REGULATION OF ENDOTHELIN-1 (ET-1) SYNTHESIS AND SECRETION AT THE OUTER BLOOD-RETINAL BARRIER.

Santosh Narayan, Department of Pharmacology & Neuroscience, University of North Texas Health Science Center Fort Worth, TX 76107.

SUMMARY

The retinal pigment epithelium (RPE) constitutes the outer blood retinal barrier at the posterior segment of the eye. The RPE provides metabolic support to the photoreceptors in the neural retina. A breakdown in the barrier supported by RPE is a hallmark in several retinopathies including proliferative vitreoretinopathy, choroidal neovascularization and macular edema. Characteristic to all epithelial cells, mature RPE cells display a polarized phenotype both in culture (ARPE-19 cells) and *in vivo*, with specific apical and basolateral domains. This provides a testable model to study the RPE *in vitro*. The purpose of this study was to characterize the RPE as a source for endothelin-1, using both *in vitro* and *in situ* models.

Endothelins (ET-1,-2, and -3) are known regulators of vascular tone, that are produced at sites close to their target. ET-1, being a potent vasoconstrictor may be involved in regulating blood supply to the choroid and the neural retina. We identified the RPE to be a major source for endothelin-1 (ET-1) *in situ* in the human retina as well as in pigmented and albino rat retinas. Additionally, using a cell-culture model of mature polarized ARPE-19 cells, we studied the synthesis and expression of ET-1 in response to muscarinic receptor stimulation, TNF-α and more recently to thrombin. We have identified other components involved in the synthesis and turnover of ET-1 in ARPE-19

cells including the proprotein convertase- furin, endothelin-converting enzyme-1 and its isoforms and the endothelin receptor B subtype. ARPE-19 cells grown on collagen filters helped determine if secretion of ET-1 was polarized or discriminative towards either the apical or basolateral surface.

We consistently observed changes in cell shape and tight junction disassembly in ARPE-19 cells following TNF-α and thrombin addition. Additionally, thrombin caused an increase in preproET-1 mRNA at earlier time points that was dependent on the rho-kinase (ROCK1/2) pathway. We report a novel signaling mechanism for regulating preproET-1 mRNA and mature ET-1 secretion in ARPE-19 cells that involves the thrombin receptor (protease activated recepotor-1/PAR-1) dependent activation of the rho/ROCK1/2 signaling pathway that may also be involved in thrombin induced changes in the cytoskeleton.
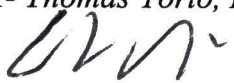
In conclusion, the RPE may be an important source for ET-1 at the posterior segment of the eye, secretion of which is greatly enhanced by substances that promote breakdown of blood retinal barriers, inflammation and changes in the RPE cytoskeleton. ET-1 secreted by the RPE, under physiological conditions may provide an autoregulatory mechanism for controlling blood flow at the outer blood retinal barrier. Excessive ET-1 secretion following breakdown of the barrier may either promote wound repair or may mediate further damage to the retina, the substrates of which are presently unknown. Future experimental approaches are planned to address these possibilities.
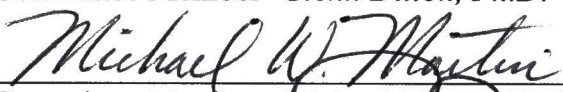
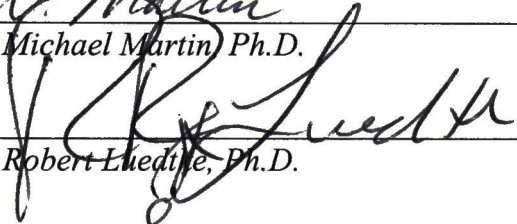# REGULATION OF ENDOTHELIN-1 (ET-1) SYNTHESIS AND SECRETION AT THE OUTER BLOOD RETINAL BARRIER.
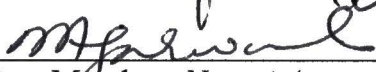
Santosh Narayan

APPROVED BY:

_____
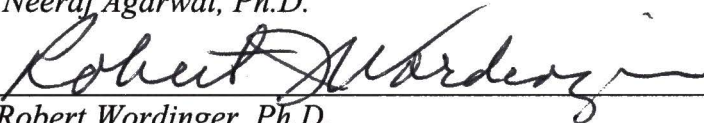
Major Professor- *Thomas Yorio, Ph.D.*

_____

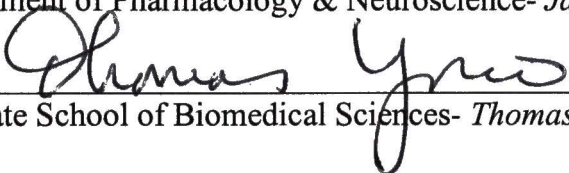Committee Member- *Glenn Dillon, Ph.D.*

_____

Committee Member- *Michael Martin, Ph.D.*

_____

Committee Member- *Robert Luedtke, Ph.D.*

_____

Committee Member- *Neeraj Agarwal, Ph.D.*

_____

University Member- *Robert Wordinger, Ph.D.*

_____

Chair, Department of Pharmacology & Neuroscience- *James Simpkins, Ph.D.*

_____

Dean, Graduate School of Biomedical Sciences- *Thomas Yorio, Ph.D.*

REGULATION OF ENDOTHELIN-1 (ET-1) SYNTHESIS AND SECRETION AT

THE OUTER BLOOD-RETINAL BARRIER.

Ph.D. Dissertation

Presented to the Graduate Council of the University of North Texas Health Science

Center at Fort Worth.

In Partial Fulfillment of the Requirements for the

Degree of Doctorate of Philosophy

By

Santosh Narayan

Department of Pharmacology and Neuroscience

UNTHSC, Fort Worth, Texas 76107.

August 28, 2003.

ACKNOWLEDGEMENTS

---

[*] Elder uncle in the South Indian languange, Tamil.

ABBREVIATIONS AND DEFINITIONS

ARPE-19: Adult Retinal Pigment Epithelial Cells from a 19-year-old donor
ARVO: Association for Research in Vision and Ophthalmology
BAB: Blood-Aqueous Barrier
BigET-1: Big Endothelin-1
BRB: Blood-Retinal Barrier
$[Ca^{2+}]_i$: Intracellular Calcium
CCh: Carbachol
4-DAMP: Muscarinic Receptor subtype 3 selective antagonist
DAPI: Nuclear Stain
DIC: Differential Interference Contrast
ECE: Endothelin Converting Enzyme
EM: Electron Microscopy
ET-1: Endothelin-1
ET_A: Endothelin Receptor A
ET_B: Endothelin Receptor B
GPCR: G-protein Coupled Receptor
ir-ET-1: Immunoreactive ET-1
mRPE: mature or polarized ARPE-19 cells
M_{1-5}: Muscarnic Receptor subtypes 1-5
NO: Nitric Oxide
NPE: Non-pigmented Ciliary Epithelium
PAR 1-4: Protease Activated Receptor subtypes 1-4
PE: Pigmented Ciliary Epithelium
PLC: Phospholipase C
PKC: Protein Kinase C
pPAR-1: Peptide agonist for PAR-1 receptor (SFLLR)
pPAR-4: Peptide agonist for PAR-4 receptor (AYPGKF)
ProET-1: Proendothelin-1
ppET-1: Preproendothelin-1
PZE: Pirenzepine, Muscarinic receptor subtype 1 selective antagonist
Q-PCR: Quantitative Polymerase Chain Reaction
RIA: Radioimmunoassay
ROCK: Rho-Kinase or Rho-associated Kinase
Ro 31-8425: Nonselective Protein Kinase C (or pan-PKC) Inhibitor
RPE: Retinal Pigment Epithelium
RPE65: RPE protein-65kD (resident protein used as a marker for RPE)
RT-PCR: Reverse Transcriptase Polymerase Chain Reaction
TJ: Tight Junction
TNF-α: Tumor Necrosis Factor-α
TNF-R1: TNF-Receptor type-1
U73122: Phospholipase C inhibitor

yRPE: young or non-polarized ARPE-19 cells
Y27632: Rho Kinase Inhibitor
ZO-1: Zona Occludens-1

CONTENTS

Chapter 5. Thrombin Induced Endothelin-1 Synthesis and Secretion in Retinal Pigment Epithelial Cells is Rho Kinase (ROCK) Dependent.

LIST OF FIGURES

The Endothelin-1 Axis in the Retinal Pigment Epithelium

LIST OF TABLES

CHAPTER 1

INTRODUCTION

The introduction is divided into three broad sections- the first section provides an overview on the biology of endothelins, the second section provides a brief introduction to ocular blood circulation and blood-ocular barriers and the third section describes the retinal pigment epithelium (RPE) as one of components of the blood-ocular barrier and the clinical relevance associated with it.

I. *Endothelin Biology*

[Prasanna G., Narayan S., Krishnamoorthy R.R., and Yorio T. Eyeing Endothelins: a cellular perspective. *Mol. Cell. Biochem.* 283: 71-88, 2003]

Endothelins (ET) belong to the class of well-conserved neuropeptides that are ubiquitously present in vertebrate systems and in other diverse species including the marine mollusk aplysia.[1, 2] Signaling events following its cognate receptor activation sustains a spectrum of essential functions from development and migration in the fetus [3-6] to vascular homeostasis and proliferation in the adult.[7-9] Endothelin-1, the first of the three isoforms originally isolated from porcine aortic endothelial cells[10] was found to be a potent vasoconstricting agent. Following its initial discovery, several groups have reported and confirmed their presence (transcript and/or translated products) at other sites including the brain,[11, 12] eye,[13-15] heart,[16-18] lung,[13] kidney,[19] intestine and bladder.[13, 20]

The spatiotemporal expression of ET along with its receptors is indicative of its absolute functional requirement at these sites. Endothelin and its receptors are required

for proper migration of neural crest cells and differentiation postmigration.[6, 21] Ablating endothelin or its receptors have generated lethal phenotypes that include developmental abnormalities [4, 6, 21] and cardiovascular defects.[21, 22] Endothelin along with certain other proinflammatory cytokines, nitric oxide and reactive oxygen species constitute the growing list of the 'usual suspects' implicated in several pathologies including myocardial infarction, congestive heart failure, atherosclerosis, hypertension, stroke and more recently, in glaucoma.[23]

Like most neuropeptides, endothelins are expressed in minimal amounts including areas besides the cardiovascular system. Its role in areas like the hypothalamus[12] and the retina [24] remain largely unascertained. Because of these reasons and because endothelin levels are elevated in several pathologies both systemically and locally, it is important to understand how these peptides are produced and regulated.

Isoforms of Endothelin

The ET family of peptides comprise mainly three isoforms, ET-1, -2 and –3.[25] All three isoforms are derived from separate genes and undergo post-translational proteolytic processing yielding the mature peptide that is 21 amino acids in length.[16] The isoforms share similar characteristics that include an N-terminal domain and a hydrophobic C-terminal domain. There are two cysteine bridges that link residues 1 and 15 and residues 3 and 11. Residues at position 2, 4-7 and 14 make up for variable regions of these peptides. The hydrophobic tail comprising residues 16-21 are highly conserved between the three isoforms with a terminal tryptophan (Trp21) residue important for activity.[16, 26]

14

Synthesis of Endothelins

The biogenesis of endothelin is believed to occur in three steps that involve successive proteolytic processing from a larger precursor to a smaller form of the peptide. The precursor, preproendothelin-1 (ppET-1) mRNA is translated into a 212 amino acid product.[27] The first 17 amino acids represent a signal sequence that gets cleaved by a signal peptidase to form proET-1. A dibasic amino acid convertase with furin-like specificity cleaves proET-1 at the paired basic amino acid residues Lys^{51}-Arg^{52} and Lys^{91}-Arg^{92} to form big ET-1.[28] The cleavage at Arg^{92} is essential for processing of big ET-1 to its mature form- ET-1 catalyzed by endothelin converting enzyme-1 (ECE-1).[29] The processing of big ET-2 to ET-2 involves cleavage at the Trp-Val bond while the conversion of bigET-3 to ET-3 involves the Trp-Ile bond. ECE is a zinc dependent phosphoramidon-sensitive metalloprotease that hydrolyzes big ET-1 at the Trp^{21}-Val^{22} bond to yield the 21 amino acid form of mature ET-1.[30-32] ECE shares significant homology with the membrane-bound neural endopeptidase-24.11 (NEP/E-24.11/neprilysin) and Kell blood group protein.[33] E-24.11 regulates the levels of peptides in several tissues.[34]

The general consensus supports the finding that ECE is a type II integral membrane (plasma membrane and/ or vesicular membrane) protein with its large C-terminal catalytic domain facing the extracellular region,[35, 36] and may thus act as an ectoenzyme. The catalytic domain of ECE-1 comprises almost 90% of the protein (681 residues), tethered by a single membrane spanning domain of 21 residues and a cytoplasmic N-terminal domain which is 51-56 residues long.[32] The enzyme is highly

glycosylated (approximately 33%) with ten putative glycoslation sites in the extracellular catalytic domain. Unlike E-24.11, functional ECE exists as a disulfide-linked homodimer in the catalytic domain of subunit MW 120-130 kD.[37, 38] Alternative splice variants of ECE-1 i.e. ECE-1a, 1b, and 1c have been reported and they differ in their N-terminus.[39, 40] Consistent with this finding, there appears to be no significant difference in substrate specificity or k_{cat} for big ET conversion between the three ECE-1 isoforms.[41]

CCh, TNF-α, Thrombin

ppET-1 mRNA → PreproET-1 (212 a.a)

Signal Peptidase

ProET-1 (196 a.a)

Furin/ Proprotein convertase

Big ET-1 (38 a.a)

ECE-1

ET-1 (21 a.a)

ETA receptor

ETB receptor
('Clearance receptor')
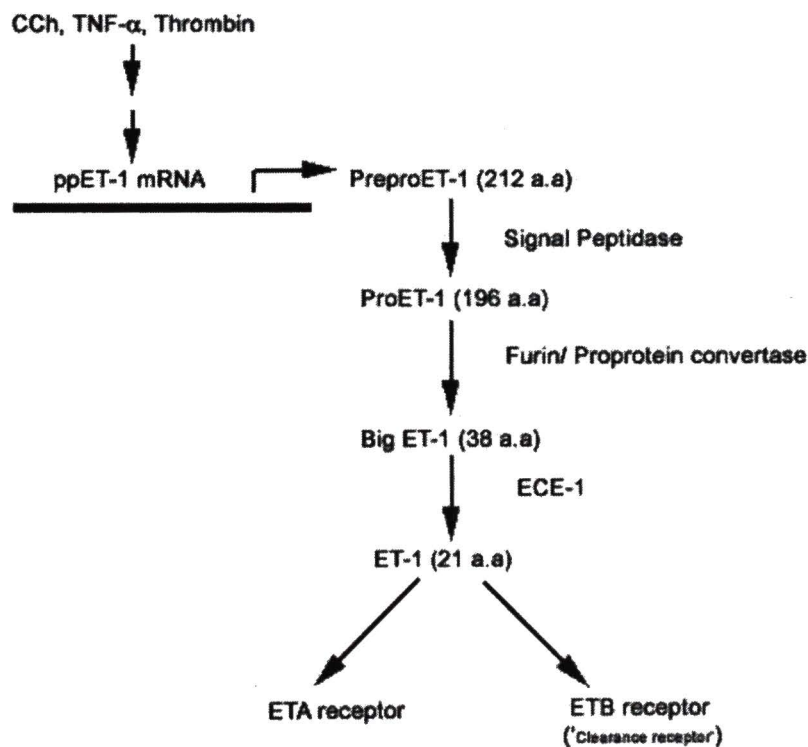
Biogenesis of ET-1

Storage and Exocytosis of Endothelin

Secretory proteins and neurotransmitters are stored in small or large dense core vesicles that discharge their contents into extracellular space either constitutively or

following stimulation.[42] They are transported from the site for synthesis-the rough endoplasmic reticulum to the golgi cisternae where they undergo post-translational processing and finally to the plasma membrane where vesicular fusion and subsequent fission results in exocytosis.[43] Protein transportation and secretion may be achieved either via a constitutive pathway involving constant release and/or a regulated pathway involving stimulated and instantaneous release. The constitutive pathway is regulated at the level of transcription and involves *de novo* synthesis.[44]

Secretion of endothelin can be either constitutive and/or regulated.[45] Immunoreactive-ET-1 was found to be localized in the rough endoplasmic reticulum, golgi cisternae, golgi vesicles and smaller storage vesicles beneath the plasma membrane of endothelial cells suggesting that ET-1 is synthesized and segregated in the rough endoplasmic reticulum, transported to golgi complex, packed and condensed into golgi vesicles and secreted by exocytosis.[46] The microtubular system has been implicated in the transport of storage vesicles and granules containing synthesized ET-1 to the cell surface.[47]

Endothelin-like immunoreactivity was detected in secretory vesicles in bovine aortic and human coronary artery endothelial cells implicating constitutive secretion.[48, 49] Vascular endothelial cells contain elongated storage granules called Weibel-Palade bodies[50] that are involved in regulated exocytosis.[51] Weibel-Palade bodies store several vasoactive substances including von Willebrand factor (vWF),[52] P-selectin,[53] calcitonin gene-related peptide[54], big endothelin, endothelin[48, 55, 56] and other substances including CD63/lamp3,[57] tissue-type plasminogen activator[58] and α1,3-fucosyltransferase VI.[59] It

has been proposed that vWF itself may be involved in the formation of Weibel Palade bodies [60, 61] and may act as a chaperone for targeting selective proteins that are structurally unrelated, including P-selectin and IL-8 into these granules[62,48, 55] have proposed that these storage granules specific for endothelial cells may also represent a site for the conversion of big ET to mature ET. In human umblical vein endothelial cells, big ET-1 along with ECE-1 were found to co-localize with vWF in Weibel Palade bodies.[45] The presence of big ET-1 and ET-1 in both secretory vesicles and Weibel Palade bodies implies that ET-1 and/or big ET-1 can be released in a constitutive and regulated manner.

Polarity of endothelin secretion

Studies have shown that secretion of ET-1 is polarized in endothelial cells. Masaki (1989) had proposed a polar secretion of the peptide by endothelial cells towards the underlying intimal smooth muscle implicating a paracrine role for endothelin.[63] Almost 80% of ET-1 was released from the basolateral (abluminal) compartment in human umblical vein endothelial cells (HUVECs) cultured in acellular amniotic membranes[64] and in procine cerebral endothelial cells.[65] This is in agreement with the observation that ET-1 released in this manner can act on the underlying vascular smooth muscle and modulate vasomotor tone.[66]

The Rho family of small GTPases that belong to the ras superfamily have been implicated in regulation of actin cytoskeletal organization, vesicular trafficking ,exocytosis and establishment of cell polarity.[67] Thrombin, a known activator of endothelin-1 synthesis and secretion[47] has been shown to regulate endothelial cell

permeability by way of actin stress fiber assembly and increase in intercellular gap formation.[68] It has been shown that thrombin mediated effects on ET-1 production in HUVECs is rho and mitogen-activated protein kinase (MAPK) dependent[69]. These observations indicate the possibility that during inflammation involving a breakdown of the tight junction barrier and perturbation of polarity by thrombin or other chemokines, it is feasible to cause a greater release of ET-1 in the luminal/apical side.

Signals for Endothelin Synthesis and Secretion

Several physiological or pathophysiological stimuli can cause the release of endothelin by way of the regulated pathway. Cytokines including TGF-β,[70] IL-1,[71] TNFα,[72, 73] interferon-γ (IFN–γ)[74] and thrombin[75] can induce both transcription as well as release of ET-1. The above studies have implicated Ca^{2+} and/or protein kinase C (PKC) to be involved in the transcriptional regulation of preproET-1. An increase in intracellular Ca^{2+} has been also shown to regulate both the expression of preproET-1 as well as ET-1 secretion. Ca^{2+} released from intracellular stores along with calcium-calmodulin complexes can elicit phosphorylation of the myosin light chain that can result in cytoskeletal rearrangement favorable for transport and exocytosis of secretory vesicles.[76] Natriuretic factors including atrial natriuretic peptide (ANP) and brain derived natriuretic peptide (BNP)[77] along with nitric oxide donors have been shown to inhibit secretion of ET-1 from endothelial cells.[78] These reports have implicated a cGMP dependent pathway to be involved in the inhibition of ET-1 secretion. Nitric oxide (NO) has also been shown to displace ET-1 from its receptor.[79] Heparin has also been shown to inhibit thrombin

mediated perproET-1 transcription and ET-1 secretion presumably by inhibiting IP$_3$ receptors and subsequent Ca^{2+} mobilization and PKC activation in endothelial cells.[80] Phosphoramidon, a non-selective metalloprotease inhibitor has also been shown to decrease ET-1 production via its direct inhibitory effect on ECE.[81]

Small G-proteins have been implicated in vesicular exocytosis and recently it was shown that Ral, a small GTPase is associated with Weibel-Palade bodies.[82] Ral associates with GDP (ral-GDP bound state) when inactive. Stimuli that promote intracellular Ca^{2+} mobilization events (eg. thrombin) results in activation of a Ca^{2+}dependent calmodulin complex that in turn binds to ral-GDP associated with Weibel-Palade bodies. This association promotes GTP exchange on ral by a ral-guanine exchange factor (ralGEF) and interacts downstream with effectors like RLIP76, a GTPase activating protein for Cdc42 and Rac. GTP hydrolysis on Cdc42 or rac may promote cytoskeletal rearrangement and regulated exocytosis of Weibel-Palade bodies.[51, 83]

ET Receptors, Signaling and Trafficking of ET receptors.

Endothelin receptors belong to the family of G-protein coupled receptors (GPCR) and exist mainly as ET$_A$ and ET$_B$ receptor subtypes.[84] Signaling via the ET$_A$ receptor mediates the vasoconstrictive action of ET-1[85] while ET$_B$ mediated actions on endothelial cells result in vasodilation caused by nitric oxide (NO).[86] ET$_B$ receptors are also involved in the clearance of circulating ET-1 and is referred to as the 'clearance receptor' for ET-1.[87, 88] Human ET$_A$ and ET$_B$ receptors share 55% homology indicating that signaling events following stimulation of each of the subtype may be distinct and may be differentially regulated by other interacting proteins.

Cellular adaptation to prolonged stimuli acting on GPCRs occurs by way of receptor desensitization and/or internalization. This may be particularly vital in ET-receptor mediated signaling because under physiological conditions ET binds irreversibly to its receptors.[89] Phosphorylation of serine-threonine residues in the C-terminal tail of activated GPCRs is implicated in receptor desensitization.[90, 91] The G-protein receptor kinase (GRK), specifically GRK2 has been shown to cause phosphorylation and subsequent desensitization of both ET_A and ET_B receptors in an agonist dependent manner.[92] GRK-mediated receptor phosphorylation subsequently facilitates binding of β-arrestin to the receptor, resulting in uncoupling of the receptor from its G-protein and receptor internalization ensues in a dynamin/ clathrin mediated manner.[93-95] Bremnes (2000)[96] have shown that both ET_A and ET_B receptors undergo β-arrestin2-dynamin/clathrin-dependent receptor internalization following GRK-mediated phosphorylation in transfected chinese hamster ovary (CHO) cells. The study also revealed different subcellular trafficking routes for ET_A and ET_B receptors. Internalized ET_A receptors were targeted to the pericentriolar recycling compartment while ET_B receptors were sorted to the lysosome and degraded. The differential adaptation of ET receptors to the same stimuli i.e. endothelin, may explain the prolonged vasoconstrictive effects mediated by ET_A receptors due to maintenance/ recycling of receptors on the cell surface as opposed to the clearance of circulating endothelin mediated by ET_B by subsequent internalization and degradation in lysosomes.

Truncation and domain-swapping experiments of ET-receptors revealed the differential sorting mechanisms were due to the differences in their C-terminal tails.[97]

Novel roles for arrestin-mediated signaling are emerging. Recent studies show that arrestins may not only be involved in signal termination but may also act as a scaffolding protein for GPCR-dependent activation of MAPKs.[98, 99] β-arrestin mediated regulation of the Ral-GDS-Ral pathway may also regulate the chemoattractant formyl-Met-Leu-Phe (fMLP) receptor-induced granule exocytosis in polymorphonuclear leukocytes (PMNs)[100] Lee et al (2001)[101] have reported the histone acetyltransferase Tip60 and the histone deacetylase HDAC7 interact with internalized ET_A receptors in the recycling compartment, a mechanism that ensued in a ligand-dependent fashion and resulted in ERK1/2 phosphorylation. Scaffolding proteins like Tip60 and HDAC7 may stabilize the receptor in the recycling compartment and may protect against degradation.

II. Ocular Circulation and Blood Ocular Barriers

Ocular Circulation

Blood flow to the eye, especially to the retina is critical for the maintenance of vision. This was clinically confirmed when it was first observed that irreparable damage occurs if ocular ischemia due to occlusion of retinal vessels persists for over an hour.[102, 103] Ocular blood vessels in humans are mainly derived from the ophthalmic artery, which is a branch of the internal carotid.[104] The ophthalmic artery branches into the central retinal artery, anterior ciliary arteries and the posterior ciliary arteries. The central retinal artery in turn branches into 4 major vessels, each supplying a quadrant of the inner retina. The anterior ciliary artery supplies blood to the anterior uvea that includes the ciliary body, anterior choroid and the iris. The posterior ciliary artery supplies blood to the

posterior uvea mainly at the posterior pole of the eye including the choroid beneath the retina and the anterior optic nerve.

Venous drainage of the eye empties into the superior and inferior ophthalmic veins. Blood from the retina and the anterior optic nerve is drained into the central retinal vein that in turn drains into the superior ophthalmic vein. The choroid and the anterior uvea drain blood into the vortex veins and the episcleral veins respectively, that in turn drain into both the superior and inferior ophthalmic veins.

Blood-ocular barriers

The hallmark of any blood-organ barrier is that they protect and metabolically support the underlying tissue. The 'barrier' function is mainly provided by apically localized tight junctions in epithelial and endothelial cells that constitute most barriers and prevents permeability to macromolecules (>40 Å).[105] Blood-ocular barriers are functionally similar to other blood-organ barriers in that it provides a controlled environment within the organ or tissue. In the retinal and the brain vasculature for example, the blood barrier comprising mainly of endothelial cells provides an interface between the neuron and the blood and controls the exchange of oxygen and other nutrients between either sides.

Based on the anatomy of the eye, blood-ocular barriers comprise mainly of two types- the anterior blood-aqueous barrier (BAB) and the posterior blood-retinal barrier (BRB). The blood-aqueous barrier is formed by the ciliary epithelium (both the pigmented and the non-pigmented ciliary epithelium) and the endothelium of the iridial vessels. The blood-retinal barrier can be further classified into the outer BRB formed by

the retinal pigment epithelium and the inner BRB formed by endothelial cells of retinal vessels in the inner retina.[106] Blood barriers differ in their barrier properties based on the permissible size of molecules across it. The vascular barriers are highly permeable to oxygen, carbon dioxide and nitric oxide that readily pass through endothelial cells. Water diffuses across these barriers via the para- and trans-cellular routes. The BAB has tight junctions of the 'leaky' type similar to the kidney epithelium and the BRB membranes have tight junctions of the 'non-leaky' type similar to that seen in the blood-brain barrier. Both receptor mediated and non-receptor mediated stimuli can regulate permeability across blood ocular barriers.

III. *The Retinal Pigment Epithelium (RPE) and Clinical Implications*

The retinal pigment epithelium, as mentioned above forms the outer blood retinal barrier and provides the interface between the highly vascular choroid and the avascular anterior neural retina. The apical domain of the RPE faces the apical domain of the photoreceptor outer segments.[107, 108] This arrangement allows the apical microvilli of the RPE to engulf and phagocytize shed photoreceptor outer segments. The RPE additionally, provides metabolic support to the photoreceptors including the transport of vitamin A from the basal choriocappilaries to the photoreceptors that sustains the phototransduction cascade.[107] Additionally the RPE maintains the fluid and ionic balance at the subretinal space (region between the RPE and the photoreceptor outer segments), important for retinal adhesiveness.[109] All these functions require the structural integrity of the RPE monolayer at the posterior pole. Tight junctions at the apical RPE maintain the barrier. Additionally, tight junctions in epithelial cells function as a 'lipid fence' that

The maintenance of structural integrity of blood-ocular barriers is of major concern for the clinician, in diseases and surgical procedures that alter their permeability. Several abnormalities are associated with the RPE involving perturbation of its monolayer integrity, that alters the RPE cytoskeleton and permits excessive proliferation, a condition known as proliferative vitreoretinopathy.[117] In diabetic retinopathy and choroidal neovascularization, excessive RPE proliferation and migration results in deposition of newly formed RPE cells on the epiretinal surface that results in blurred vision. Surgical procedures including retinal reattachment can damage the RPE which in turn results in altered permeability and proliferation.[107, 109] In conditions like uveitis, a breakdown of the inner blood-retinal barrier can result in inflammation, which in turn exposes the RPE to blood-borne substances that can perturb its integrity. Similarly, breakdown or compromised choroidal blood vessels at the basal side can predispose the RPE to further injury.

CHAPTER 2

RESEARCH DESIGN, RATIONALE AND METHODS

In the anterior chamber of the eye, ET-1 has been shown to regulate intraocular pressure and aqueous humor dynamics[23, 118] and in the posterior segment, ET-1 and nitric oxide (NO) have been shown to influence retinal and choroidal blood flow.[119] Exogenously administered ET-1 either intravitreally or at the region of the optic nerve head produces neuropathy analogous to that seen in glaucoma. The precise source of endothelin especially in the posterior segment is not completely understood. In addition to targeting the source of ET-1 production, it is also important to identify factors that regulate ET-1 synthesis at the posterior segment that may help understand conditions that promote its secretion.

In the light of the above knowledge about endothelins, ocular barriers and the RPE, we hypothesized that the RPE, due to its specific location can act as a source for endothelin-1 (ET-1) and that breakdown of the blood retinal barrier would allow cytokines like TNF-α and blood derived proteases including thrombin to act on the RPE and regulate ET-1 synthesis and secretion. Additionally, we compared how different stimuli including muscarinic receptor stimulation, TNF-α and thrombin altered the RPE cytoskeleton and have identified a novel signaling cascade that is involved in both ET-1 synthesis and cytoskeletal remodeling.

The overall goal of this proposal is to demonstrate that ET-1 is synthesized and secreted constitutively by the retinal pigment epithelium (outer blood retinal barrier) and that secretion can be regulated by different factors including TNF-α, thrombin and cholinergic (muscarinic) stimulation.

Our approach has been to map regions of the eye that expresses immunoreactive ET-1 (ir-ET-1) by light microscopy. The non-pigmented ciliary epithelium has been identified as one of the source for ET-1 in the anterior chamber.[118] We confirmed this *in situ* using rat retinas, that additionally provided a control for the anti-ET-1 antibody used in our studies. At the region of the outer blood retinal barrier, we have used immunoelectron microscopy to determine the distribution of ET-1. In addition, using a human cell culture model of the retinal pigment epithelium (posterior segment) we have attempted to study how secretion of ET-1 by these cells may be regulated in response to different naturally occurring stimuli.

The following specific aims were designed to address our hypothesis:

1) Identifying the distribution for ET-1 at the anterior and posterior segments (Chapter 3).

2) To determine if synthesis and secretion of ET-1 is constitutive and/or regulated and is it polarized or discriminative towards the apical or basal surfaces of the RPE? (Chapters 1-3)

3) To elucidate the signaling mechanism for regulated ET-1 synthesis and secretion in response to thrombin in ARPE-19 cells (Chapter 4).

The following section outlines the methods that were employed to address the above specific aims, details of which have been included in individual chapters.

Specific Aim 1. Identifying the distribution for ET-1 at the anterior and posterior segments (Chapter 3)

1.1 Immunoreactive ET-1 (intracellular) distribution in pigmented and albino rat eyes

Immunoreactive ET-1 (ir-ET-1) expression patterns were determined by indirect immunofluorescence. Freshly enucleated eyes from Brown Norway rats (pigmented) and Wistar rats (albinos) were fixed and sectioned for light microscopy. Pigmented eyes are autofluorescent. We included albino eyes in our study to compare distribution patterns of ET-1 between pigmented and albino eyes. Sections (5 μm thickness) were labeled with rabbit anti-ET-1 antibody (Bachem/Peninsula Labs, CA) and mouse anti-RPE65 (gift from Dr. Debra Thompson, University of Michigan Medical School) and DAPI (Molecular Probes, OR) for nuclear staining. RPE-65 is a resident protein that is exclusively expressed in the RPE, and serves as a marker to differentiate the RPE from the underlying Bruch's membrane and choroid.

1.2 Immunoreactive ET-1 (intracellular) distribution at the outer blood retinal barrier in human eyes.

Adult human retinas (aged 74 and 86) were used for this study. Ultrathin sections (50nm thickness) were mounted on nickel grids and immunostained with rabbit anti-

ET-1 (Bachem/Peninsula Labs, CA) and anti-rabbit antibody conjugated to 12nm colloidal gold particles. Sections were visualized under an electron microscope at different magnifications. Control sections using rabbit IgG at the same concentration as the primary antibody were included in the study.

Specific Aim 2. To determine if secretion of ET-1 constitutive and/or regulated and is it polarized or discriminative towards the apical or basal surfaces of the RPE ? (Chapters 1-3). Specific aims 2.1 and 2.2 address constitutive secretion of ET-1 in ARPE-19 cells and the polarity of secreted ET-1. Specific aims 2.3 and 2.4 address regulated secretion of ET-1 following muscarinic receptor stimulation and TNF-α.

2.1 <u>Constitutive ET-1 secretion (mature form) in ARPE-19 cells.</u>

Radioimmunoassay (RIA)-based techniques are sensitive and more importantly quantitative. We used a commercially available kit to detect ET-1 (Bachem/Peninsula Labs, CA) secreted by ARPE-19 cells in the culture medium. ET-1 released from untreated cells is a measure of constitutive synthesis and secretion of ET-1. Secretion profile of ET-1 was analyzed at different time points.

2.2 <u>Polarization and Secretion of ET-1 in ARPE-19 cells</u>

ARPE-19 cells were grown on transwell collagen coated filters with a thin coat of matrigel. Cells were maintained in culture for at least 4 weeks before collecting media from apical and basal compartments in the well. The RPE monolayer integrity on collagen filters was determined by a paracellular flux assay using C^{14}-mannitol added to the apical chamber. Fractions from the basolateral chamber were collected over time and

counted. To determine whether ET-1 was secreted vectorially in polarized RPE cells, apical and basolateral media were assayed separately for ET-1 content by RIA.

2.3 Regulated secretion of ET-1 in ARPE-19 cells following muscarinic receptor stimulation and TNF-α.

The rationale for considering the actions of cholinergics on RPE stems from observations that the uvea including the choroid is parasympathetically innervated by varicosities arising postganglionically from the pterygopalatine and ciliary ganglions. The dense plexus of cholinergic innervation at the choriocapillaries just beneath the RPE is thought to act post-synaptically on choroidal smooth muscles as well as the RPE.[120] Additionally, both immunofluorescence and binding studies have shown that mammalian and avian RPE express abundant muscarinic receptors throughout development and adult stages, similar to that seen in the brain.[120-124] Aceylcholine unlike TNF-α, is not known to cause inflammation or breakdown of epithelial barriers. However, both muscarinic receptor activation and TNF-α have been reported to influence ET-1 secretion.[73, 125, 126] This provided us with tools to identify and differentiate receptor-mediated regulation of ET-1 synthesis and secretion in ARPE-19 cells.

2.3a. Intracellular calcium [Ca^{2+}]$_i$ mobilization following carbachol stimulation. Carbachol induced changes in [Ca^{2+}]$_i$ mobilization were studied in real-time by fura-2AM fluorescence microscopy. Pharmacological characterization of muscarinic receptors was performed using selective muscarinic receptor antagonists- pirenzepine (M_1 subtype antagonist), 4-DAMP (M_1 and M_3 subtype antagonist) and himbacine (M_2 and M_4 syptype antagonist). U73122, a phospholipase C inhibitor was also used to

delineate IP_3 mediated Ca^{2+} release following carbachol stimulation. Receptor desensitization and/or internalization was determined by pre incubating cells with carbachol at different concentrations followed by a carbachol challenge.

2.3b. <u>Western blot analysis for the M_1 and M_3 muscarinic receptor sybtypes</u>. The expression of M1 and M3 muscarinic receptors (rabbit anti M_1 and goat anti M_3 antibodies from Santacruz Biotechnology, CA) as well as the TNF-R1 receptor (Santacruz Biotechnology, CA) in ARPE-19 cells were determined by western blotting using membrane fractions.

2.3c. <u>ET-1 RIA</u> was employed to determine regulated release of mature ET-1 following different concentrations of carbachol in the presence or absence of selective muscarinic receptor antagonists (as mentioned in 2.3 a). TNF-α mediated ET-1 secretion was in the presence and absence of a TNF-R1 monoclonal antibody (R & D Systems, MN). Additionally, temporal aspects of TNF-α mediated ET-1 secretion was compared with untreated cells at the same time points.

2.3d. <u>Indirect immunofluorescence analysis in ARPE-19 cells</u>. TNF-α and carbachol mediated changes in the expression patterns of the tight junction protein, ZO-1 and intracellular ET-1 was performed by indirect immunofluorescence. TNF-α mediated disruption of RPE tight junctions was analyzed temporally and in the presence of the TNF-R1 receptor antibody (R & D Systems, MN).

2.3e <u>Real time (quantitative) reverse transcriptase polymerase chain reaction (RT-PCR)</u>. TNF-α and carbachol mediated changes in preproET-1 mRNA was determined at

different time points using SYBR-green PCR core reagents for fluorescence-based detection of PCR products in real time.

2.4 <u>The ET-1 Axis in the RPE- Expression of the proprotein convertase furin, endothelin-converting enzyme-1 (ECE-1) isoforms and ET receptors in ARPE-19 cells.</u>

2.4a. Furin belongs to the family of proprotein convertases (PC) that is involved in the conversion of precursor proproteins to their active mature forms.[127] In the biogenesis of endothelins, furin is involved in converting the proET (212 amino acids) form to bigET-1 (38 amino acids). The presence of furin in ARPE-19 cells was determined by western blot analysis using an antibody specific for furin (rabbit anti-furin proprotein convertase from Affinity Bioreagents, CO).

2.4b. Endothelin-converting enzymes (ECE) are type II membrane metalloproteases that are involved in the final step that proteolytically converts precursor bigET (38 amino acids) to the biologically active and mature form of ET (21 amino acids). ECE-1 isoforms have been implicated in the processing of ET-1. So far, four splice variants (ECE-1a,b,c,d) differing at their N-terminals have been identified and sequenced. The catalytic activity of ECE is at the C-terminal, thus the four isoforms are considered to have similar activities. We designed specific primers that spanned the N-terminal regions of ECE-1 cDNA isoforms and PCR amplified to determine the presence of the genes in RPE cells.

2.4c. ET-1 secreted by the RPE is likely to act on its receptors ET_A and ET_B, both of which are G-protein coupled receptors. Secreted ET-1 is thought to act either in an autocrine and/or paracrine manner. ET_B receptors are known to regulate the turnover of secreted ET-1 and like LDL receptors, they internalize following ligand dependent activation. Internalized ET_B receptors are lysosomally degraded with the ligand (ET) thus providing a means to regulate extracellular levels of ET. ET_A receptors unlike ET_B are recycled to the plasma membrane following activation and internalization of the receptor. We sought to determine if ET_A and ET_B receptors were present in ARPE-19 by western blotting (rabbit anti-ET_A and anti-ET_B antibodies from Alomone Labs, Israel). Additionally, to determine if ET_B receptors were internalized, the level of ET_B receptors in membrane fractions following ET-1 stimulation at different concentrations were analyzed by western blotting.

Specific Aim 3. To elucidate the signaling mechanism for regulated ET-1 synthesis and secretion in response to thrombin in ARPE-19 cells (Chapter 4).

This study was designed to specifically determine if thrombin mediated synthesis and secretion of ET-1 was dependent on receptor-mediated alternation of the RPE cytoskeleton.

3.1 ET-1 RIA. Thrombin, a serine protease acts on protease-activated receptors (PAR-1, -3 and -4) that belong to the atypical class of G-protein coupled receptors. Details regarding the pharmacology and mechanism of action of PARs is included in Chapter 4. Thrombin mediated ET-1 secretion in ARPE-19 cells were analyzed by ET-1 RIA in the

presence of thrombin at different concentrations, the PAR-1 receptor agonist (SFLLR) and the PAR-4 receptor agonist (AYPGKF). Hirudin, a direct inhibitor of thrombin was included in the study. Temporal aspects of ET-1 secretion following thrombin were also studied by RIA. U73122, a phospholipase C inhibitor, Y27632, a rho-associated kinase (ROCK1/2) inhibitor and Ro 31-8425, a pan-protein kinase C (PKC) inhibitor were included to study the signaling mechanism of thrombin mediated ET-1 secretion.

3.2 <u>Intracellular Ca^{2+} measurements</u>. Thrombin induced changes in $[Ca^{2+}]_i$ mobilization were studied in real-time by fura-2AM fluorescence microscopy. Pharmacological characterization of the PAR-1 and PAR-4 receptor subtypes were performed using specific receptor agonists. U73122, a phospholipase C inhibitor was included in this study to determine the contribution of the G_q/PLC/IP$_3$-dependent cascade on ET-1 production.

3.3 <u>Indirect immunofluorescence</u>. Thrombin mediated alteration in the RPE tight junction assembly was analyzed as mentioned in specific aim 2.3d.

3.4 <u>Rho pull-down assay.</u> Protease-activated receptors for thrombin are known activators of the small GTPase rho. To determine if thrombin activates rho at similar time scales as the $[Ca^{2+}]_i$ mobilization event, we performed a glutathione-based fusion protein assay that specifically pulls down active rho. Active and total rho levels were determined by western blot analysis and scanning densitometry.

3.5 <u>Real time (quantitative) reverse transcriptase polymerase chain reaction (RT-PCR).</u>

As mentioned in specific aim 2.3e, thrombin mediated preproET-1 (ppET-1) mRNA synthesis was determined at different time points following stimulation. U73122, a

phospholipase C inhibitor, and Y27632, a rho-associated kinase (ROCK1/2) inhibitor were included to study the signaling mechanism of thrombin mediated ppET-1 mRNA synthesis.

REFERENCES (for Introduction, Research Design, Rationale and Methods)

1. Brain, S. D., Crossman, D. C., Buckley, T. L. & Williams, T. J. Endothelin-1: demonstration of potent effects on the microcirculation of humans and other species. *J Cardiovasc Pharmacol* **13 Suppl 5**, S147-9; discussion S150 (1989).

2. Giaid A, Masaki T, Ouimet T, et al. Expression of endothelin-like peptide in the nervous system of the marine mollusk Aplysia. *J Cardiovasc Pharmacol* **17 Suppl 7**, S449-51 (1991).

3. Baynash AG, Hosoda K, Giaid A, et al. Interaction of endothelin-3 with endothelin-B receptor is essential for development of epidermal melanocytes and enteric neurons. *Cell* **79**, 1277-85 (1994).

4.   Clouthier DE, Williams SC, Yanagisawa H, Wieduwilt M, Richardson JA,Yanagisawa M. Signaling pathways crucial for craniofacial development revealed by endothelin-A receptor-deficient mice. *Dev Biol* **217**, 10-24 (2000).

5.   Hosoda K, Hammer RE, Richardson JA, et al. Targeted and natural (piebald-lethal) mutations of endothelin-B receptor gene produce megacolon associated with spotted coat color in mice. *Cell* **79**, 1267-76 (1994).

6.   Yanagisawa H, Hammer RE, Richardson JA, Williams SC, Clouthier DE,Yanagisawa M. Role of Endothelin-1/Endothelin-A receptor-mediated signaling pathway in the aortic arch patterning in mice. *J Clin Invest* **102**, 22-33 (1998).

7.   Wenzel, R. R., Zbinden, S., Noll, G., Meier, B. & Luscher, T. F. Endothelin-1 induces vasodilation in human skin by nociceptor fibres and release of nitric oxide. *Br J Clin Pharmacol* **45**, 441-6 (1998).

8.   Wright, C. E. & Fozard, J. R. Regional vasodilation is a prominent feature of the haemodynamic response to endothelin in anaesthetized, spontaneously hypertensive rats. *Eur J Pharmacol* **155**, 201-3 (1988).

9.   Takuwa, Y., Yanagisawa, M., Takuwa, N. & Masaki, T. Endothelin, its diverse biological activities and mechanisms of action. *Prog Growth Factor Res* **1**, 195-206 (1989).

10.   Yanagisawa M, Kurihara H, Kimura S, et al. A novel potent vasoconstrictor peptide produced by vascular endothelial cells. *Nature* **332**, 411-5 (1988).

11. MacCumber, M. W., Ross, C. A. & Snyder, S. H. Endothelin in brain: receptors, mitogenesis, and biosynthesis in glial cells. *Proc Natl Acad Sci U S A* **87**, 2359-63 (1990).

12. Lee, M. E., de la Monte, S. M., Ng, S. C., Bloch, K. D. & Quertermous, T. Expression of the potent vasoconstrictor endothelin in the human central nervous system. *J Clin Invest* **86**, 141-7 (1990).

13. MacCumber, M. W., Ross, C. A., Glaser, B. M. & Snyder, S. H. Endothelin: visualization of mRNAs by in situ hybridization provides evidence for local action. *Proc Natl Acad Sci U S A* **86**, 7285-9 (1989).

14. MacCumber, M. W., Jampel, H. D. & Snyder, S. H. Ocular effects of the endothelins. Abundant peptides in the eye. *Arch Ophthalmol* **109**, 705-9 (1991).

15. Wollensak, G., Schaefer, H. E. & Ihling, C. An immunohistochemical study of endothelin-1 in the human eye. *Curr Eye Res* **17**, 541-5 (1998).

16. Yanagisawa M, Inoue A, Ishikawa T, et al. Primary structure, synthesis, and biological activity of rat endothelin, an endothelium-derived vasoconstrictor peptide. *Proc Natl Acad Sci U S A* **85**, 6964-7 (1988).

17. Sakai S, Miyauchi T, Kobayashi M, Yamaguchi I, Goto K,Sugishita Y. Inhibition of myocardial endothelin pathway improves long-term survival in heart failure. *Nature* **384**, 353-5 (1996).

18. Plumpton, C., Ashby, M. J., Kuc, R. E., O'Reilly, G. & Davenport, A. P. Expression of endothelin peptides and mRNA in the human heart. *Clin Sci (Lond)* **90**, 37-46 (1996).

19.   Karet, F. E. Endothelin peptides and receptors in human kidney. *Clin Sci (Lond)*
      91, 267-73 (1996).

20.   Koseki, C., Imai, M., Hirata, Y., Yanagisawa, M. & Masaki, T. Binding sites for
      endothelin-1 in rat tissues: an autoradiographic study. *J Cardiovasc Pharmacol* **13**
      Suppl 5, S153-4 (1989).

21.   Kurihara Y, Kurihara H, Suzuki H, et al. Elevated blood pressure and craniofacial
      abnormalities in mice deficient in endothelin-1. *Nature* **368**, 703-10 (1994).

22.   Kurihara Y, Kurihara H, Oda H, et al. Aortic arch malformations and ventricular
      septal defect in mice deficient in endothelin-1. *J Clin Invest* **96**, 293-300 (1995).

23.   Yorio, T., Krishnamoorthy, R. & Prasanna, G. Endothelin: is it a contributor to
      glaucoma pathophysiology? *J Glaucoma* **11**, 259-70 (2002).

24.   MacCumber, M. W. & D'Anna, S. A. Endothelin receptor-binding subtypes in the
      human retina and choroid. *Arch Ophthalmol* **112**, 1231-5 (1994).

25.   Inoue A, Yanagisawa M, Kimura S, et al. The human endothelin family: three
      structurally and pharmacologically distinct isopeptides predicted by three separate
      genes. *Proc Natl Acad Sci U S A* **86**, 2863-7 (1989).

26.   Kimura S, Kasuya Y, Sawamura T, et al. Structure-activity relationships of
      endothelin: importance of the C-terminal moiety. *Biochem Biophys Res Commun*
      156, 1182-6 (1988).

27.   Itoh Y, Yanagisawa M, Ohkubo S, et al. Cloning and sequence analysis of cDNA
      encoding the precursor of a human endothelium-derived vasoconstrictor peptide,

endothelin: identity of human and porcine endothelin. *FEBS Lett* **231**, 440-4 (1988).

28.   Denault JB, Claing A, D'Orleans-Juste P, et al. Processing of proendothelin-1 by human furin convertase. *FEBS Lett* **362**, 276-80 (1995).

29.   Kido, T., Sawamura, T. & Masaki, T. The processing pathway of endothelin-1 production. *J Cardiovasc Pharmacol* **31 Suppl 1**, S13-5 (1998).

30.   Xu D, Emoto N, Giaid A, et al. ECE-1: a membrane-bound metalloprotease that catalyzes the proteolytic activation of big endothelin-1. *Cell* **78**, 473-85 (1994).

31.   Sawamura T, Shinmi O, Kishi N, et al. Characterization of phosphoramidon-sensitive metalloproteinases with endothelin-converting enzyme activity in porcine lung membrane. *Biochim Biophys Acta* **1161**, 295-302 (1993).

32.   Turner, A. J. & Murphy, L. J. Molecular pharmacology of endothelin converting enzymes. *Biochem Pharmacol* **51**, 91-102 (1996).

33.   Turner, A. J. Endothelin-converting enzymes and other families of metallo-endopeptidases. *Biochem Soc Trans* **21 (Pt 3)**, 697-701 (1993).

34.   Roques, B. P., Noble, F., Dauge, V., Fournie-Zaluski, M. C. & Beaumont, A. Neutral endopeptidase 24.11: structure, inhibition, and experimental and clinical pharmacology. *Pharmacol Rev* **45**, 87-146 (1993).

35.   Waxman L, Doshi KP, Gaul SL, Wang S, Bednar RA,Stern AM. Identification and characterization of endothelin converting activity from EAHY 926 cells: evidence for the physiologically relevant human enzyme. *Arch Biochem Biophys* **308**, 240-53 (1994).

36. Corder, R., Khan, N. & Barker, S. Studies of endothelin-converting enzyme in bovine endothelial cells and vascular smooth-muscle cells: further characterization of the biosynthetic process. *J Cardiovasc Pharmacol* **31 Suppl 1**, S46-8 (1998).

37. Schmidt M, Kroger B, Jacob E, et al. Molecular characterization of human and bovine endothelin converting enzyme (ECE-1). *FEBS Lett* **356**, 238-43 (1994).

38. Shimada, K., Takahashi, M., Turner, A. J. & Tanzawa, K. Rat endothelin-converting enzyme-1 forms a dimer through Cys412 with a similar catalytic mechanism and a distinct substrate binding mechanism compared with neutral endopeptidase-24.11. *Biochem J* **315 (Pt 3)**, 863-7 (1996).

39. Schweizer A, Valdenaire O, Nelbock P, et al. Human endothelin-converting enzyme (ECE-1): three isoforms with distinct subcellular localizations. *Biochem J* **328 (Pt 3)**, 871-7 (1997).

40. Valdenaire, O., Rohrbacher, E. & Mattei, M. G. Organization of the gene encoding the human endothelin-converting enzyme (ECE-1). *J Biol Chem* **270**, 29794-8 (1995).

41. Turner, A. J., Barnes, K., Schweizer, A. & Valdenaire, O. Isoforms of endothelin-converting enzyme: why and where? *Trends Pharmacol Sci* **19**, 483-6 (1998).

42. Jamieson, J. D. & Palade, G. E. Intracellular transport of secretory proteins in the pancreatic exocrine cell. II. Transport to condensing vacuoles and zymogen granules. *J Cell Biol* **34**, 597-615 (1967).

43. Palade, G. Intracellular aspects of the process of protein synthesis. *Science* **189**, 347-58 (1975).

44. Burgess, T. L. & Kelly, R. B. Constitutive and regulated secretion of proteins. *Annu Rev Cell Biol* **3**, 243-93 (1987).

45. Russell, F. D. & Davenport, A. P. Secretory pathways in endothelin synthesis. *Br J Pharmacol* **126**, 391-8 (1999).

46. Nakamura, S., Naruse, M., Naruse, K., Demura, H. & Uemura, H. Immunocytochemical localization of endothelin in cultured bovine endothelial cells. *Histochemistry* **94**, 475-7 (1990).

47. Kitazumi, K., Mio, M. & Tasaka, K. Involvement of the microtubular system in the endothelin-1 secretion from porcine aortic endothelial cells. *Biochem Pharmacol* **42**, 1079-85 (1991).

48. Russell, F. D., Skepper, J. N. & Davenport, A. P. Evidence using immunoelectron microscopy for regulated and constitutive pathways in the transport and release of endothelin. *J Cardiovasc Pharmacol* **31**, 424-30 (1998).

49. Harrison, V. J., Corder, R., Anggard, E. E. & Vane, J. R. Evidence for vesicles that transport endothelin-1 in bovine aortic endothelial cells. *J Cardiovasc Pharmacol* **22 Suppl 8**, S57-60 (1993).

50. Weibel, E. R. & Palade, G. E. New cytoplasmic components in arterial endothelia. *J. Cell Biol.* **23**, 101-112 (1964).

51. van Mourik, J. A., Romani de Wit, T. & Voorberg, J. Biogenesis and exocytosis of Weibel-Palade bodies. *Histochem Cell Biol* **117**, 113-22 (2002).

52. Wagner, D. D., Olmsted, J. B. & Marder, V. J. Immunolocalization of von Willebrand protein in Weibel-Palade bodies of human endothelial cells. *J Cell Biol* **95**, 355-60 (1982).

53. McEver, R. P., Beckstead, J. H., Moore, K. L., Marshall-Carlson, L. & Bainton, D. F. GMP-140, a platelet alpha-granule membrane protein, is also synthesized by vascular endothelial cells and is localized in Weibel-Palade bodies. *J Clin Invest* **84**, 92-9 (1989).

54. Ozaka, T., Doi, Y., Kayashima, K. & Fujimoto, S. Weibel-Palade bodies as a storage site of calcitonin gene-related peptide and endothelin-1 in blood vessels of the rat carotid body. *Anat Rec* **247**, 388-94 (1997).

55. Russell, F. D., Skepper, J. N. & Davenport, A. P. Human endothelial cell storage granules: a novel intracellular site for isoforms of the endothelin-converting enzyme. *Circ Res* **83**, 314-21 (1998).

56. Sakamoto, Y., Doi, Y., Ohsato, K. & Fujimoto, S. Immunoelectron microscopy on the localization of endothelin in the umbilical vein of perinatal rabbits. *Anat Rec* **237**, 482-8 (1993).

57. Vischer, U. M. & Wagner, D. D. CD63 is a component of Weibel-Palade bodies of human endothelial cells. *Blood* **82**, 1184-91 (1993).

58. Datta, Y. H., Youssoufian, H., Marks, P. W. & Ewenstein, B. M. Targeting of a heterologous protein to a regulated secretion pathway in cultured endothelial cells. *Blood* **94**, 2696-703 (1999).

59. Schnyder-Candrian, S., Borsig, L., Moser, R. & Berger, E. G. Localization of alpha 1,3-fucosyltransferase VI in Weibel-Palade bodies of human endothelial cells. *Proc Natl Acad Sci U S A* **97**, 8369-74 (2000).

60. Denis, C. V., Andre, P., Saffaripour, S. & Wagner, D. D. Defect in regulated secretion of P-selectin affects leukocyte recruitment in von Willebrand factor-deficient mice. *Proc Natl Acad Sci U S A* **98**, 4072-7 (2001).

61. Gebrane-Younes, J., Drouet, L., Caen, J. P. & Orcel, L. Heterogeneous distribution of Weibel-Palade bodies and von Willebrand factor along the porcine vascular tree. *Am J Pathol* **139**, 1471-84 (1991).

62. Hop, C. et al. Assembly of multimeric von Willebrand factor directs sorting of P-selectin. *Arterioscler Thromb Vasc Biol* **20**, 1763-8 (2000).

63. Masaki, T. The discovery, the present state, and the future prospects of endothelin. *J Cardiovasc Pharmacol* **13 Suppl 5**, S1-4; discussion S18 (1989).

64. Wagner OF, Christ G, Wojta J, et al. Polar secretion of endothelin-1 by cultured endothelial cells. *J Biol Chem* **267**, 16066-8 (1992).

65. Yoshimoto, S., Ishizaki, Y., Sasaki, T. & Murota, S. Effect of carbon dioxide and oxygen on endothelin production by cultured porcine cerebral endothelial cells. *Stroke* **22**, 378-83 (1991).

66. Pohl, U. & Busse, R. Differential vascular sensitivity to luminally and adventitially applied endothelin-1. *J Cardiovasc Pharmacol* **13 Suppl 5**, S188-90 (1989).

67.   Hall, A. G proteins and small GTPases: distant relatives keep in touch. *Science* **280**, 2074-5 (1998).

68.   Wojciak-Stothard, B., Potempa, S., Eichholtz, T. & Ridley, A. J. Rho and Rac but not Cdc42 regulate endothelial cell permeability. *J Cell Sci* **114**, 1343-55 (2001).

69.   Eto M, Barandier C, Rathgeb L, et al. Thrombin suppresses endothelial nitric oxide synthase and upregulates endothelin-converting enzyme-1 expression by distinct pathways: role of Rho/ROCK and mitogen-activated protein kinase. *Circ Res* **89**, 583-90 (2001).

70.   Kurihara H, Yoshizumi M, Sugiyama T, et al. Transforming growth factor-beta stimulates the expression of endothelin mRNA by vascular endothelial cells. *Biochem Biophys Res Commun* **159**, 1435-40 (1989).

71.   Yoshizumi M, Kurihara H, Morita T, et al. Interleukin 1 increases the production of endothelin-1 by cultured endothelial cells. *Biochem Biophys Res Commun* **166**, 324-9 (1990).

72.   Marsden, P. A. & Brenner, B. M. Nitric oxide and endothelins: novel autocrine/paracrine regulators of the circulation. *Semin Nephrol* **11**, 169-85 (1991).

73.   Prasanna, G., Dibas, A., Tao, W., White, K. & Yorio, T. Regulation of endothelin-1 in human non-pigmented ciliary epithelial cells by tumor necrosis factor-alpha. *Exp Eye Res* **66**, 9-18 (1998).

74.   Woods M, Mitchell JA, Wood EG, et al. Endothelin-1 is induced by cytokines in human vascular smooth muscle cells: evidence for intracellular endothelin-converting enzyme. *Mol Pharmacol* **55**, 902-9 (1999).

75.   Kitazumi, K. & Tasaka, K. The role of c-Jun protein in thrombin-stimulated expression of preproendothelin-1 mRNA in porcine aortic endothelial cells. *Biochem Pharmacol* **46**, 455-64 (1993).

76.   Kitazumi, K. & Tasaka, K. Thrombin-stimulated phosphorylation of myosin light chain and its possible involvement in endothelin-1 secretion from porcine aortic endothelial cells. *Biochem Pharmacol* **43**, 1701-9 (1992).

77.   Kohno M, Yasunari K, Yokokawa K, Murakawa K, Horio T,Takeda T. Inhibition by atrial and brain natriuretic peptides of endothelin-1 secretion after stimulation with angiotensin II and thrombin of cultured human endothelial cells. *J Clin Invest* **87**, 1999-2004 (1991).

78.   Saijonmaa, O., Ristimaki, A. & Fyhrquist, F. Atrial natriuretic peptide, nitroglycerine, and nitroprusside reduce basal and stimulated endothelin production from cultured endothelial cells. *Biochem Biophys Res Commun* **173**, 514-20 (1990).

79.   Wiley, K. E. & Davenport, A. P. Nitric oxide-mediated modulation of the endothelin-1 signalling pathway in the human cardiovascular system. *Br J Pharmacol* **132**, 213-20 (2001).

80. Imai, T., Hirata, Y. & Marumo, F. Heparin inhibits endothelin-1 and proto-oncogene c-fos gene expression in cultured bovine endothelial cells. *J Cardiovasc Pharmacol* **22 Suppl 8**, S49-52 (1993).

81. Ikegawa, R., Matsumura, Y., Tsukahara, Y., Takaoka, M. & Morimoto, S. Phosphoramidon, a metalloproteinase inhibitor, suppresses the secretion of endothelin-1 from cultured endothelial cells by inhibiting a big endothelin-1 converting enzyme. *Biochem Biophys Res Commun* **171**, 669-75 (1990).

82. de Leeuw, H. P., Wijers-Koster, P. M., van Mourik, J. A. & Voorberg, J. Small GTP-binding protein RalA associates with Weibel-Palade bodies in endothelial cells. *Thromb Haemost* **82**, 1177-81 (1999).

83. de Leeuw HP, Fernandez-Borja M, Reits EA, et al. Small GTP-binding protein Ral modulates regulated exocytosis of von Willebrand factor by endothelial cells. *Arterioscler Thromb Vasc Biol* **21**, 899-904 (2001).

84. Sakurai, T., Yanagisawa, M. & Masaki, T. Molecular characterization of endothelin receptors. *Trends Pharmacol Sci* **13**, 103-8 (1992).

85. Marsault, R., Feolde, E. & Frelin, C. Receptor externalization determines sustained contractile responses to endothelin-1 in the rat aorta. *Am J Physiol* **264**, C687-93 (1993).

86. Yanagisawa, M. & Masaki, T. Endothelin, a novel endothelium-derived peptide. Pharmacological activities, regulation and possible roles in cardiovascular control. *Biochem Pharmacol* **38**, 1877-83 (1989).

87.   Berthiaume, N., Yanagisawa, M., Labonte, J. & D'Orleans-Juste, P. Heterozygous knock-Out of ET(B) receptors induces BQ-123-sensitive hypertension in the mouse. *Hypertension* **36**, 1002-7 (2000).

88.   Fukuroda T, Fujikawa T, Ozaki S, Ishikawa K, Yano M,Nishikibe M. Clearance of circulating endothelin-1 by ETB receptors in rats. *Biochem Biophys Res Commun* **199**, 1461-5 (1994).

89.   Sokolovsky, M. Endothelin receptor subtypes and their role in transmembrane signaling mechanisms. *Pharmacol Ther* **68**, 435-71 (1995).

90.   Freedman NJ, Liggett SB, Drachman DE, Pei G, Caron MG,Lefkowitz RJ. Phosphorylation and desensitization of the human beta 1-adrenergic receptor. Involvement of G protein-coupled receptor kinases and cAMP-dependent protein kinase. *J Biol Chem* **270**, 17953-61 (1995).

91.   Lohse, M. J. Molecular mechanisms of membrane receptor desensitization. *Biochim Biophys Acta* **1179**, 171-88 (1993).

92.   Freedman NJ, Ament AS, Oppermann M, Stoffel RH, Exum ST,Lefkowitz RJ. Phosphorylation and desensitization of human endothelin A and B receptors. Evidence for G protein-coupled receptor kinase specificity. *J Biol Chem* **272**, 17734-43 (1997).

93.   Pierce, K. L. & Lefkowitz, R. J. Classical and new roles of beta-arrestins in the regulation of G-protein-coupled receptors. *Nat Rev Neurosci* **2**, 727-33 (2001).

94. Schleicher, S., Boekhoff, I., Arriza, J., Lefkowitz, R. J. & Breer, H. A beta-adrenergic receptor kinase-like enzyme is involved in olfactory signal termination. *Proc Natl Acad Sci U S A* **90**, 1420-4 (1993).

95. Roth, N. S., Campbell, P. T., Caron, M. G., Lefkowitz, R. J. & Lohse, M. J. Comparative rates of desensitization of beta-adrenergic receptors by the beta-adrenergic receptor kinase and the cyclic AMP-dependent protein kinase. *Proc Natl Acad Sci U S A* **88**, 6201-4 (1991).

96. Bremnes T, Paasche JD, Mehlum A, Sandberg C, Bremnes B,Attramadal H. Regulation and intracellular trafficking pathways of the endothelin receptors. *J Biol Chem* **275**, 17596-604 (2000).

97. Paasche, J. D., Attramadal, T., Sandberg, C., Johansen, H. K. & Attramadal, H. Mechanisms of endothelin receptor subtype-specific targeting to distinct intracellular trafficking pathways. *J Biol Chem* **276**, 34041-50 (2001).

98. McDonald PH, Chow CW, Miller WE, et al. Beta-arrestin 2: a receptor-regulated MAPK scaffold for the activation of JNK3. *Science* **290**, 1574-7 (2000).

99. Luttrell LM, Ferguson SS, Daaka Y, et al. Beta-arrestin-dependent formation of beta2 adrenergic receptor-Src protein kinase complexes. *Science* **283**, 655-61 (1999).

100. Bhattacharya M, Anborgh PH, Babwah AV, et al. beta-Arrestins regulate a Ral-GDS Ral effector pathway that mediates cytoskeletal reorganization. *Nat Cell Biol* **4**, 547-55 (2002).

101. Lee, H. J., Chun, M. & Kandror, K. V. Tip60 and HDAC7 interact with the endothelin receptor a and may be involved in downstream signaling. *J Biol Chem* **276**, 16597-600 (2001).

102. Cioffi, G. A., Granstam, E. & Alm, A. in *Adler's Physiology of the Eye* (eds. Kaufman, P. L. & Alm, A.) 747-784 (Mosby, St. Louis, MO, 2002).

103. Fujino, T. & Hamasaki, D. I. Effect of intraocular pressure on the electroretinogram. *Arch. Ophthalmol.* **78**, 757 (1967).

104. Leber, T. in *Handbuch der gesamten augenheikunde* (eds. Graefe, A. & Saemisch, T.) (Springer-Verlag, Leipzig, Germany., 1903).

105. Lindemann, B. & Solomon, A. K. Permeability of luminal surface in intertinal mucosal cells. *J. Gen. Physiol.* **45**, 801-810 (1962).

106. Cunha-Vaz, J. The blood-ocular barriers. *Surv Ophthalmol* **23**, 279-96 (1979).

107. Marmor, M. F. in *The Retinal Pigment Epithelium* (eds. Marmor, M. F. & Wolfensberger, T. J.) 3-9 (Oxford University Press, New York, NY, 1998).

108. Wolfensberger, T. J. *The historical discovery of the retinal pigment epithelium* (eds. Marmor, M. F. & Wolfensberger, T. J.) (Oxford University Press, New York, NY, 1998).

109. Marmor, M. F. *Mechanisms of retinal adhesiveness* (eds. Marmor, M. F. & Wolfensberger, T. J.) (Oxford University Press, New York, NY, 1998).

110. Tsukita, S., Furuse, M. & Itoh, M. Multifunctional strands in tight junctions. *Nat Rev Mol Cell Biol* **2**, 285-293 (2001).

111. Nusrat A, Parkos CA, Verkade P, et al. Tight junctions are membrane microdomains. *J Cell Sci* **113 (Pt 10)**, 1771-81 (2000).

112. Balda, M. S., Garrett, M. D. & Matter, K. The ZO-1-associated Y-box factor ZONAB regulates epithelial cell proliferation and cell density. *J Cell Biol* **160**, 423-32 (2003).

113. Campochiaro, P. A. in *The Retinal Pigment Epithelium* (eds. Marmor, M. F. & Wolfensberger, T. J.) 459-477 (Oxford University Press, New York, NY, 1998).

114. Sheedlo, H. J., Li, L., Fan, W. & Turner, J. E. Retinal pigment epithelial cell support of photoreceptor survival in vitro. *In Vitro Cell Dev Biol Anim* **31**, 330-3 (1995).

115. Dunn, K. C., Aotaki-Keen, A. E., Putkey, F. R. & Hjelmeland, L. M. ARPE-19, a human retinal pigment epithelial cell line with differentiated properties. *Exp Eye Res* **62**, 155-69 (1996).

116. Dunn KC, Marmorstein AD, Bonilha VL, Rodriguez-Boulan E, Giordano F,Hjelmeland LM. Use of the ARPE-19 cell line as a model of RPE polarity: basolateral secretion of FGF5. *Invest Ophthalmol Vis Sci* **39**, 2744-9 (1998).

117. Hiscott, P. & Sheridan, C. M. in *The Retinal Pigment Epithelium* (eds. Marmor, M. F. & Wolfensberger, T. J.) 478-491 (Oxford University Press, New York, NY, 1998).

118. Lepple-Wienhues A, Becker M, Stahl F, et al. Endothelin-like immunoreactivity in the aqueous humour and in conditioned medium from cultured ciliary epithelial cells. *Curr Eye Res* **11**, 1041-6 (1992).

119.	Haefliger, I. O., Flammer, J. & Luscher, T. F. Nitric oxide and endothelin-1 are important regulators of human ophthalmic artery. *Invest Ophthalmol Vis Sci* **33**, 2340-3 (1992).

120.	Friedman, Z., Hackett, S. F. & Campochiaro, P. A. Human retinal pigment epithelial cells possess muscarinic receptors coupled to calcium mobilization. *Brain Res* **446**, 11-6 (1988).

121.	Salceda, R. Muscarinic receptors binding in retinal pigment epithelium during rat development. *Neurochem Res* **19**, 1207-10 (1994).

122.	Osborne, N. N., FitzGibbon, F. & Schwartz, G. Muscarinic acetylcholine receptor-mediated phosphoinositide turnover in cultured human retinal pigment epithelium cells. *Vision Res* **31**, 1119-27 (1991).

123.	Feldman, E. L., Randolph, A. E., Johnston, G. C., DelMonte, M. A. & Greene, D. A. Receptor-coupled phosphoinositide hydrolysis in human retinal pigment epithelium. *J Neurochem* **56**, 2094-100 (1991).

124.	Fischer, A. J., McKinnon, L. A., Nathanson, N. M. & Stell, W. K. Identification and localization of muscarinic acetylcholine receptors in the ocular tissues of the chick. *J Comp Neurol* **392**, 273-84 (1998).

125.	Prasanna, G., Dibas, A. I. & Yorio, T. Cholinergic and adrenergic modulation of the Ca2+ response to endothelin-1 in human ciliary muscle cells. *Invest Ophthalmol Vis Sci* **41**, 1142-8 (2000).

126.	Tasaka, K. & Kitazumi, K. The control of endothelin-1 secretion. *Gen Pharmacol* **25**, 1059-69 (1994).

127. Thomas, G. Furin at the cutting edge: from protein traffic to embryogenesis and disease. *Nat Rev Mol Cell Biol* **3**, 753-66 (2002).

CHAPTER 3

Endothelin-1 synthesis and secretion in human retinal pigment epithelial cells

(ARPE-19): differential regulation by cholinergics and TNF-α.

*Santosh Narayan, Ganesh Prasanna, Raghu R. Krishnamoorthy, Xinyu Zhang and
Thomas Yorio.*

Department of Pharmacology and Neuroscience, University of North Texas Health
Science Center, Fort Worth, Texas 76107, U.S.A.

Section code: PH

Running title: RPE and endothelin-1 secretion.

Total word count: 5098 (including abstract, introduction, methods, results, discussion and
acknowledgements)

Number of figures and tables: 9 figures and 2 tables.

Corresponding author:

Thomas Yorio, Ph.D.
Professor and Dean
Department of Pharmacology and Neuroscience
University of North Texas Health Science Center (UNTHSC)
3500 Camp Bowie Blvd,
Fort Worth, Texas 76107.

ABSTRACT

Purpose: Endothelin-1 (ET-1) can produce nerve damage analogous to that seen in optic neuropathies, like glaucoma. The precise source of endothelin in the posterior segment of the eye remains unclear. Presently we report that the retinal pigment epithelium (RPE), which helps maintain the outer blood retinal barrier, is a local source for ET-1 and that the amount of ET-1 secreted by the RPE may be differentially regulated by cholinergics and the cytokine TNF-α.

Methods: Human retinal pigment epithelial cells (ARPE-19) were cultured either to a mature state (mature RPE or mRPE) for four weeks with well-defined tight junctions or as a young culture of RPE (young RPE or yRPE) for four days with incompletely formed tight junctions. ET-1 like immunoreactivity was determined by immunocytochemistry and secreted ET-1 was quantified by radioimmunoassay in both cell types. Cells were stimulated with a cholinergic agonist, carbachol or with the cytokine, TNF-α, for specified time points. The expression of muscarinic receptor subtypes M_1 and M_3 and the peripheral membrane protein ZO-1, were analyzed by immunoblotting and immunocytochemistry respectively. Expression of preproendothelin-1 (ppET-1) mRNA following different stimuli at specified time points was determined by real-time RT-PCR. Carbachol mediated elevation in intracellular calcium ($[Ca^{2+}]_i$) was also measured in the presence or absence of a selective muscarinic receptor antagonist.

Results: Constitutive synthesis and secretion of ET-1 was greater in mRPE compared to yRPE. TNF-α caused a significant increase in ppET-1 mRNA levels and ET-1 secretion in both phenotypes. The disruption and subsequent breakdown of the tight junction barrier was evident in either phenotype following treatments with TNF-α. There was a concentration dependent rise in [Ca^{2+}]$_i$ in both y- and mRPE in response to carbachol. Carbachol at 1 μM significantly increased ET-1 secretion, a response observed in yRPE but not in mRPE cells. This effect may be mediated primarily by the M$_3$ receptor subtype and is phospholipase C (PLC) dependent.

Conclusions: Regulation of ET-1 release in human retinal pigment epithelial cells (ARPE-19) was differentially regulated by TNF-α and carbachol and was dependent on the age of the culture. RPE may be a source for ET-1 in the retina and its increased release may become more important during breakdown of the blood retinal barrier, as seen following TNF-α treatment.

INTRODUCTION

Endothelins (ET) are 21 amino acid potent vasoactive peptides, processed and secreted locally in the eye,[1-4] with immunoreactive ET-1 and ET-3 expressed most notably in the iris, choroid, retina, optic nerve head, ciliary body, lens and the corneal endothelium.[1, 3-5] ET-1 is also present in aqueous and vitreous humors.[6,7] Within in the retina, the retinal pigment epithelium (RPE), photoreceptor inner segments, the innerplexiform layer, the retinal ganglion cells and retinal pericytes were also shown to be immunoreactive for ET-1 mRNA and mature ET-1 protein.[3, 5, 8-10] Our laboratory has demonstrated that non-pigmented ciliary epithelium can serve as a source of ET-1 in the anterior chamber and that cholinergics, TNF-α and glucocorticoids may regulate its secretion.[4,11] The ciliary pigment and non-pigmented epithelium (NPE) together constitute the blood aqueous barrier in the anterior segment that is contiguous with the outer blood retinal barrier formed by the RPE at the ora serrata. The ciliary epithelium, primarily the NPE and the RPE secrete a multitude of growth factor-like substances and thus act as source cells for peptides within the immune-privileged environment of the eye.[12, 13] Based on these reports and similarities between the NPE and the RPE in regulating fluid transport and acting as secretory cells within their respective local environments, we hypothesized that RPE can act as a source for ET-1.

Our primary intent was to provide a quantitative description of both the mRNA and protein levels of ET-1 in a cell culture model of human RPE. Additionally, we have quantitatively analyzed both constitutive and regulated secretory pathways for ET-1 in these cells that emphasizes the temporal aspects of ET-1 synthesis and secretion in the

RPE. The rationale for considering the actions of cholinergics on RPE stems from observations that the uvea including the choroid is parasympathetically innervated by varicosities arising postganglionically from the pterygopalatine and ciliary ganglions.[14] The dense plexus of cholinergic innervation at the choriocapillaries just beneath the RPE is thought to act post-synaptically on choroidal smooth muscles as well as the RPE.[15] Additionally, both immunofluorescence and binding studies have shown that mammalian and avian RPE express abundant muscarinic receptors throughout development and adult stages, similar to that seen in the brain.[15-19]

The physiological and pathophysiological implications of endothelins at specific regions in the eye, including the RPE are not well understood. ET-1 along with ET-3 and nitric oxide (NO) may help regulate optic nerve head, retinal and choriodal blood flow.[20-23] Higher levels of ET-1 have been implicated in severe cardiovascular and developmental dysfunctions[24] and more recently in the pathophysiology of glaucoma.[25] Exogenous ET-1 administered at the retrobulbar region of the optic nerve results in a neuropathy in a manner similar to glaucoma,[26] and intravitreally injected ET-1 can significantly alter the rate of membrane-bound organelles associated with fast axonal transport in the optic nerve.[27] Presently, we have established that the retinal pigment epithelium (RPE) can act as a local source for ET-1.

The RPE, like most epithelia, develop apical tight junctions and polarize with distinct apical and basolateral domains.[28] The development of the outer blood retinal barrier is a gradual, multi-step process that parallels changes in expression and recruitment of proteins involved in formation of the tight junction complex with concomitant decrease in paracellular permeability, akin to most epithelia including the

RPE.[28-32] Sorting and secretion of proteins in epithelial cells are critically dependent on cell polarity.[33, 34] We have, therefore, used two phenotypes of RPE to delineate differences in ET-1 secretion that may be dependent on the polarity and maturity of the epithelium. We report that secretion of ET-1 may be differentially regulated (muscarinic or TNF-α mediated stimulation) in a cell culture system of polarized or mature RPE (mRPE) and non-polarized or young RPE (yRPE).

MATERIAL AND METHODS

Antibodies

The rabbit anti-muscarinic receptor M1 (epitope corresponding to part of the i3 loop-residues 231-350) and goat anti-M3 subtypes (epitope corresponding to the C-terminal region) were purchased from SantaCruz, La Jolla, CA. Rat heart lysate and the blocking peptide purchased from SantaCruz were used as controls for M1 and M3 receptor detection respectively. Mouse anti-ZO-1 was purchased from Zymed Laboratories, San Francisco, CA. Rabbit anti-endothelin-1 (anti-ET-1) was purchased from Bachem/ Peninsula laboratories, Belmont, CA. The same antibody was used in radioimmunoassay measurements (secreted ET-1) and immunofluorescence experiments (intracellular ET-1). Rabbit IgG and mouse IgG were purchased from Vector laboratories, Burlingame, CA. Secondary antibodies including donkey anti-rabbit IgG, donkey anti-mouse IgG and bovine anti-goat IgG conjugated to HRP were purchased from Amersham Biosciences, Piscataway, NJ. Fluorescent probes including goat anti-rabbit Alexa 488 and goat anti-mouse Alexa 594 were purchased from Molecular Probes, Eugene, OR.

Cell culture

Human retinal pigment epithelial cells (ARPE-19), a spontaneously transformed cell line, was purchased from American Type Culture Collection (ATCC, VA). ARPE-19 cells (passage #s: 20-23) were maintained at 37 °C and 5% CO_2 in a 1:1 mixture of Dulbecco's modified Eagle's medium (DMEM) and Ham's F-12 medium (Invitrogen, Carlsbad, CA) supplemented with 10% fetal bovine serum (Hyclone, Logan, UT), 2mM L-glutamine, 23mM $NaHCO_3$ and penicillin and streptomycin (Invitrogen, Carlsbad, CA). The spontaneously arising human retinal pigment epithelial cells (ARPE-19), characterized by Dunn et al.[35] displays the typical polarized epithelial morphology when grown according to conditions described by them. Additionally, mature polarized ARPE-19 cells that were maintained in culture for 3-4 weeks had reduced paracellular permeability and higher transepithelial resistance (TER) compared to cultures that were grown for 1 week.[35] We followed similar culture conditions that were described by Dunn et al. to obtain mature RPE cells. Cellular morphology for both 'young' (3-4 days in culture) and mature phenotypes was similar to those shown by Dunn et al. Cells were seeded at 1.4×10^5 cells/ well (6 well plate) or 4×10^5 cells/ 100mm dish and maintained in culture according to Dunn et al.[35, 36] ARPE-19 cells were grown either for 4-5 weeks (mature RPE or mRPE) with well-defined tight junctions or for 3-4 days with incompletely formed tight junctions (young RPE or yRPE).

Treatments

ARPE-19 cells were subjected to different treatments in serum free DMEM-F12 medium for various time periods as specified in each experiment. The agonists used in this study were carbachol (Sigma-Aldrich, St.Louis, MO) and tumor necrosis factor-α (TNF-α)

(PeproTech, NJ). The antagonists used were pirenzepine, 4-DAMP (both from Sigma-Aldrich, St.Louis, MO), and U73122 (Biomol, Plymouth Meeting, PA). In treatments that included an antagonist or inhibitor, cells were pretreated for 20-30 minutes prior to treating with the agonist. Each treatment condition was performed at least 6 times in most experiments.

ET-1 extraction and measurement by radioimmunoassay

ARPE-19 cells were grown to either young (3-4 days in culture, yRPE) or mature states (4 weeks in culture, mRPE) in 6-well culture plates (35mm diameter/ well, ~ 1.4 x 10^5 cells/ well) in 1:1 DMEM + Ham's F12 culture medium containing 10% FBS. On the day of treatments, cells were rinsed three times with serum-free 1:1 DMEM + Ham's F12 culture media (SF-DMEM/ F12) and treated with 1 ml SF-DMEM/ F12 containing either carbachol (CCh: 1,10,100μM) or TNF-α (10 nM), a concentration previously shown to stimulate ET-1 synthesis and secretion in human non-pigmented epithelial cells.[4] Treatment incubations were for 24 hours in most of the experiments or during a time course (1, 4, 8, 16, 24hr). The extraction protocol for ET-1 was performed as previously described by Prasanna et al.[4] Efficiency of ET-1 recovery was 75 ± 3 % (n = 3). Measurement of immunoreactive ET-1 (ir-ET-1) was according to manufacturer's instructions in a commercially available RIA kit for ET-1 (Peninsula Laboratories, Belmont, CA).[4]

Intracellular Ca^{2+} ([Ca^{2+}]$_i$) measurement

Intracellular Ca^{2+} in y- and mRPE cells was measured at 37 ^{o}C by the ratiometric technique using fura-2AM (excitation at 340 nm and 380 nm, emission at 500 nm) according to Prasanna et al.[37]

Total RNA extraction, cDNA synthesis and Quantitative Reverse Transcriptase-Polymerase Chain Reaction (RT-PCR)

Total RNA was isolated from y- and mRPE cells, grown in 100mm dishes to subconfluent or confluent states and treated as described above. Using the Trizol reagent (Invitrogen, Carlsbad, CA) total RNA extraction was performed as previously described.[38] Five micrograms of total RNA was used to synthesize the corresponding cDNA, using AMV-reverse transcriptase (Promega, Madison, WI) and random primers (Promega, Madison, WI) in a reaction volume of 50 µl at 42 ^{o}C for 30 minutes. QPCR primers for human preproET-1 (ppET-1) (Fisher-Scientific Genosys, Plano, TX) were designed from the respective cDNA sequence using the GeneJockey II program (Biosoft, Ferguson, MO). The primer sequences for human ppET-1 were designed such that they span different exons. β-actin served as an internal control that accounted for variability in the initial concentration, quality of the total RNA and for the conversion efficiency of the reverse transcription reaction. The primer sequences for ppET-1 and β-actin were as follows: ppET-1-forward/sense 5'-TATCAGCAGTTAGTGAGAGG-3' and reverse/antisense 5'-CGAAGGTCTGTCACCAATGTGC-3' with an expected amplicon/product size of 180 bp; β-actin- forward/sense 5'-TGTGATGGTGGGAATGGGTCAG-3' and reverse/antisense 5'-

TTTGATGTCACGCACGATTTCC-3' with an expected amplicon/product size of 514 bp.

Quantitative PCR (QPCR) was performed as described by Zhang et al.[11]. Product authenticity was confirmed by DNA sequencing followed by a BLAST homology search of the resulting sequences (data not shown). Quantitation of relative ppET-1 transcript levels in ARPE-19 was achieved using the comparative C_T method (as described in the

PE   Biosystems   User   Bulletin   #2:

http://docs.appliedbiosystems.com/pebiodocs/04303859.pdf

QPCR data is presented as the mean percentage to the value of its corresponding untreated control in three separate experiments.

Membrane isolation and immunoblot analysis

Membrane preparation and immunoblot analysis was performed according to Zhang et al.[11]. Either 60 μg/ lane (for M_1 receptor detection), 100 μg/ lane (for M_3 receptor detection) or 50 μg/lane (for ZO-1 detection) of the membrane protein was boiled with the SDS page sample buffer and loaded onto 7.5% SDS-PAGE gels and run at 80V for 2-3 hours. Gel contents were electrophoretically transferred to 0.45 μm pore-sized PVDF membrane (Millipore, Billerica, MA) overnight at 30V and at 4 °C. Blots were probed with the desired primary antibody (in 3% non-fat dry milk): rabbit anti-muscarinic M_1 receptor (final concentration 0.7 ug/ml), goat anti-muscarinic M_3 receptor (2 ug/ml) or mouse anti-ZO-1 (1.5ug/ml) for 1 hour. The rat heart lysate was used as a control for the muscarinic M_1 receptor (SantaCruz, La Jolla, CA) and the M_3 blocking peptide (control antigen) (SantaCruz, La Jolla, CA) for the M_3 receptor detection as per manufacturer's

instructions. Following secondary antibody incubation, blots were rinsed and developed using the enhanced chemiluminescence (ECL) reagents (Amersham Pharmacia Biotech, Piscataway, NJ).

Immunofluorescence microscopy

y- and mRPE cells were grown on 25mm glass coverslips for the desired period and treated as indicated. Cells were fixed in 4% paraformaldehyde in PBS (15mM KCl, 468mM NaCl, 580mM $Na_2HPO_4.7H_2O$ and 27mM KH_2PO_4) for 30 minutes at room temperature followed by permeabilization with 0.2 % Triton-X 100 for 15 minutes. Cells were rinsed in PBS and incubated twice in 50 mM glycine, 15 minutes/ incubation. Each coverslip was carefully inverted (cell-side facing solution) onto 200ul of blocking solution containing 3% BSA + 3% normal goat serum in PBS for 30 minutes. The coverslips were then incubated in rabbit anti-ET-1 (10 µg/ml) for 4 hours at 4 °C followed by incubation in a mixture containing rabbit anti-ET-1 (10 µg/ml) and mouse anti-ZO-1 (10 µg/ml), overnight at 4 °C. The antibody used for intracellular ET-1 detection was same antibody as that used in the ET-1 RIA measurements. Coverslips were rinsed and allowed to incubate in a mixture of secondary antibodies containing donkey anti-mouse alexa 594 conjugated (5 µg/ml) and donkey anti-rabbit alexa 488 conjugated (5 µg/ml) for 1 hour in the dark at room temperature. Nuclei were stained with DAPI (300 nM) (Molecular Probes, Eugene, OR) for 10 minutes. Coverslips were mounted on glass slides using FluorSave (Calbiochem, San Diego, CA) and allowed to dry for 20 minutes in the dark. Cells were viewed with a Nikon Microphot FXA digital fluorescent microscope and images at the red, green and blue wavelengths were acquired

using a CCD-camera, digitally processed using the IPLab (Scanalytics, Fairfax, VA) image analysis software. All images were deconvolved using the IPLab software and transferred to Adobe Photoshop 7.0 (Adobe Systems, San Jose, CA) for further analysis.

Data Analysis

Quantitative data is represented as mean $\pm$ SEM. Statistical comparisons were performed by t-test in most experiments except ET-1 RIA measurements where comparisons between control and multiple treatments were made using ANOVA and SNK test. In $[Ca^{2+}]_i$ measurements, comparisons between baseline, peak and one minute post peak values were made by one way repeated measures ANOVA. Sample size and p values for each experiment are indicated in the figure legends.

RESULTS

In the present study we compared two different phenotypes of the RPE in cell culture. A mature culture (4-5 weeks, mRPE), similar to an intact polarized and differentiated epithelium with few intercellular gaps and a young culture (3-4 days, yRPE) that has an incomplete barrier formed with more intercellular gaps and possible lack of polarization. The two RPE cell phenotypes were tested for their ability to secrete endothelin-1 (ET-1) following a cytokine (TNF-α) or a cholinergic agonist (CCh) treatment.

Secretion and regulation of ET-1 in ARPE-19 cells

Young RPE (yRPE) and mature RPE (mRPE) cells were incubated with either TNF-α (10nM) or carbachol (CCh, 0.01-100 μM), a non-selective muscarinic receptor agonist for 24 hours (Figs. 1A, B). In yRPE cells (Fig. 1A), TNF-α and CCh 1 μM significantly enhanced ir-ET-1 secretion compared with the untreated control. The extent by which

TNF-α potentiated ir-ET-1 secretion was higher than that produced by CCh 1 μM. Interestingly, it was only at the 1 μM concentration that CCh was consistently able to stimulate ET-1 release in yRPE. There are 5 muscarinic receptor subtypes (M_{1-5}) [39-26] of which the M_1, M_3 and M_5 are directly coupled to the G_q-IP_3-Ca^{2+} signaling pathway while the M_2 and M_4 subtypes are coupled to the G_i-cAMP cascade. Activation of the IP_3-Ca^{2+} cascade requires prior activation of the G-protein coupled receptor-mediated transducer phospholipase Cβ (PLCβ).[40, 41] To determine if this was the mechanism responsible for cabachol-mediated ir-ET-1 release, yRPE cells were preincubated with 2 μM U73122, a PLC inhibitor for 20-30 minutes with subsequent stimulation with 1μM CCh. U73122 completely inhibited ET-1 release suggesting that activation of PLC was a critical determinant in CCh mediated ET-1 release (Fig. 1A). Selective muscarinic receptor antagonists were then used to further delineate the receptor subtype(s) that were involved in ET-1 release in yRPE cells. The compounds 4-diphenylacetoxy-N-methylpiperidine methiodide (4-DAMP), a selective M_1/M_3 receptor antagonist (pKi: 9.4 and 9.1 for M_1 and M_3 respectively) and pirenzepine (PZE), an M_1 selective antagonist (pKi: 6.9 for M_1)[42,43] were employed in our study. Both 4-DAMP and PZE were effective in inhibiting CCh induced ET-1 release with an apparent relative order of potency as 4-DAMP> PZE (Fig. 1A). mRPE cells were allowed to grow for 4 weeks to form an intact epithelial barrier (Fig. 5). The basal amounts (untreated controls) of both ppET-1 mRNA (Fig. 8) and secreted ir-ET-1 measured in these cells (mRPE) was higher than yRPE cells after 24 hours (compare scales in Fig. 1A and B). TNF-α continued to potentiate ET-1 secretion in mRPE cells to the same degree as that observed in yRPE (4-5 fold increase over

control). A similar increase in released ET-1 was not observed in mRPE following CCh treatments for 24 hours (Fig. 1B).

M_1 and M_3 muscarinic receptors in ARPE-19

Differences in secretion of ir-ET-1 in mRPE and yRPE cells in response to CCh and TNF-α may be due to differential expression of M_1 and M_3 receptors or differences in the intracellular calcium ($[Ca^{2+}]_i$) trends following muscarinic receptor activation. The primary reason M_1 and M_3 receptor subtypes were considered was because 4-DAMP and PZE were effective in inhibiting CCh mediated ET-1 release in the yRPE (Fig. 1A). Additionally, carbachol mediated phosphoinositide hydrolysis and subsequent rise in intracellular Ca^{2+} in human RPE cells may be predominantly M_3 receptor mediated.[16] Since 4-DAMP has 6-13 fold lower affinity for M_5 compared to M_3 or M_1 receptors[42] and the concentrations we employed in our studies and previous reports on mucarinic receptor expression in RPE [44,15] it was evident that either the M_3 or M_1 or both subtypes were principal targets for carbachol induced ET-1 secretion in yRPE.

Both M_1 and M_3 receptors are expressed in ARPE-19 cells (y-and mRPE) (Fig. 2A and 2B- western blots). The apparent molecular weights of the protein bands (M_1R: 60kD and M_3R: 70kD) were confirmed using appropriate controls (rat heart lysate for M_1R and the blocking peptide for M_3R). Detection of the M_3 receptor subtype in y- and mRPE cells required higher amounts of total protein (100 μg/lane for M_3 detection as opposed to 60 μg/lane for M_1 detection).

Carbachol mediated $[Ca^{2+}]_i$ mobilization in y- and mRPE cells

M_1 and M_3 muscarinic receptors belong to the class of G_q coupled receptors that upon activation mobilize $[Ca^{2+}]_i$ in an IP_3 dependent manner.[45] Receptor mediated increase in $[Ca^{2+}]_i$ can activate several downstream effectors including those involved in regulated exocytosis in both excitable and non-excitable cells.[46] Retinal pigment epithelial cells express muscarinic receptors that mobilize $[Ca^{2+}]_i$ but not cAMP following acetylcholine or carbachol.[15] Since the immunoblot analysis indicated there were differences in the expression of M_1 and M_3 receptors between y- and mRPE cells, it was possible that functional differences between the receptors existed as well. Representative $[Ca^{2+}]_i$ trends in y- and mRPE cells following CCh (1, 10, 100 μM) stimulation are shown in Fig. 3A and 3B respectively and a summary of the results are shown in Tables 1 and 2. There was a concentration dependent increase in the mean $[Ca^{2+}]_i$ mobilized by CCh in both y- and mRPE with characteristic biphasic transients observed in both phenotypes (Fig. 3A and B). Since 1μM CCh was effective in evoking significant release of ET-1 in yRPE cells (Fig. 1A), this concentration was used for all future experiments in these cells. To address the receptor subtypes that were functionally coupled to the CCh response, different concentrations of 4-DAMP (M_1/M_3 selective inhibitor) and pirenzepine (PZE) (M_1 selective inhibitor) were used. 2μM U73122 blocked CCh mediated $[Ca^{2+}]_i$ mobilization (Table 1), consistent with results observed when similar treatments effectively blocked CCh mediated ET-1 secretion in yRPE cells (Fig. 1). Interestingly, PZE at 100 nM failed to inhibit CCh mediated $[Ca^{2+}]_i$ elevation and required a concentration of ≥ 400nM to do so (Table 1). 4-DAMP unlike PZE, continued to inhibit CCh mediated $[Ca^{2+}]_i$ elevation at concentrations similar to those employed in Fig.1A.

To determine if the RIA results were due to functional uncoupling of muscarinic receptors (receptor desensitization and /or internalization) in their ability to mobilize $[Ca^{2+}]_i$, cells were pre-incubated with CCh (1 and 100 μM) for 24 hours followed by CCh (1 and 100 μM) challenge (Table 1). Cells pretreated with CCh 1 μM were able to retain ~ 50% of their response to acute CCh 1 μM as opposed to CCh 100 μM where the response was reduced to ~10% of the initial response without pretreatment. Similar results were observed in mRPE cells (Table 2) in their ability to mobilize $[Ca^{2+}]_i$ following CCh (1, 10, 100 μM) additions before or after pretreatments. A comprehensive study using muscarinic receptor antagonists were not performed in the mRPE cells because CCh failed to evoke any significant increase in ET-1 release in these cells (Fig. 1B). However, 4-DAMP (5 and 10nM) completely inhibited CCh mediated $[Ca^{2+}]_i$ elevation in these cells (data not shown), similar to that observed in yRPE cells suggesting that both phenotypes had similar responses to CCh in their ability to mobilize $[Ca^{2+}]_i$.

Disruption of tight junctions by TNF-α and its influence on intracellular and secreted ET-1

Several recent studies have proposed that tight junction and sub-tight junction domains form clusters of scaffolding proteins that could be important in regulating paracellular transport, cell motility, membrane integrity and recruitment of exocytotic machinery.[47] We hypothesized that the presence of a mature tight junction complex may regulate secretion of ET-1 in mRPE cells. mRPE cells expressed abundant amounts of ZO-1, a peripheral tight junction-associated protein in epithelial cells. Immunoblot and

immunofluorescence analysis was employed to determine the extent of ZO-1 expression in both phenotypes. There was a significant increase in ZO-1 expression in mRPE as opposed to yRPE cells (50 μg/ lane, n =3) with both isoforms of ZO-1 (α+ and α-) (data not shown). Immunofluorescence studies demonstrated that the mRPE cells expressed greater amounts of ZO-1 with well-defined tight junctions compared to yRPE cells (Fig. 4 and 5).

TNF-α caused visible changes in morphology, an increase in intercellular gaps and disruption of tight junctions in both y- and mRPE cells (Fig. 4 and 5). These changes were not observed following CCh treatment. Intracellular ET-1 was detected as punctate stains in both phenotypes. Although there were differences in the intensities of intracellular ET-1 content between cells in the same coverslip, basal intracellular ET-1 in yRPE was visibly higher than in mRPE cells (compare Fig. 4C and 5C). Negative controls including non-immune serum (Fig. 5), no primary and no secondary antibodies (data not shown) confirmed the authenticity of detection.

Time-dependent changes in ZO-1 and ET-1 following TNF-α

To determine if TNF-α mediated changes in mRPE cells were time-dependent, we measured the amount of secreted ir-ET-1 (Fig. 7), immunofluorescent ZO-1 and intracellular ET-1 expression (Fig. 7) at 1, 4, 8, 16 and 24 hours following treatment with TNF-α. Constitutive ppET-1 (preproET-1) mRNA expression in mRPE cells was over 4 fold higher compared to yRPE cells over 24 hours (Fig. 8). This finding was in agreement with differences in constitutive secretion of mature ir-ET-1 over the same time period (Fig. 1A, B). ppET-1 mRNA expression was measured in response to TNF-α or CCh in

70

y- and mRPE cells at indicated time points (Fig. 9). TNF-α significantly increased the amount of secreted ET-1 at the end of 8 hours (Fig. 6) and continued to do so until 16 and 24 hours where the highest amounts of secreted ET-1 was measured. In addition, TNF-α caused visible alteration in cellular morphology and disruption of tight junctions, an effect that was first detected at 8 hours and persisted until 24 hours (Fig. 7). ppET-1 mRNA levels in mRPE cells was significantly elevated by about four fold at the end of the first hour following TNF-α stimulation and gradually decreased to about 1.5 fold of control at the end of 24 hours (Fig. 9B). There was a gradual and delayed increase in ET-1 release during the same time period (Fig. 6). CCh failed to increase ppET-1 transcription in both phenotypes at the end of 24 hours.

DISCUSSION

Several physiological or pathophysiological stimuli can cause the release of endothelin-1 and is considered as regulated secretion of ET-1. Cytokines including TGF-β,[48] IL-1,[49] TNFα,[50,4] and interferon-γ (IFN–γ)[51] can induce both transcription as well as release of ET-1. ET-1 secretion typically results from activation of the constitutive or regulated pathways.[52,53]

Unlike CCh, TNF-α can influence mRNA synthesis and secretion of ET-1 [54] and several studies have reported the ability of TNF-α to cause cytoskeletal changes including breakdown of the tight junction barrier in epithelial cells and RPE.[55-57] TNF-α has been shown to decrease the turnover of occludin, one of the integral proteins of the tight junction complex.[58] In yRPE cells the tight junction complex appears to be premature and the epithelial phenotype to be non-polarized and undifferentiated.[59,31]

Failure to recruit desired proteins at the tight-junction complex and execution of the barrier, fence and signaling functions[47] may alter both constitutive and regulated release (by carbachol and TNF-α) of ET-1 in RPE cells. Constitutive synthesis and secretion of ET-1 was higher in mature RPE cells compared to young RPE cells. However, basal intracellular ET-1 (endogenous ET-1) content appeared to be higher in yRPE compared to mRPE. This suggests that rate of constitutive secretion may be higher in mRPE vs. yRPE. Constitutive and regulated secretion may be influenced by several factors including polarization by plasma membrane asymmetry and/or golgi asymmetry, differential sorting of proteins including membrane receptors and decreased paracellular permeability. The finding that CCh-mediated ET-1 secretion was higher in yRPE (non-polarized) cells as opposed to mRPE (polarized) cells, was consistent with this view. In contrast, TNF-α was able to enhance secretion of ET-1 by 4-5 fold at the end of 24 hours in both phenotypes. This was probably due to TNF-α's ability to not only enhance ET-1 secretion but also significantly increase ppET-1 transcription and disrupt tight junctions in RPE, all of which were time dependent in mRPE cells. CCh, on the contrary, although able to regulate ET-1 secretion in yRPE cells, failed to enhance ppET-1 transcription or cause significant alterations in cell shape and membrane integrity. Interestingly, CCh was able to mobilize $[Ca^{2+}]_i$ to a similar degree in both y- and mRPE, indicating that the cumulative muscarinic receptor mediated $[Ca^{2+}]_i$ trends remained unaltered in either phenotype and that ET-1 release mechanisms may not necessarily be coupled to calcium mobilization alone. This was particularly evident in yRPE where significant ET-1 release only occurred at 1μM concentration of CCh. The inability of lower (<1μM) and higher

(10 and 100μM) concentrations of CCh failing to elicit similar or greater release of ET-1 may have been due to the inability to mobilize required $[Ca^{2+}]_i$ and activate the ET-1 secretory pathway at lower concentrations and/or due to receptor desensitization and internalization at higher concentrations.

Our results suggest that CCh mediated ET-1 release may predominantly involve the M_3 muscarinic receptor subtype. However, we cannot totally exclude the participation of M_1 receptors, because 4-DAMP has similar affinities for M_1 vs. M_3 receptors.[42, 43] Additionally, pirenzepine (PZE) at 100nM was able to inhibit CCh mediated ET-1 release in yRPE cells. Interestingly concentrations of $\geq$ 400nM PZE were required to inhibit 1 μM CCh mediated $[Ca^{2+}]_i$ increase in yRPE cells suggesting that most of this increase was M_3 mediated and that CCh mediated ET-1 release was both M_1 and M_3 dependent. The inability of CCh to increase ET-1 secretion in mRPE may have been due to limited paracellular permeability in mRPE cells in addition to recruitment of the tight junction complex that may effect its actions on M_1 receptors.

In conclusion, these results favor an action of CCh on the regulated release of ET-1 in yRPE cells, whereas the actions of TNF-α reflect a generalized disturbance in cell morphology, disruption of tight junctions and enhanced ppET-1 transcription such that the increased release of ET-1 following TNF-α may occur due to de novo synthesis and release of ET-1. Such actions would be reminiscent of an inflammatory response during breakdown of the blood retinal barrier as seen in proliferative vitreoretinopathy (PVR) and diabetic retinopathy.[12] Our results suggest the RPE may be the source for ET-1 at the posterior pole of the eye. The implications for physiological function of ET-1 under

normal conditions in the RPE are presently unknown. In diseased conditions, a pathologic increase in ET-1 secretion by barrier-compromised RPE may be important in cell migration and proliferation as seen in PVR. Locally secreted ET-1 could act to produce vasoconstriction and affect cellular responses that minimize damage to a compromised blood retinal barrier. Additionally, released ET-1 may mediate vascular homeostasis as a mechanism to balance vasodilator influences however with excessive secretion, ET-1 may promote prolonged vasoconstriction and induce ischemic episodes in the retina. We are presently working on models that will address the role of ET-1 at the outer blood retinal barrier.

ACKNOWLEDGEMENTS

REFERENCES

1. MacCumber MW, Ross CA, Glaser BM,Snyder SH. Endothelin: visualization of mRNAs by in situ hybridization provides evidence for local action. *Proc Natl Acad Sci U S A*. 1989;86:7285-9.

2. MacCumber MW, Jampel HD,Snyder SH. Ocular effects of the endothelins. Abundant peptides in the eye. *Arch Ophthalmol*. 1991;109:705-9.

3. Wollensak G, Schaefer HE,Ihling C. An immunohistochemical study of endothelin-1 in the human eye. *Curr Eye Res*. 1998;17:541-5.

4. Prasanna G, Dibas A, Tao W, White K,Yorio T. Regulation of endothelin-1 in human non-pigmented ciliary epithelial cells by tumor necrosis factor-alpha. *Exp Eye Res*. 1998;66:9-18.

5. Stitt AW, Chakravarthy U, Gardiner TA,Archer DB. Endothelin-like immunoreactivity and receptor binding in the choroid and retina. *Curr Eye Res*. 1996;15:111-7.

6. Lepple-Wienhues A, Becker M, Stahl F, et al. Endothelin-like immunoreactivity in the aqueous humour and in conditioned medium from cultured ciliary epithelial cells. *Curr Eye Res*. 1992;11:1041-6.

7. Kallberg ME, Brooks DE, Garcia-Sanchez GA, Komaromy AM, Szabo NJ,Tian L. Endothelin 1 levels in the aqueous humor of dogs with glaucoma. *J Glaucoma*. 2002;11:105-9.

8. Chakrabarti S, Gan XT, Merry A, Karmazyn M,Sima AA. Augmented retinal endothelin-1, endothelin-3, endothelinA and endothelinB gene expression in chronic diabetes. *Curr Eye Res*. 1998;17:301-7.

9. Ripodas A, de Juan JA, Roldan-Pallares M, et al. Localisation of endothelin-1 mRNA expression and immunoreactivity in the retina and optic nerve from human and porcine eye. Evidence for endothelin-1 expression in astrocytes. *Brain Res*. 2001;912:137-43.

10. Murata M, Nakagawa M,Takahashi S. Selective expression of endothelin 1 mRNA in rat retina. *Ophthalmologica*. 1998;212:331-3.

11. Zhang X, Krishnamoorthy RR, Prasanna G, Narayan S, Clark A,Yorio T. Dexamethasone regulates endothelin-1 and endothelin receptors in human non-pigmented ciliary epithelial (HNPE) cells. *Exp Eye Res*. 2003;76:261-72.

12. Campochiaro PA. Growth factors in the retinal pigment epithelium and retina. Marmor, MF and Wolfensberger, TJ. *The Retinal Pigment Epithelium*. New York, NY: Oxford University Press;1998:459-477.

13. Coca-Prados M, Escribano J,Ortego J. Differential gene expression in the human ciliary epithelium. *Prog Retin Eye Res*. 1999;18:403-29.

14. Ruskell GL. Facial parasympathetic innervation of the choroidal blood vessels in monkeys. *Exp Eye Res*. 1971;12:166-72.

15. Friedman Z, Hackett SF,Campochiaro PA. Human retinal pigment epithelial cells possess muscarinic receptors coupled to calcium mobilization. *Brain Res*. 1988;446:11-6.

16. Feldman EL, Randolph AE, Johnston GC, DelMonte MA,Greene DA. Receptor-coupled phosphoinositide hydrolysis in human retinal pigment epithelium. *J Neurochem*. 1991;56:2094-100.

17. Fischer AJ, McKinnon LA, Nathanson NM,Stell WK. Identification and localization of muscarinic acetylcholine receptors in the ocular tissues of the chick. *J Comp Neurol.* 1998;392:273-84.

18. Osborne NN, FitzGibbon F,Schwartz G. Muscarinic acetylcholine receptor-mediated phosphoinositide turnover in cultured human retinal pigment epithelium cells. *Vision Res.* 1991;31:1119-27.

19. Salceda R. Muscarinic receptors binding in retinal pigment epithelium during rat development. *Neurochem Res.* 1994;19:1207-10.

20. Haefliger IO, Flammer J,Luscher TF. Nitric oxide and endothelin-1 are important regulators of human ophthalmic artery. *Invest Ophthalmol Vis Sci.* 1992;33:2340-3.

21. Polak K, Petternel V, Luksch A, et al. Effect of endothelin and BQ123 on ocular blood flow parameters in healthy subjects. *Invest Ophthalmol Vis Sci.* 2001;42:2949-56.

22. Polak K, Luksch A, Frank B, Jandrasits K, Polska E,Schmetterer L. Regulation of human retinal blood flow by endothelin-1. *Exp Eye Res.* 2003;76:633-40.

23. Kawamura H, Oku H, Li Q, Sakagami K,Puro DG. Endothelin-induced changes in the physiology of retinal pericytes. *Invest Ophthalmol Vis Sci.* 2002;43:882-8.

24. Kedzierski RM,Yanagisawa M. Endothelin system: the double-edged sword in health and disease. *Annu Rev Pharmacol Toxicol.* 2001;41:851-76.

25. Yorio T, Krishnamoorthy R,Prasanna G. Endothelin: is it a contributor to glaucoma pathophysiology? *J Glaucoma.* 2002;11:259-70.

26. Cioffi GA, Orgul S, Onda E, Bacon DR, Van Buskirk EM. An in vivo model of chronic optic nerve ischemia: the dose-dependent effects of endothelin-1 on the optic nerve microvasculature. *Curr Eye Res*. 1995;14:1147-53.

27. Stokely ME, Brady ST, Yorio T. Effects of endothelin-1 on components of anterograde axonal transport in optic nerve. *Invest Ophthalmol Vis Sci*. 2002;43:3223-30.

28. Marmorstein AD. The polarity of the retinal pigment epithelium. *Traffic*. 2001;2:867-72.

29. Ban Y, Rizzolo LJ. Differential regulation of tight junction permeability during development of the retinal pigment epithelium. *Am J Physiol Cell Physiol*. 2000;279:C744-50.

30. Ban Y, Rizzolo LJ. A culture model of development reveals multiple properties of RPE tight junctions. *Mol Vis*. 1997;3:18.

31. Rizzolo LJ. Polarity and the development of the outer blood-retinal barrier. *Histol Histopathol*. 1997;12:1057-67.

32. Williams CD, Rizzolo LJ. Remodeling of junctional complexes during the development of the outer blood-retinal barrier. *Anat Rec*. 1997;249:380-8.

33. Mostov K, Su T, Ter Beest M. Polarized epithelial membrane traffic: conservation and plasticity. *Nat Cell Biol*. 2003;5:287-93.

34. Kreitzer G, Schmoranzer J, Low SH, et al. Three-dimensional analysis of post-Golgi carrier exocytosis in epithelial cells. *Nat Cell Biol*. 2003;5:126-36.

35. Dunn KC, Aotaki-Keen AE, Putkey FR,Hjelmeland LM. ARPE-19, a human retinal pigment epithelial cell line with differentiated properties. *Exp Eye Res*. 1996;62:155-69.

36. Dunn KC, Marmorstein AD, Bonilha VL, Rodriguez-Boulan E, Giordano F,Hjelmeland LM. Use of the ARPE-19 cell line as a model of RPE polarity: basolateral secretion of FGF5. *Invest Ophthalmol Vis Sci*. 1998;39:2744-9.

37. Prasanna G, Dibas AI,Yorio T. Cholinergic and adrenergic modulation of the Ca2+ response to endothelin-1 in human ciliary muscle cells. *Invest Ophthalmol Vis Sci*. 2000;41:1142-8.

38. Krishnamoorthy R, Agarwal N,Chaitin MH. Upregulation of CD44 expression in the retina during the rds degeneration. *Brain Res Mol Brain Res*. 2000;77:125-30.

39. Bonner TI, Buckley NJ, Young AC,Brann MR. Identification of a family of muscarinic acetylcholine receptor genes. *Science*. 1987;237:527-32.

40. Abdel-Latif AA. Acetylcholine and the incorporation of (P32) phosphate into phospholipids and phosphoproteins of nerve endings of developing rat brain. *Nature*. 1966;211:530-1.

41. Fain JN,Berridge MJ. Relationship between 5-hydroxytryptamine activation of phosphatidylinositol hydrolysis and calcium-ion entry in Calliphora salivary glands. *Biochem Soc Trans*. 1978;6:1038-9.

42. Eglen RM, Choppin A,Watson N. Therapeutic opportunities from muscarinic receptor research. *Trends Pharmacol Sci*. 2001;22:409-14.

43. http://PDSP.cwru.edu/PDSP.asp. Pharmacokinetics unbound. Science NetWatch. *Science*. 2000;287:543.

44. Crook RB, Song MK, Tong LP, Yabu JM, Polansky JR, Lui GM. Stimulation of inositol phosphate formation in cultured human retinal pigment epithelium. *Brain Res*. 1992;583:23-30.

45. Neher E, Marty A, Fukuda K, Kubo T, Numa S. Intracellular calcium release mediated by two muscarinic receptor subtypes. *FEBS Lett*. 1988;240:88-94.

46. Penner R, Neher E. The role of calcium in stimulus-secretion coupling in excitable and non-excitable cells. *J Exp Biol*. 1988;139:329-45.

47. Tsukita S, Furuse M, Itoh M. Multifunctional strands in tight junctions. *Nat Rev Mol Cell Biol*. 2001;2:285-293.

48. Kurihara H, Yoshizumi M, Sugiyama T, et al. Transforming growth factor-beta stimulates the expression of endothelin mRNA by vascular endothelial cells. *Biochem Biophys Res Commun*. 1989;159:1435-40.

49. Yoshizumi M, Kurihara H, Morita T, et al. Interleukin 1 increases the production of endothelin-1 by cultured endothelial cells. *Biochem Biophys Res Commun*. 1990;166:324-9.

50. Marsden PA, Brenner BM. Transcriptional regulation of the endothelin-1 gene by TNF-alpha. *Am J Physiol*. 1992;262:C854-61.

51. Woods M, Mitchell JA, Wood EG, et al. Endothelin-1 is induced by cytokines in human vascular smooth muscle cells: evidence for intracellular endothelin-converting enzyme. *Mol Pharmacol*. 1999;55:902-9.

52. Kido T, Sawamura T, Masaki T. The processing pathway of endothelin-1 production. *J Cardiovasc Pharmacol*. 1998;31 Suppl 1:S13-5.

53. Russell FD, Davenport AP. Secretory pathways in endothelin synthesis. *Br J Pharmacol*. 1999;126:391-8.

54. Maemura K, Kurihara H, Morita T, Oh-hashi Y, Yazaki Y. Production of endothelin-1 in vascular endothelial cells is regulated by factors associated with vascular injury. *Gerontology*. 1992;38 Suppl 1:29-35.

55. Walsh SV, Hopkins AM, Nusrat A. Modulation of tight junction structure and function by cytokines. *Adv Drug Deliv Rev*. 2000;41:303-13.

56. Zech JC, Pouvreau I, Cotinet A, Goureau O, Le Varlet B, de Kozak Y. Effect of cytokines and nitric oxide on tight junctions in cultured rat retinal pigment epithelium. *Invest Ophthalmol Vis Sci*. 1998;39:1600-8.

57. Mullin JM, Snock KV. Effect of tumor necrosis factor on epithelial tight junctions and transepithelial permeability. *Cancer Res*. 1990;50:2172-6.

58. Mankertz J, Tavalali S, Schmitz H, et al. Expression from the human occludin promoter is affected by tumor necrosis factor alpha and interferon gamma. *J Cell Sci*. 2000;113 (Pt 11):2085-90.

59. Yeaman C, Grindstaff KK, Nelson WJ. New perspectives on mechanisms involved in generating epithelial cell polarity. *Physiol Rev*. 1999;79:73-98.

Figure legends-

Fig. 1. <u>ET-1 RIA in young RPE (yRPE) (ARPE-19 cells grown for 4 days) and mature RPE (mRPE) (ARPE-19 cells grown for 4 weeks).</u> Cells were treated with various agonists and/or antagonists for 24 hours in serum-free DMEM/F-12 medium. Immunoreactive ET-1 (ir-ET-1) released in the media was extracted and measured by RIA (refer Methods). **(A)**. In yRPE cells, TNF-α and CCh 1 μM were able to significantly increase ir-ET-1 secretion vs. control. U73122, 4-DAMP and PZE were able to inhibit CCh mediated ir-ET-1 secretion. **(B)**. In mRPE cells, TNF-α significantly increased ir-ET-1 secretion vs. control. Note the difference in the X-axis values. mRPE cells produced higher amounts of ir-ET-1 (compare controls in A and B). Data is represented as mean $\pm$ SEM. Statistical comparisons were performed using ANOVA and SNK test. * denotes significance vs. control (p<0.05) (n= atleast 6/ treatment).

Fig. 2. <u>Immunoblot analysis in yRPE and mRPE cells.</u> **(A)** 60 μg of total membrane fraction was loaded per lane. Blots probed with the rabbit anti-M_1 receptor. Rat heart lysate (30 μg) was used as control to verify apparent size (~60 kD) and expression of the M_1 receptor **(B)** 100 μg of total membrane fraction/ lane was required to detect M_3 receptor expression in both phenotypes. The goat anti-M_3 receptor antibody was used for detection. The apparent size of the M_3 receptor was ~70 kD. Control antigen (lower blots in **B**) pre incubated with the M_3 antibody for 1h at room temperature was used as the negative control. (n= 4 per condition)

Fig. 3. <u>Intracellular [Ca^{2+}]$_i$ measurements in yRPE and mRPE cells</u> **(A)** Representative [Ca^{2+}]$_i$ trends in response to CCh (1,10,100 μM) in yRPE. **(B)** Representative [Ca^{2+}]$_i$

trends in response to CCh (1,10,100 μM) in mRPE cells. In both phenotypes there was a concentration dependent rise in CCh mediated mean $[Ca^{2+}]_i$ mobilization (see tables 1 and 2) as well as an increase in biphasic transients.

Fig. 4. <u>Indirect immunofluorescence microscopy in yRPE cells.</u> Cells were treated with TNF-α or CCh for 24 hours and expression of ZO-1 and ET-1 were analyzed by light microscopy. A-D: control/ untreated, E-H: TNF-α (10 nM) treated and I-L: CCh (1 μM) treated cells. Fixed cells were probed with mouse anti ZO-1. (B-F) and rabbit anti ET-1. (C-K) followed by incubation with goat anti-mouse-alexa 594 antibody and goat anti-rabbit-alexa 488 antibody. Nuclei were stained with DAPI (blue fluorescence) and merged images are shown in D, H and L. A, E and I represent the differential interference contrast (DIC) images. TNF-α but not CCh caused visible changes in morphology and disruption of tight junctions (ZO-1 staining). Atleast 5 different fields were viewed per coverslip and a total of 3 coverslips per condition (n =4) were tested under similar conditions. (scale = 10μm)

Fig. 5. <u>Indirect immunofluorescence microscopy in mRPE cells.</u> Cells were treated with TNF-α or CCh for 24 hours and expression of ZO-1 and ET-1 were analyzed by light microscopy. A-D: control/ untreated, E-H: TNF-α (10 nM) treated and I-L: CCh (1 μM) treated cells. Fixed cells were probed with mouse anti ZO-1. (B-F) and rabbit anti ET-1. (C-K) followed by incubation with donkey anti-mouse-alexa 594 antibody (5ug/ml, red fluorescence) and donkey anti-rabbit-alexa 488 antibody (5ug/ml, green fluorescence). Nuclei were stained with DAPI (300nM, blue fluorescence) and merged images are shown in D, H and L. A, E and I represent the differential interference contrast (DIC)

images. TNF-α but not CCh caused visible changes in morphology and disruption of tight junctions (ZO-1 staining). Atleast 5 different fields were viewed per coverslip and a total of 3 coverslips per condition (n =3) were tested under similar conditions. Negative controls using non-immune IgG at concentrations identical for anti ZO-1 and anti ET-1 showed little of no staining. (scale = 10μm).

Fig. 6. <u>Time dependent increase in ir-ET-1 secretion in confluent ARPE-19 cells (4 weeks old) following TNF-α stimulation.</u> Confluent ARPE-19 cells were treated with TNF-α (10nM) for 1, 4, 8, 16 and 24 hours. The media was collected and assayed for ir-ET-1 content as previously described. ◆ indicates control, ■ indicates TNF-α treated cells. TNF-α stimulated ir-ET-1 secretion in a time- dependent manner. A significant increase in ir-ET-1 was observed at the end of 8, 16 and 24 hours compared to control. Secretion of ir-ET-1 reached a plateau after 16 hours. Data is represented as mean $\pm$ SEM. Statistical comparisons were performed by t-test. Asterisk (*) denotes significance vs. controls at 8, 16 and 24 hours respectively ($p < 0.001$) (n = 6).

Fig. 7. <u>Immunofluorescence analysis in mRPE cells following TNF-α at the indicated time points.</u> The top row (A-F) represents differential interference contrast (DIC) images and the bottom row (G-L) represents merged fluorscent images of cells labeled using mouse anti-ZO-1 (red), rabbit anti-ET-1 (green) and DAPI (blue) (similar to Fig. 5). TNF-α (10nM) caused visible breakdown of cell-cell contact and tight junction disruption that was time-dependent. The first detectable change in cell-cell contact was observed at 4 hours and progressive damage thereafter. (scale = 10μm). Experiments were performed on at least 3 separate coverslips (n=3) per time point.

Fig. 8. <u>Quantitative RT-PCR in yRPE and mRPE cells.</u> Quantitative RT-PCR was performed using the SYBR-green PCR core reagents (Applied Biosystems). Quantitation of ppET-1 transcripts was done by the comparative C_T method (refer Methods). Basal levels of ppET-1 mRNA expression in y- and mRPE. Data is represented as mean $\pm$ SEM. Statistical comparisons were performed by t-test. * denotes significance vs. control (p< 0.05) (n = 4 per treatment).

Fig. 9. <u>Quantitative RT-PCR in yRPE and mRPE cells.</u> (A) and (B) ppET-1 mRNA levels following CCh (1, 10, 100 μM) and TNF-α (10nM) in y- and mRPE cells respectively. CCh (1, 10 and 100 μM) did not result in significant elevation of ppET-1 mRNA in yRPE (A) or mRPE cells (B) following 24 hours. TNF-α (10nM) significantly increased ppET-1 mRNA following 24 hours (A) and within 1, 4, and 8 hours vs. control (B). Data is represented as mean $\pm$ SEM. Statistical comparisons were performed by t-test. * denotes significance vs. control (p< 0.05) (n = 4 per treatment).
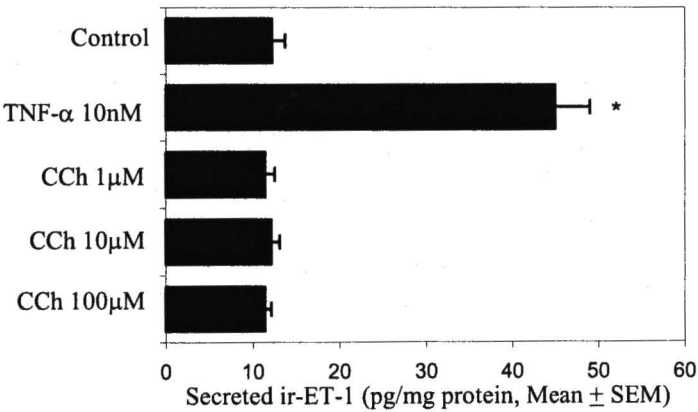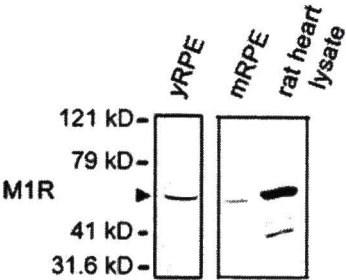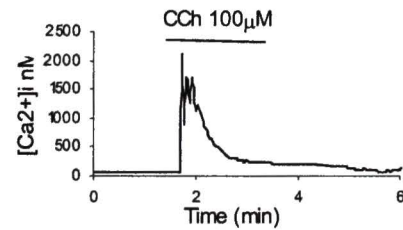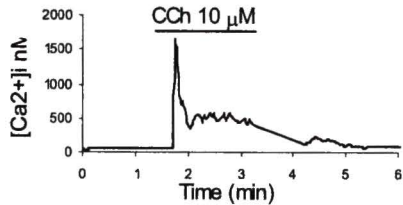
Fig. 1

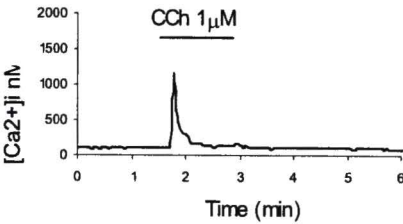A. yRPE
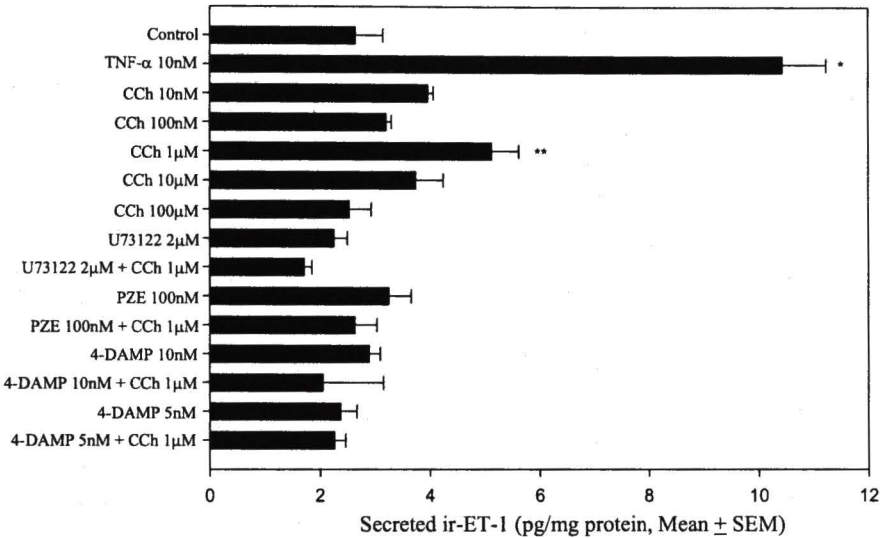
B. mRPE

Fig 2.

A.

B.

Fig. 3

A. yRPE

B. mRPE
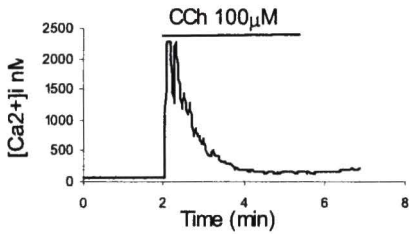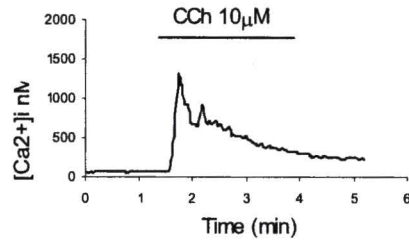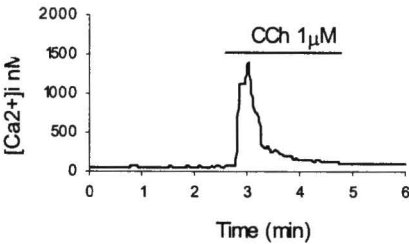
Table 1. Summary of CCh mediated $[Ca^{2+}]_i$ mobilization in yRPE cells measured by fura-2AM imaging. * denotes statistical significance between baseline, peak and one minute postpeak (not shown) mean values, performed by one way repeated measures ANOVA (p<0.001).

CCh dose response-

Treatment	$[Ca^{2+}]_i$ nM, Mean ± SEM	Number of cells (n)
Baseline	74 ± 5	98
CCh 1 μM	1504 ± 154 *	98
Baseline	57 ± 5	55
CCh 10 μM	1629 ± 276 *	55
Baseline	137 ± 21	26
CCh 100 μM	2851 ± 1392 *	26

Antagonist studies with CCh 1 μM-

Treatment	$[Ca^{2+}]_i$ nM, Mean ± SEM	Number of cells (n)
Baseline	65 ± 5	34
CCh 1 μM	1414 ± 203 *	34
U73122, 2 μM/ Baseline	132 ± 12	26
U73122, 2 μM + CCh 1 μM	177 ± 14	26
PZE 100nM/ Baseline	68 ± 7	16
PZE 100nM + CCh 1 μM	1584 ± 360 *	16
PZE 400nM/ Baseline	90 ± 8	17
PZE 400nM + CCh 1 μM	181 ± 30	17
4-DAMP 10nM/ Baseline	130 ± 6	68
4-DAMP 10nM + CCh 1 μM	122 ± 5	68

Receptor internalization studies-

| Treatment	$[Ca^{2+}]_i$ nM, Mean ± SEM	Number of cells (n)
Baseline	65 ± 5	34
CCh 1 μM	1414 ± 203 *	34
Pretreatment with CCh 1 μM (24 h)		
Baseline	77 ± 5	21
CCh 1 μM	736 ± 308 *	21
Baseline	137 ± 21	26
CCh 100 μM	2851 ± 1392 *	26
Pretreatment with CCh 100 μM (24 h)		
Baseline	156 ± 9	35
CCh 100 μM	202 ± 16	35

Table 2. Summary of CCh mediated $[Ca^{2+}]_i$ mobilization in mRPE cells measured by fura-2AM imaging. * denotes statistical significance between baseline, peak and one minute postpeak (not shown) mean values, performed by one way repeated measures ANOVA ($p<0.001$).

CCh dose response-

Treatment	$[Ca^{2+}]_i$ nM, Mean ± SEM	Number of cells (n)
Baseline	101 ± 8	35
CCh 1 μM	1260 ± 270 *	35
Baseline	105 ± 11.1	57
CCh 10 μM	1352 ± 158 *	57
Baseline	72 ± 6	54
CCh 100 μM	2349 ± 209 *	54

Receptor internalization studies-

Treatment	$[Ca^{2+}]_i$ nM, Mean ± SEM	Number of cells (n)
Baseline	100 ± 9	33
CCh 1 μM	1236 ± 316 *	33
Pretreatment with CCh 1 μM (24 h)		
Baseline	117 ± 28	22
CCh 1 μM	411 ± 134 *	22

Baseline	65 ± 9	16
CCh 100 μM	2500 ± 532 *	16
Pretreatment with CCh 100 μM (24 h)		
Baseline	87 ± 10	22
CCh 100 μM	82 ± 22	22

Fig. 4

	DIC	anti ZO-1	anti ET-1	Merge + DAPI
CONTROL	A	B	C	D
TNF-α 10nM	E	F	G	H
CCh 1 µM	I	J	K	L

Fig. 5

	DIC	anti ZO-1	anti ET-1	Merge + DAPI
CONTROL	A	B	C	D
TNF-α 10nM	E	F	G	H
CCh 1 μM	I	J	K	L

Negative controls

	DIC	Goat anti-mouse IgG-alexa 594	Goat anti-rabbit IgG-alexa 488	Merge + DAPI
Non-immune serum	A	B	C	D
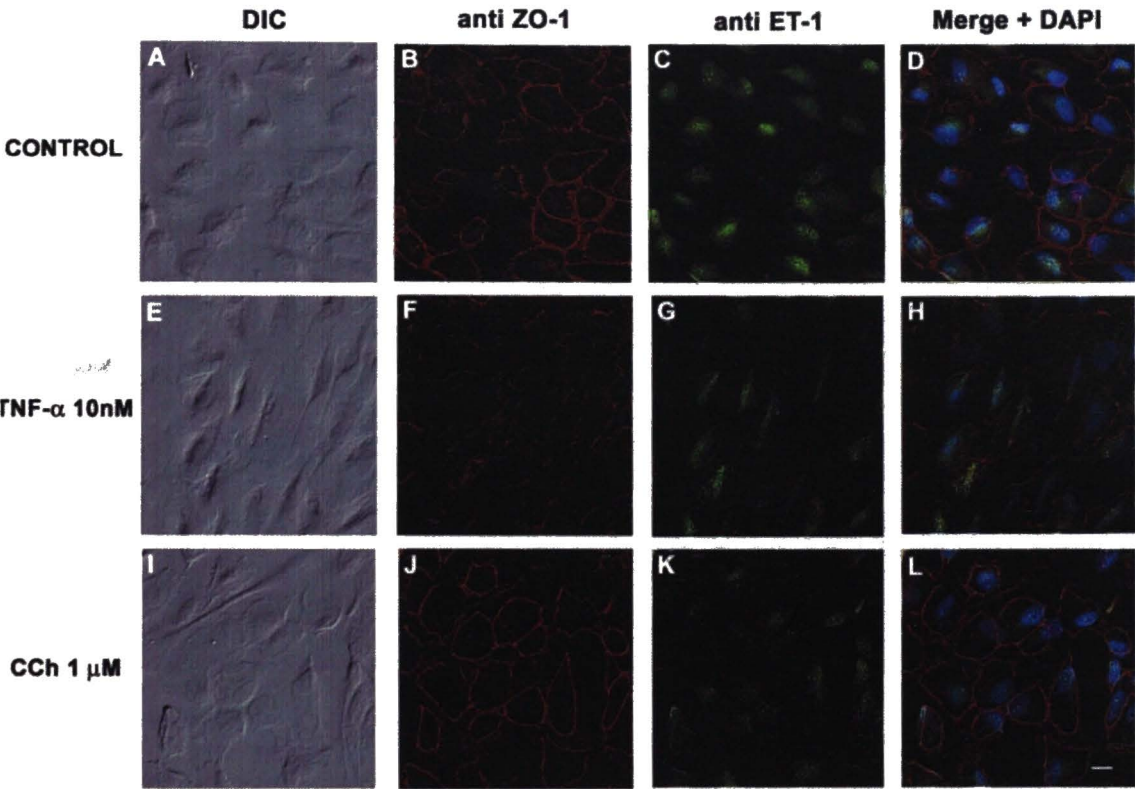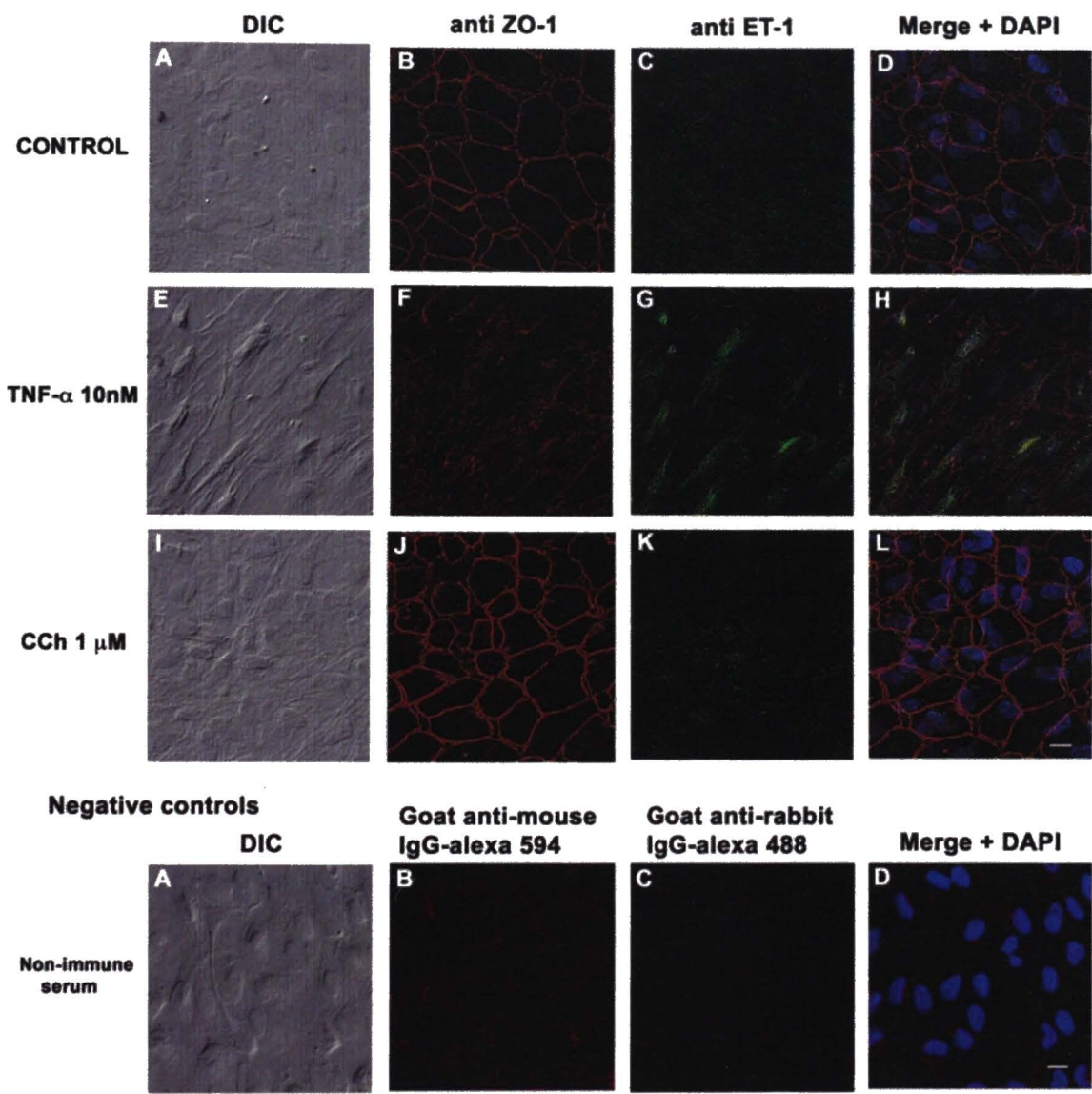
Fig. 6
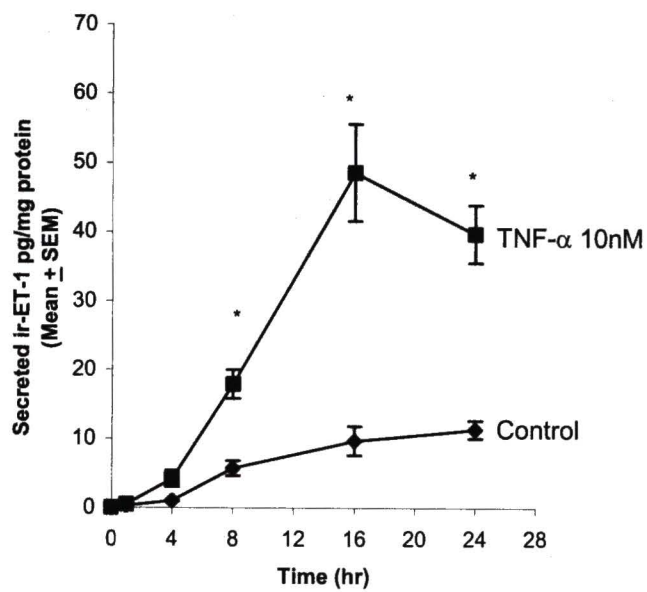
mRPE

Fig. 7
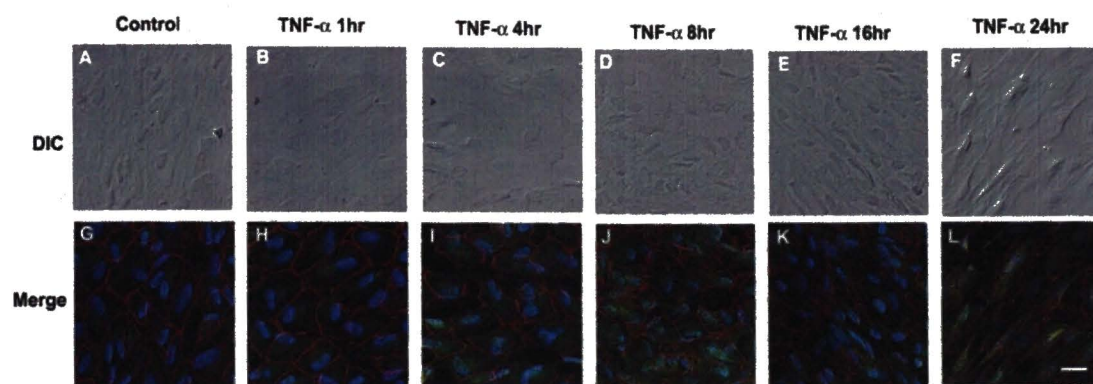
Fig. 8

A. y- and mRPE
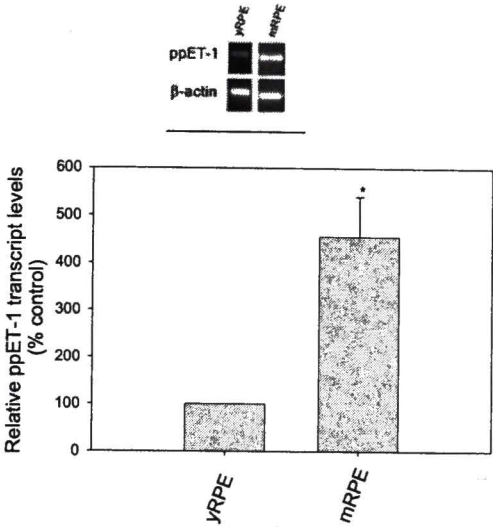
Fig. 9

A. yRPE
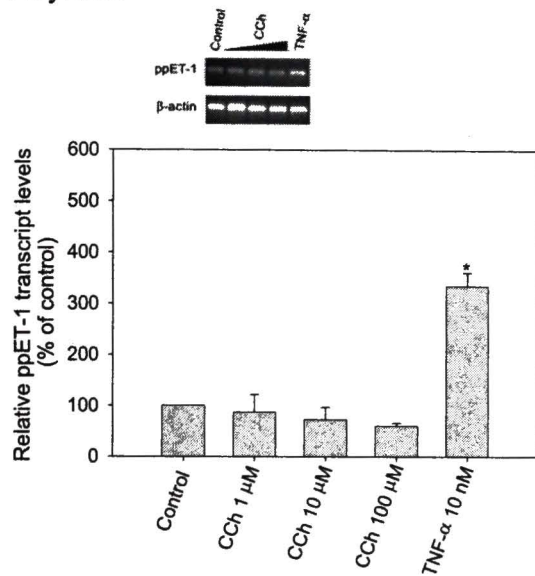
B. mRPE
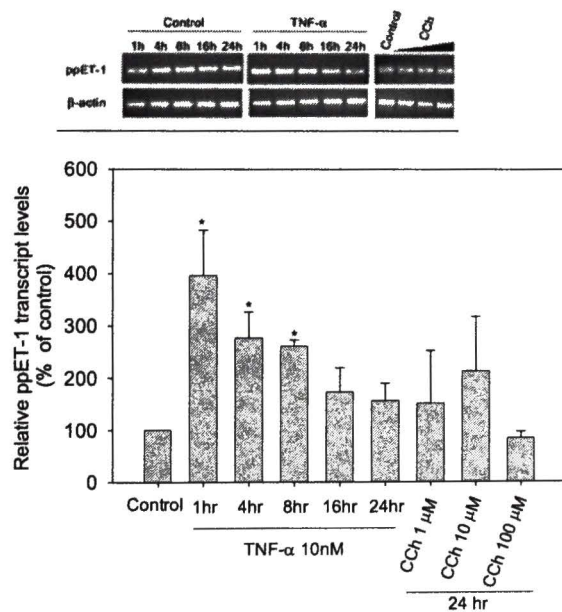
CHAPTER 4

Polarity of Endothelin-1 Distribution and Secretion in the Retinal Pigment Epithelium.

Santosh Narayan[1], Anne Marie Brun[2], and Thomas Yorio[1]

[1]Department of Pharmacology and Neuroscience and [2]Department of Cell Biology and

Genetics, University of North Texas Health Science Center, Fort Worth, Texas 76107,

U.S.A.

Corresponding author:

Thomas Yorio, Ph.D.
Professor and Dean
Department of Pharmacology and Neuroscience
University of North Texas Health Science Center (UNTHSC)
3500 Camp Bowie Blvd,
Fort Worth, TX 76107.

SUMMARY

Endothelins are a family of conserved vasoactive peptides that are widely expressed in different biological systems including the eye. In the cell culture model of retinal pigment epithelium, ARPE-19, the synthesis and secretion of endothelin-1 (ET-1) is regulated by cholinergics and TNF-α. In the present study we investigated the expression of ET-1 in RPE in situ, in rat and human eyes. Additionally, we have employed the human retinal pigment epithelial (ARPE-19) cells to delineate the apical and basolateral ET-1 expression and secretion by confocal microscopy and radioimmunoassay, respectively. Our results suggest a possible conservation of ET-1 expression predominantly in the mammalian RPE underlining its importance at this site. Additionally, our results suggest that constitutive ET-1 secretion may be non-selective in cultured RPE possibly allowing ET-1 to activate its receptors located in the apical and/or basal side of the RPE.

INTRODUCTION

The retinal pigment epithelium (RPE) is a monolayer of cells that forms the outer blood retinal barrier with the neural retina on the apical side and Bruch's membrane and the choroid on the basal side . Due to its unique location, the RPE serves as a communicating link between the neural retina and choroid. The specific orientation of the RPE with distinct apical and basal domains confers a polarized phenotype to the cell with different functions performed by each domain (Marmor, 1998). The establishment and maintenance of RPE polarity is therefore crucial in preserving a controlled environment at this region (Burke, 1998). Loss in RPE polarity is seen in inflammatory conditions that involve breakdown or a compromised barrier including uveitis (Luna et al., 1997), proliferative vitreoretinopathy (Hiscott and Sheridan, 1998; Nagasaki et al., 1998), diabetic retinopathy (Cunha-Vaz et al., 1993; Cunha-Vaz et al., 1979), choroidal neovascularization (Campochiaro, 1998), age-related macular degeneration (Campochiaro et al., 1999), retinitis pigmentosa (Vinores et al., 1995a) and ocular melanoma (Vinores et al., 1995b).

The RPE is known to constitutively secrete several growth factors and cytokines both *in vitro* and *in vivo* (Campochiaro, 1998; Sheedlo et al., 1995) the physiological relevance of which are not completely understood. We have recently identified the RPE as a source for one such peptide, endothelin-1 (ET-1) *in vitro*, in ARPE-19 cells (Narayan et al., 2003).

Endothelins are a family of 21 amino acid peptides that are differentially expressed and secreted locally at sites including the brain, eye, heart, lung, kidney, intestine and bladder (Kedzierski and Yanagisawa, 2001; MacCumber et al., 1991; Yorio et al., 2002). Of the three isoforms, ET-1 and ET-3 are predominantly found in the eye, including the cornea, iris, ciliary epithelium, aqueous humor, lens, sclera, choroid, the retina and the optic nerve (MacCumber et al., 1991; MacCumber et al., 1989; Stitt et al., 1996; Wollensak et al., 1998). Endothelin-1 (ET-1) acts on its receptors ET_A and ET_B, both belonging to the rhodopsin-like superfamily of seven transmembrane G-protein coupled receptors. Activation of ET_A receptors in the smooth muscle results in prolonged vasoconstriction while activation of ET_B receptors is thought to mediate vasodilation via nitric oxide (NO) production (Kedzierski and Yanagisawa, 2001). The precise role of ET-1 in the RPE remains unknown.

Both endothelial and epithelial cells have been shown to secrete ET-1 preferentially towards the basolateral side (Masaki, 1989; Uchida et al., 1991; Wagner et al., 1992; Yoshimoto et al., 1991). Studies using MDCK cells have shown ET-1 to be secreted towards both apical and basolateral sides in unstimulated cells but more towards the basolateral side following stimulation with TGF-β (Uchida et al., 1991). Preferential sorting and secretion of ET-1 towards a particular domain in the RPE may provide insights for its function at this region.

Unfortunately, secretion of growth factors and peptides can be induced merely by culturing cells in vitro (Terracio et al., 1988). This criticism is particularly relevant in case of RPE cells considering their phenotypic variability following isolation and culture

compared to their morphology *in vivo* (Burke, 1998). It is important to compare expression patterns of molecules of interest *in vivo* as a first step towards deducing their physiological relevance. In the present study we have confirmed the expression of ET-1 in situ, in both rat and human retinas. In addition, ARPE-19 cells grown on filter supports have been employed as a model to study polarized secretion of growth factors and cytokines by these cells *in vitro* (Dunn et al., 1998). We employed a similar model to study polarized secretion of ET-1 in ARPE-19 cells grown on collagen-coated filters.

MATERIALS AND METHODS

Human eyes were obtained within 12 hours post-mortem from the Rochester Eye and Human Parts Bank, Inc., Rochester, NY. The donor eyes were handled in compliance with the provisions of the Declaration of Helsinki for research involving human tissue. Experiments involving adult male Brown Norway rats and Wistar Kiyoto rats (both strains from Harlan Sprague-Dawley, Indianapolis, IN) adhered to the ARVO statement for the Use of Animals in Ophthalmic and Vision Research, the tenets of the Declaration of Helsinki, and the guidelines of the University of North Texas Health Science Center Committee on Animal Welfare.

Rat eye tissue preparation for immunohistochemistry (fixing, embedding and sectioning)

Prior to the removal of eyes, the animals were sacrificed using a CO_2 inhalation (30 seconds-1 min) technique. The eyes were immediately enucleated along with part of the optic nerve attached and transferred to a vial containing freshly made 4% paraformaldehyde for 1 hour with gentle rocking at room temperature after which approximately 5mm incisions were made on the sclera to facilitate permeation of the

fixative. Eyes were further incubated in the fixative for 1-2 hours at room temperature with gentle rocking, and transferred to 4 °C overnight. The following day, the eyes were dehydrated using a graded ethanol series (70%, 75%, 85%, 95%, for 1 hour each and 2 x 100% for 30 minutes). Eyes were placed on a petridish containing 100% ethanol, under a dissecting microscope and an incision was made on the sclera to gently remove the lens. The lens was removed to aid ease of sectioning. Lens removal did not alter morphology of the retina as determined by hemotoxylin and eosin (H & E) staining after embedding and sectioning (not shown). A few eyes with intact lenses were also included in the study. Their morphology (by H & E and by indirect immunofluorescence for detection of ET-1) and staining patterns were no different from eyes with lenses removed prior to sectioning (data not shown). Each eye was enclosed in Tissue-Tek embedding cassettes (Electron Microscopy Sciences, Fort Washington, PA), labeled and placed in a mixture containing 50% ethanol and 50% xylene, 2 x 100% xylene and a mixture with 50% xylene and 50% paraffin (in a pressurized oven at 50-60 °C) respectively for 30 minutes each. The cassettes were transferred to100% paraffin for incubation overnight in the oven. Prior to embedding, the cassettes were placed in fresh paraffin, 2 x 1 hour. Eyes were removed from cassettes and placed in steel molds and embedded in 100% paraffin devoid of air bubbles, on an embedding station at 65 °C. Molds were covered, labeled and transferred to a cold block maintained at 4 °C and allowed to solidify overnight. Paraffin blocks were removed from the mold and 5 μm thick sections on a microtome. Sections were floated in warm water before picking them on glass slides and placed in an incubator maintained at 37 °C overnight.

Immunohistochemistry

Paraffin sections that included the entire retina were used for immunohistochemical analysis. Slides were immersed twice in xylene, 15 minutes per incubation and hydrated using a graded ethanol series (100%-twice, 95%, 75%, and 50%) for 10 minutes per incubation and finally in PBS (15mM KCl, 468mM NaCl, 580mM $Na_2HPO_4.7H_2O$ and 27mM KH_2PO_4) for 10 minutes. Some slides were stained using H & E to confirm the presence of an intact retina with the RPE/choroid and the sclera. The remaining sections were processed for immunostaining. Briefly, the slides were immersed in 0.2% Triton-X 100 for 15 minutes. Slides were rinsed three times before immersing them in 50mM glycine for 15 minutes. Sections were then marked using a hydrophobic pen (PAP pen; Electron Microscopy Sciences, Fort Washington, PA) and allowed to incubate in blocking solution containing 5% BSA and 5% normal goat serum in PBS for 30 minutes. Slides were then drained off by tilting and sections were incubated in an antibody diluting solution containing 1% BSA and 1% normal goat serum with rabbit anti-ET-1 (10µg/ml; Peninsula labs/ Bachem, Belmont, CA) and mouse anti-RPE65 (8B11.37; 3.2µg/ml, generously gifted by Dr. Debra Thompson, W.K. Kellogg Eye Center, University of Michigan Medical School). Sections were incubated either with primary antibodies or non-immune rabbit (10µg/ml) and mouse IgG (3.2µg/ml) (Vector Laboratories, Burlingame, CA.) or the antibody diluting solution (no primary control) overnight at 4 °C. Slides were placed in a slide holder box with paper towels wetted in PBS underneath the holders to prevent evaporation of the antibody solution. All subsequent steps were performed as described below for immunocytochemistry with the exception of the red

fluorophore conjugated to goat anti-mouse IgG was Alexa 594 (10µg/ml; Molecular

Probes, Eugene, OR). Images were acquired on a Nikon Microphot FXA digital

fluorescent microscope (40X objective lens, NA=0.7) at the red, green and blue

wavelengths using a CCD-camera at same exposure settings and digitally processed using

the IPLab (Scanalytics, Fairfax, VA) image analysis software. All images were

deconvolved using the IPLab software and transferred to Adobe Photoshop 7.0 (Adobe

Systems, San Jose, CA) for further analysis

Immuno electron microscopy

Human donor eyes were fixed in 4% paraformaldehyde and 1% glutaradehyde overnight

at 4 °C with gentle rocking. The following day, eyes were rinsed with PBS three times for

5 minutes each. Samples were then dehydrated in 10%, 30%, and 50% ethanol, 10

minutes each at room temperature and with cold 70%, 95% and 2 x 100% ethanol for 1

hour each at 4 °C. Samples were infiltrated with either 1:1 Lowicryl mixture A + B or

LRWhite (both from Polysciences, Inc., Warrington, PA) in ethanol according to the

manufacturer, and allowed to incubate at 4 °C overnight followed by 2:1 lowicryl or

LRWhite in ethanol for 6-8 hours. The lowicryl mixture was replaced with 100%

lowicryl plus a UV catalyst and incubated overnight at 4 °C. LRWhite samples were

mixed in 100% LRWhite and also incubated at 4 °C, overnight. The next morning,

solutions were replaced with fresh lowicryl or LRWhite plus the UV accelerator

(Polysciences, Inc., Warrington, PA) and incubated at 4 °C for atleast 1 hour. Samples were

then embedded in plastic molds and UV polymerized. Lowicryl samples were

polymerized first at 4 °C overnight followed by polymerization at room temperature for

72 hours. LRWhite samples were allowed to polymerize in UV for 24-48 hours. Following embedding, ultrathin sections (50nm thick) were taken on a Reichert Ultracut S microtome and collected on Formvar/Carbon-coated glow-discharged 200-mesh nickel grids. Sections on grids were placed on 20-30 µl droplets of PBS for 3 x 5 minutes and permeabilized with 0.2% triton X100 for 15 minutes at 37 °C. Free aldehydes in sections were quenched by incubating sections in 0.5M glycine in PBS (3 x 5 minutes). Immunostaining was performed section side facing down on to droplets. Non specific sites were blocked using 5% normal donkey serum (SantaCruz Biotechnology, SantaCruz, CA) for 15 minutes. Sections were either incubated in rabbit anti-ET-1 (100mg/ml; from Bachem/ Peninsula laboratories, Belmont, CA.) in 1% donkey serum or non immune rabbit IgG (100mg/ml, Vector Laboratories, Burlingame, CA). Few sections were incubated in antibody diluting solution (1% donkey serum in PBS) as the no primary controls. Following overnight incubation at 4 °C, sections were rinsed in PBS, 5 x 5minutes and incubated in donkey anti rabbit IgG conjugated to 12nm colloidal gold (Jackson ImmunoResearch Laboratories, Inc., West Grove, PA) for 1 hour at room temperature. Following 3 x 5 minutes rinse in PBS, sections were post-fixed in 1% glutaraldehyde for 15 minutes. After 3 x 5 minutes rinse in PBS and sterile water, the grids were placed in 0.2% uranyl acetate and lead citrate solution for 10 minutes, air dried and viewed on a Zeiss 910 electron microscope at 100kV accelerating voltage. Images taken were recorded on Kodak SO-163 electron films and processed in a Mohr Pro 8 film processor. All images were scanned and labeled on Adobe Photoshop 7.0.

Cell Culture

Human retinal pigment epithelial cells (ARPE-19), a spontaneously arising cell line was purchased form the American Type Culture Collection (ATCC, Manassas, VA). Cells were maintained at 37 °C and 5% CO_2 in a 1:1 mixture of Dulbecco's modified Eagle's medium (DMEM) (Gibco- Life Technologies, Grand Island, NY) and Ham's F12 medium (Gibco- Life Technologies, Grand Island, NY) containing 1% fetal bovine serum (FBS) (Hyclone, Logan, Utah), 23 mM $NaHCO_3$ and penicillin/ streptomycin (Gibco- Life Technologies, Grand Island, NY). Cells were maintained in culture (containing 10% FBS) for atleast two weeks prior to harvesting them on 24-mm diameter Transwell-COL (collagen coated) polycarbonate filters (Corning Costar, Cambridge, MA) with a pore size of 0.4 μm. Filters were coated using matrigel (BD Biosciences, Bedford, MA) at a dilution of 1:40 in serum free DMEM-F-12 medium by the thin coating technique as described by the manufacturer. Cells were harvested at a density of 1.5 x 10^5 cells/cm^2 and maintained in culture for 3-4 weeks as described by Dunn et al.(Dunn et al., 1996)

Indirect immunofluorescence on ARPE-19 cells

ARPE-19 cells maintained in culture for 3-4 weeks on filters as mentioned above were fixed, permeabilized, blocked and labeled overnight with rabbit anti-ET-1 (5μg/ml; Bachem/Peninsula labs, Belmont, CA) and mouse anti-ZO-1 (10μg/ml) according to Narayan et al., 2003. Filters were rinsed with phosphate buffered saline (PBS) and incubated with goat anti- rabbit IgG Alexa 488 (10μg/ml; Molecular Probes, Eugene, OR) and goat anti-mouse IgG Alexa 633 (10μg/ml; Molecular Probes, Eugene, OR) in PBS for 1 hour in the dark at room temperature. Nuclei were labeled with DAPI (300nM; Molecular Probes, Eugene, OR) for 10-15 minutes. Filters were rinsed again with

distilled water before inverting and excising them with a sharp scalpel blade onto glass slides such that cell-side (apical) always faced the top and the basal side (filter) faced the slide. Glass coverslips were placed with a drop of Fluoro Save (EMD Biosciences, San Diego, CA) over the filter and allowed to air dry in dark for 20-30 minutes. En face (xy plane) and xz plane images were acquired on a Zeiss laser scanning confocal microscope using a 25X objective lens (NA=1.2).

Paracellular flux measurements

ARPE-19 cells grown on transwell collagen filters (24mm diameter) coated with matrigel as mentioned above were maintained in culture for 3-4 weeks. D-$[C^{14}]$ mannitol (56 mCi/mM; American Radiolabeled Chemicals, St. Louis, MO) diffusion across cells (paracellular transport) were measured as previously described (Ban and Rizzolo, 2000). Cells were rinsed twice with serum free DMEM-F12 medium before start of each assay. The assay was performed by adding 3 μCi/ml to the apical side in a total volume of 1.5 ml. The coated filter alone served as blank. Cells were maintained in a 5% CO_2 incubator at 37 °C for 15, 30, 60 or 90 minutes at the end of which 5 μl aliqouts were taken from the basal chamber and counted in a liquid scintillation counter. Flux ($J_{apical\ to\ basal}$) was calculated as nmoles/min/cm^2.

ET-1 Radioimmunoassay

ARPE-19 cells grown on filter supports (12 mm diameter; Transwell-COL, Corning Costar, Cambridge, MA) and maintained in culture for 3-4 weeks were employed to

determine the polarity of ET-1 secretion. Media containing 1% FBS was replaced with serum free media after 3 rinses with the same. Cells were incubated in serum free media alone (control and untreated) or in presence of thrombin (10nM) a known stimulator of ET-1 synthesis and secretion. Thrombin was added either to the apical or the basal side and allowed to incubate for 24 hours, at the end of which media was separately collected from both apical and basal chambers and assayed for ET-1 content by radioimmunoassay (ET-1 RIA; Peninsula labs/ Bachem, Belmont, CA). ET-1 extraction was performed according to Prasanna et al (1998) and the RIA was performed according to the manufacturer.

RESULTS

The retinal pigment epithelium is of the same neural lineage as rest of the retina and differentiates into a secretory epithelium. Several growth factors and cytokines are expressed and secreted by the RPE both in vivo and in vitro (Campochiaro, 1998). Mature polarized ARPE-19 cells as well as non polarized cells can synthesize and secrete ET-1 in a constitutive and regulated manner (Narayan et al., 2003). In this study we sought to determine if the RPE expresses the mature form of ET-1 peptide *in vivo*. Previous studies have shown ET-1 labeling in the RPE layer in rat retinas (Chakrabarti and Sima, 1997; Ripodas et al., 2001) and some had attributed the RPE label to be autofluorescence (Wollensak et al., 1998) . We sought to resolve this issue by comparing retinas from pigmented and albino rats. In the human retinas that we attempted to use for light microscopy analysis, there was a high degree of autofluorescence even in the absence of an antibody (data not shown). We thus examined the human retina by

immunoelectron microscopy to determine the labeling pattern for ET-1. Additionally, polarized ARPE-19 cells grown on collagen filters were employed to determine the polarity of ET-1 secretion in culture.

ET-1 expression in pigmented and albino rat retinas

Compared to the rest of the retina, immunoreactive ET-1 was predominantly found in the RPE (arrowheads in Fig.1 and 2) that almost appeared to entirely merge with the RPE specific protein, RPE65 (Fig 1D, 1H and Fig. 2D). Labeling at the photoreceptor outer and inner segments were punctate (arrows in Fig. 1). Immunoreactive ET-1 was also present in the choroid, inner plexiform layer and the inner limiting membrane albeit the labeling was very faint (not shown). Control retinas incubated with non immune IgG at the same concentration showed little or no labeling (Fig. 1 I-L).

ET-1 expression in the human RPE

Human retinas (n=2; 74 years and 86 years) were examined for ET-1 immunoreactivity. Labeling was predominantly in the RPE layer, with clusters of immunogold particles found in between lipid droplets that were reminiscent to vesicular structures (Fig.3B, C). Additionally, parts of the Bruch's membrane and choroid were also labeled but were significantly less than that found in the RPE. The RPE displayed the characteristic localization of melanosomes in the apical side including few rounded granules towards the center and basal parts of the cell that were 'lipofuscin-like' (Fig. 3A, D). Large clear lipid droplets or inclusions were present in both the eyes examined (Fig. 3A-E) probably the result of age or contributed by yet unknown factors. Non immune rabbit IgG showed little or no staining (Fig.3E).

Polarization of ARPE-19 cells, paracellular flux and secretion of ET-1

Tight junctions or zonula occludens are the most apically localized intercellular junction in mammalian epithelial and endothelial cells that limit paracellular movements of various substances including ions and macromolecules (Madara and Dharmsathaphorn, 1985) thus constituting a diffusion barrier (Balda et al., 1991; Tsukita et al., 2001). ARPE-19 cells grown on a collagen-matrigel support for 3-4 weeks have been shown to develop a tight epithelium with distinct apical and basolateral domains and have been used to deduce polarized secretion of certain growth factors and cytokines including bFGF (Dunn et al., 1998), IL-6, and IL-8 (Holtkamp et al., 1998). We employed a similar model to determine polarity of ET-1 distribution and secretion in these cells.

Paracellular diffusion was measured on cells grown on filter supports for 4 weeks (Fig. 4). Diffusion of C^{14}-mannitol across the filter alone (collagen + thin coat matrigel) was rapid that peaked within 30 minutes of addition of serum free media containing the tracer to the apical side. As expected, diffusion of the tracer from the apical to the basal compartment was much lower in filters with cells suggesting the presence of an apical diffusion barrier. Addtionally, diffusion across cells was constant at all time points tested. This confirmed previous reports that RPE cells grown in this manner polarize *in vitro* and provide a testable model for vectorial expression and transport of proteins.

To determine the distribution of intracellular ET-1, we first determined if ARPE-19 cells maintained epithelial polarity in culture. Filter grown ARPE-19 cells were immunolabeled with anti-ZO-1 and anti-ET-1. ZO-1, a scaffolding protein, is a peripheral component of all tight junctions (Nusrat et al., 2000; Tsukita et al., 2001) and was used as

an apical marker. Mislocalization of ZO-1 results in perturbation of the tight junction barrier and loss in cellular polarity (Pelletier et al., 1997). The *en face* view (xy axes) by confocal imaging indicated the presence of a tightly packed epithelium (Fig. 5, left panels) in accordance with Fig. 4. ZO-1 was entirely localized on the apical membrane (red) while punctate labeling of immunoreactive ET-1 was seen throughout the cytoplasm (green). View from the xz plane clearly depicted a polarized morphology with apically present tight junctions (arrows in Fig. 5). Interestingly, most of the ET-1 labeling was also localized at the apical and subapical regions (arrowheads in Fig. 5). The non-immune control appeared faint and diffuse. The nuclear stain (DAPI) was included to show the presence of cells at equal density (Fig. 5, right panels).

To quantitatively assess secretion of ET-1 towards specific domains, media from the apical and basal compartments from ARPE-19 cells grown on filter inserts were collected and assayed by RIA. Apical and basolateral ET-1 content were equal following a 24 hour exposure to serum free medium (Table I) suggesting that although sorting of intracellular ET-1 may be predominantly apical or subapical, constitutive secretion of ET-1 in RPE may be non-discriminatory. Regulated secretion involves sorting vesicles for directional transport and exocytosis (Blazquez and Shennan, 2000; Gerdes and Glombik, 1999). Thrombin is a known stimulator of ET-1 synthesis and secretion and thus can regulate its production (Ota et al., 1991). Addition of thrombin to apical or basolateral side did not change the non-discriminative secretion of ET-1 in RPE cells as seen in constitutive secretion.

DICUSSION

The retinal pigment epithelium has been previously identified as a source for ET-1 both *in vitro* (Narayan et al., 2003) as well as *in vivo* (MacCumber et al., 1991). The RPE similar to the choroid is one of highest in pigment content in vivo and autofluoresces when exposed to light. Previous studies that employed immunofluorescence techniques attributed ET-1 labeling in the RPE to be difficult to resolve due to high background autofluorescence. To address this, we compared retinas from both pigmented and albino rats and found ET-1 in the retina was predominantly localized in the RPE. Additionally, we included several controls in our study to monitor autofluorescence, all of which indicated the RPE may be a major site for ET-1 synthesis at the site of the outer blood retinal barrier. Immunofluorescence studies using the human retina were more problematic due to the high degree of autofluorescence in the RPE and choroid layers (not shown) and this prompted us to examine the retina at higher resolution by electron microscopy circumventing the problem of autofluorescence at the light level as well as providing clues as to whether sorting of intracellular ET-1 was preferential towards the apical or basolateral surfaces. Our results using the human RPE confirmed the RPE as a major site for ET-1 expression. However the non preferential distribution of immunoreactive ET-1 within each cell in the RPE layer indicated a lack of directionality towards either the apical or basolateral side. There was also some minor labeling of the Bruch's membrane, the choroid on the basal side as well as the outer and inner photoreceptor segments on the apical side. These results indicate that although the RPE may be a major site for ET-1 production, the choroid and parts of the photoreceptor outer

and inner segments may also contain ET-1 or ET-1 binding sites. This later possibility seems likely as fewer gold particles at these sites could be indicative of irreversible ET-1 binding to its receptor, a feature commonly associated with the binding characteristics of endothelins to their receptors (Hirata et al., 1988).

The ARPE-19 cells grown in culture as described by (Dunn et al., 1996) can serve as a useful model to study vectorial sorting and secretion of proteins *in vitro*. Cells were grown as previously described to attain a tight and polarized epithelium. Paracellular transport of the radiolabeled tracer, C^{14}-mannitol, suggested the establishment of a diffusion barrier and that molecules secreted preferentially on either side may not easily diffuse through to the other side. This was confirmed by comparing diffusion across cells with the filter alone (blank). Thus, the fact that ET-1 was found in the media bathing each surface suggested that ET-1 was either capable of crossing tight junctional paracellular pathways or was secreted out across each domain. Cells were also labeled with ZO-1, a tight junction associated protein indicating a polarized morphology with a monolayer of tightly packed cells was achieved. Interestingly, ET-1 labeling was almost exclusively present towards the apical membrane in ARPE-19 cells *in vitro* as compared to the non preferential labeling found *in situ* with intact tissue. Previous studies have suggested that polarized distribution in cultured RPE may vary based on how polarity is established *in vitro* as opposed to its development *in vivo* (Marmorstein, 2001; Rizzolo, 1997). Our studies using cultured ARPE-19 cells indicated that although localization of intracellular ET-1 was preferentially towards the apical region, secretion of ET-1 occurred towards both apical and basolateral sides. It is not certain if this would be similar in intact tissue,

however our EM studies suggested a non-selective distribution of intracellular ET-1 that could indicate secretion across either surface.

The ET-1 receptors namely ET_A and ET_B are G-protein coupled receptors that have been shown to be expressed in the retina, including the photoreceptors, the inner plexiform layer and the ganglion cell layer (Stitt et al., 1996). The choroid, the vascular smooth muscle in retinal blood vessels and choriocapillaries have also been shown to contain receptors for ET-1 (Stitt et al., 1996). Secretion of ET-1 by the RPE could target receptors on the apical (photoreceptors) or basal (choroid) sides. Activation of ET receptors in the retinal or choroidal vasculature may be important in regulating blood flow at this region.

Studies using MDCK cells (Uchida et al., 1991) and endothelial cells (Wagner et al., 1992) suggest that ET-1 secretion may be preferentially basolateral. It is also known that the RPE can exhibit reversed polarity, the best known example is the apical localization of Na,K-ATPase in the RPE microvilli as opposed to its preferential basolateral targeting in most other epithelia (Rizzolo, 1999). Secretion of ET-1 can be regulated by substances known to activate or suppress its synthesis and secretion (Tasaka and Kitazumi, 1994). Additionally, regulated exocytosis may preferentially sort vesicles towards one particular direction. To test this possibility, polarized ARPE-19 cells were stimulated with thrombin, either on the apical or the basolateral side. Addition of thrombin, a known activator of ET-1 synthesis and secretion (Ota et al., 1991) resulted in an increase in total ET-1 secretion but failed to preferentially direct ET-1 secretion towards any particular domain. This may have been due to the fact that thrombin has been shown to perturb

paracellular permeability in a Rho-dependent manner (Wojciak-Stothard and Ridley, 2002). Almost all potent activators of ET-1 secretion can perturb permeability of tight junctions including hypoxia and oxidative stress (Meyer et al., 2001), mechanical stretch (Sumpio and Widmann, 1990), thrombin (Ota et al., 1991) and cytokines including TNF-α (Kanse et al., 1991), IL-1β and IL-2 (Corder et al., 1995). Conversely, it will be interesting to determine if selectively perturbing tight junctions can have an effect on ET-1 synthesis and secretion, especially since evidence continues to accumulate that tight junctions may act as signal integrators and may be able to influence the cytoskeletal architecture and directly regulate gene transcription (Matter and Balda, 2003). This raises the possibility that elevation of secreted ET-1 may be having a role in cell proliferation, migration and wound repair similar to that seen in corneal epithelium (Takagi et al., 1994), hepatic stellate cells (Shao and Rockey, 2002; Tangkijvanich et al., 2001) and endothelial cells (Noiri et al., 1997). Signals generated from activation of autocrine or paracrine ET-1 in the RPE may be involved in retinopathies involving breakdown of the blood retinal barrier including clinical manifestations like uveitis, macular degeneration, proliferative vitreoretinopathy, diabetic retinopathy, choroidal neovascularization and retinal detachment. Little is known about ET-1's physiological role *in vivo* in this region of the eye. We propose that challenging the blood retinal barrier either by perturbing tight junctions or by other means that generate a breakdown, may enhance ET-1 synthesis, the increased ET-1 acting in the wound repair process. Such actions may be important in understanding the molecular mechanisms involved in such pathologies.

The present study demonstrates ET-1 expression predominantly in the RPE in the retina underlining its importance at this site. Additionally, our results suggest that constitutive ET-1 secretion may be released across either surface of the RPE, possibly allowing ET-1 to activate targets located downstream from the apical and basal sides of the RPE.

ACKNOWLEDGEMENTS

REFERENCES

Balda, M.S., L. Gonzalez-Mariscal, R.G. Contreras, M. Macias-Silva, M.E. Torres-Marquez, J.A. Garcia-Sainz, and M. Cereijido. 1991. Assembly and sealing of tight junctions: possible participation of G-proteins, phospholipase C, protein kinase C and calmodulin. *J Membr Biol.* 122:193-202.

Ban, Y., and L.J. Rizzolo. 2000. Differential regulation of tight junction permeability during development of the retinal pigment epithelium. *Am J Physiol Cell Physiol.* 279:C744-50.

Blazquez, M., and K.I. Shennan. 2000. Basic mechanisms of secretion: sorting into the regulated secretory pathway. *Biochem Cell Biol.* 78:181-91.

Burke, J.M. 1998. Determinants of Retinal Pigment Epithelial Cell Phenotype and Polarity. *In The Retinal Pigment Epithelium.* M.F. Marmor and T.J. Wolfensberger, editors. Oxford University Press, New York, NY. 86-102.

Campochiaro, P.A. 1998. Growth Factors in the Retinal Pigment Epithelium and Retina. *In The Retinal Pigment Epithelium.* M.F. Marmor and T.J. Wolfensberger, editors. Oxford University Press, New York, NY. 459-477.

Campochiaro, P.A., P. Soloway, S.J. Ryan, and J.W. Miller. 1999. The pathogenesis of choroidal neovascularization in patients with age-related macular degeneration. *Mol Vis.* 5:34.

Chakrabarti, S., and A.A. Sima. 1997. Endothelin-1 and endothelin-3-like immunoreactivity in the eyes of diabetic and non-diabetic BB/W rats. *Diabetes Res Clin Pract.* 37:109-20.

Corder, R., M. Carrier, N. Khan, P. Klemm, and J.R. Vane. 1995. Cytokine regulation of endothelin-1 release from bovine aortic endothelial cells. *J Cardiovasc Pharmacol.* 26 Suppl 3:S56-8.

Cunha-Vaz, J., E. Leite, J.C. Sousa, and J.R. de Abreu. 1993. Blood-retinal barrier permeability and its relation to progression of retinopathy in patients with type 2 diabetes. A four-year follow-up study. *Graefes Arch Clin Exp Ophthalmol.* 231:141-5.

Cunha-Vaz, J.G., M.F. Goldberg, C. Vygantas, and J. Noth. 1979. Early detection of retinal involvement in diabetes by vitreous fluorophotometry. *Ophthalmology.* 86:264-75.

Dunn, K.C., A.E. Aotaki-Keen, F.R. Putkey, and L.M. Hjelmeland. 1996. ARPE-19, a human retinal pigment epithelial cell line with differentiated properties. *Exp Eye Res.* 62:155-69.

Dunn, K.C., A.D. Marmorstein, V.L. Bonilha, E. Rodriguez-Boulan, F. Giordano, and L.M. Hjelmeland. 1998. Use of the ARPE-19 cell line as a model of RPE polarity: basolateral secretion of FGF5. *Invest Ophthalmol Vis Sci.* 39:2744-9.

Gerdes, H.H., and M.M. Glombik. 1999. Signal-mediated sorting to the regulated pathway of protein secretion. *Anat Anz.* 181:447-53.

Hirata, Y., H. Yoshimi, S. Takaichi, M. Yanagisawa, and T. Masaki. 1988. Binding and receptor down-regulation of a novel vasoconstrictor endothelin in cultured rat vascular smooth muscle cells. *FEBS Lett.* 239:13-7.

Hiscott, P., and C.M. Sheridan. 1998. The Retinal Pigment Epithelium, Epiretinal Membrane Formation, and Proliferative Vitreoretinopathy. *In The Retinal Pigment Epithelium*. M.F. Marmor and T.J. Wolfensberger, editors. Oxford University Press, New York, NY. 478-491.

Holtkamp, G.M., M. Van Rossem, A.F. de Vos, B. Willekens, R. Peek, and A. Kijlstra. 1998. Polarized secretion of IL-6 and IL-8 by human retinal pigment epithelial cells. *Clin Exp Immunol*. 112:34-43.

Kanse, S.M., K. Takahashi, H.C. Lam, A. Rees, J.B. Warren, M. Porta, P. Molinatti, M. Ghatei, and S.R. Bloom. 1991. Cytokine stimulated endothelin release from endothelial cells. *Life Sci*. 48:1379-84.

Kedzierski, R.M., and M. Yanagisawa. 2001. Endothelin system: the double-edged sword in health and disease. *Annu Rev Pharmacol Toxicol*. 41:851-76.

Luna, J.D., C.C. Chan, N.L. Derevjanik, J. Mahlow, C. Chiu, B. Peng, T. Tobe, P.A. Campochiaro, and S.A. Vinores. 1997. Blood-retinal barrier (BRB) breakdown in experimental autoimmune uveoretinitis: comparison with vascular endothelial growth factor, tumor necrosis factor alpha, and interleukin-1beta-mediated breakdown. *J Neurosci Res*. 49:268-80.

MacCumber, M.W., H.D. Jampel, and S.H. Snyder. 1991. Ocular effects of the endothelins. Abundant peptides in the eye. *Arch Ophthalmol*. 109:705-9.

MacCumber, M.W., C.A. Ross, B.M. Glaser, and S.H. Snyder. 1989. Endothelin: visualization of mRNAs by in situ hybridization provides evidence for local action. *Proc Natl Acad Sci U S A*. 86:7285-9.

Madara, J.L., and K. Dharmsathaphorn. 1985. Occluding junction structure-function relationships in a cultured epithelial monolayer. *J Cell Biol.* 101:2124-33.

Marmor, M.F. 1998. Structure, Function, and Disease of the Retinal Pigment Epithelium. *In The Retinal Pigment Epithelium.* M.F. Marmor and T.J. Wolfensberger, editors. Oxford University Press, New York, NY. 3-9.

Marmorstein, A.D. 2001. The polarity of the retinal pigment epithelium. *Traffic.* 2:867-72.

Masaki, T. 1989. The discovery, the present state, and the future prospects of endothelin. *J Cardiovasc Pharmacol.* 13 Suppl 5:S1-4; discussion S18.

Matter, K., and M.S. Balda. 2003. Signalling to and from tight junctions. *Nat Rev Mol Cell Biol.* 4:225-36.

Meyer, T.N., C. Schwesinger, J. Ye, B.M. Denker, and S.K. Nigam. 2001. Reassembly of the tight junction after oxidative stress depends on tyrosine kinase activity. *J Biol Chem.* 276:22048-55.

Nagasaki, H., K. Shinagawa, and M. Mochizuki. 1998. Risk factors for proliferative vitreoretinopathy. *Prog Retin Eye Res.* 17:77-98.

Narayan, S., G. Prasanna, R.R. Krishnamoorthy, X. Zhang, and T. Yorio. 2003. Endothelin-1 synthesis and secretion in human retinal pigment epithelial cells (ARPE-19): differential regulation by cholinergics and TNF-α. *Invest Ophthalmol Vis Sci (in press).*

Noiri, E., Y. Hu, W.F. Bahou, C.R. Keese, I. Giaever, and M.S. Goligorsky. 1997. Permissive role of nitric oxide in endothelin-induced migration of endothelial cells. *J Biol Chem*. 272:1747-52.

Nusrat, A., C.A. Parkos, P. Verkade, C.S. Foley, T.W. Liang, W. Innis-Whitehouse, K.K. Eastburn, and J.L. Madara. 2000. Tight junctions are membrane microdomains. *J Cell Sci*. 113 (Pt 10):1771-81.

Ota, S., Y. Hirata, T. Sugimoto, O. Kohmoto, Y. Hata, K. Yoshiura, R. Nakada, and A. Terano. 1991. Endothelin-1 secretion from cultured rabbit gastric epithelial cells. *J Cardiovasc Pharmacol*. 17 Suppl 7:S406-7.

Pelletier, R.M., Y. Okawara, M.L. Vitale, and J.M. Anderson. 1997. Differential distribution of the tight-junction-associated protein ZO-1 isoforms alpha+ and alpha- in guinea pig Sertoli cells: a possible association with F-actin and G-actin. *Biol Reprod*. 57:367-76.

Ripodas, A., J.A. de Juan, M. Roldan-Pallares, R. Bernal, J. Moya, M. Chao, A. Lopez, A. Fernandez-Cruz, and R. Fernandez-Durango. 2001. Localisation of endothelin-1 mRNA expression and immunoreactivity in the retina and optic nerve from human and porcine eye. Evidence for endothelin-1 expression in astrocytes. *Brain Res*. 912:137-43.

Rizzolo, L.J. 1997. Polarity and the development of the outer blood-retinal barrier. *Histol Histopathol*. 12:1057-67.

Rizzolo, L.J. 1999. Polarization of the Na+, K(+)-ATPase in epithelia derived from the neuroepithelium. *Int Rev Cytol*. 185:195-235.

Shao, R., and D.C. Rockey. 2002. Effects of endothelins on hepatic stellate cell synthesis of endothelin-1 during hepatic wound healing. *J Cell Physiol*. 191:342-50.

Sheedlo, H.J., L. Li, W. Fan, and J.E. Turner. 1995. Retinal pigment epithelial cell support of photoreceptor survival in vitro. *In Vitro Cell Dev Biol Anim*. 31:330-3.

Stitt, A.W., U. Chakravarthy, T.A. Gardiner, and D.B. Archer. 1996. Endothelin-like immunoreactivity and receptor binding in the choroid and retina. *Curr Eye Res*. 15:111-7.

Sumpio, B.E., and M.D. Widmann. 1990. Enhanced production of endothelium-derived contracting factor by endothelial cells subjected to pulsatile stretch. *Surgery*. 108:277-81; discussion 281-2.

Takagi, H., P.S. Reinach, N. Yoshimura, and Y. Honda. 1994. Endothelin-1 promotes corneal epithelial wound healing in rabbits. *Curr Eye Res*. 13:625-8.

Tangkijvanich, P., S.P. Tam, and H.F. Yee, Jr. 2001. Wound-induced migration of rat hepatic stellate cells is modulated by endothelin-1 through rho-kinase-mediated alterations in the acto-myosin cytoskeleton. *Hepatology*. 33:74-80.

Tasaka, K., and K. Kitazumi. 1994. The control of endothelin-1 secretion. *Gen Pharmacol*. 25:1059-69.

Terracio, L., L. Ronnstrand, A. Tingstrom, K. Rubin, L. Claesson-Welsh, K. Funa, and C.H. Heldin. 1988. Induction of platelet-derived growth factor receptor expression in smooth muscle cells and fibroblasts upon tissue culturing. *J Cell Biol*. 107:1947-57.

Tsukita, S., M. Furuse, and M. Itoh. 2001. Multifunctional strands in tight junctions. *Nat Rev Mol Cell Biol.* 2:285-293.

Uchida, S., M. Horie, M. Yanagisawa, Y. Matsushita, K. Kurokawa, and E. Ogata. 1991. Polarized secretion of endothelin-1 and big ET-1 in MDCK cells is inhibited by cell Na+ flux and disrupted by NH4Cl. *J Cardiovasc Pharmacol.* 17 Suppl 7:S226-8.

Vinores, S.A., M. Kuchle, N.L. Derevjanik, J.D. Henderer, J. Mahlow, W.R. Green, and P.A. Campochiaro. 1995a. Blood-retinal barrier breakdown in retinitis pigmentosa: light and electron microscopic immunolocalization. *Histol Histopathol.* 10:913-23.

Vinores, S.A., M. Kuchle, J. Mahlow, C. Chiu, W.R. Green, and P.A. Campochiaro. 1995b. Blood-ocular barrier breakdown in eyes with ocular melanoma. A potential role for vascular endothelial growth factor/vascular permeability factor. *Am J Pathol.* 147:1289-97.

Wagner, O.F., G. Christ, J. Wojta, H. Vierhapper, S. Parzer, P.J. Nowotny, B. Schneider, W. Waldhausl, and B.R. Binder. 1992. Polar secretion of endothelin-1 by cultured endothelial cells. *J Biol Chem.* 267:16066-8.

Wojciak-Stothard, B., and A.J. Ridley. 2002. Rho GTPases and the regulation of endothelial permeability. *Vascul Pharmacol.* 39:187-99.

Wollensak, G., H.E. Schaefer, and C. Ihling. 1998. An immunohistochemical study of endothelin-1 in the human eye. *Curr Eye Res.* 17:541-5.

Yorio, T., R. Krishnamoorthy, and G. Prasanna. 2002. Endothelin: is it a contributor to glaucoma pathophysiology? *J Glaucoma.* 11:259-70.

Yoshimoto, S., Y. Ishizaki, T. Sasaki, and S. Murota. 1991. Effect of carbon dioxide and oxygen on endothelin production by cultured porcine cerebral endothelial cells. *Stroke.* 22:378-83.

FIGURE LEGENDS

Fig. 1 <u>Endothelin-1 (ET-1) expression in pigmented rat retinas by light microscopy.</u> Eyes from adult Brown Norway rats were enucleated, fixed, paraffin embedded and sectioned as described in the Methods section. 5μm thick sections were labeled with rabbit anti-ET-1 (10 μg/ml, green), mouse anti-RPE65 (3.2 μg/ml, red) and DAPI (blue) and visualized under a Nikon Microphot fluorescence microscope. A total of 6 animals were used in this study. Sections from two different animals (A-D and E-H) are shown here. Immunoreactive ET-1 was predominant in the RPE layer (arrowheads in C and G), that colocalized with the RPE specific protein, RPE65. Punctate labeling of ET-1 was present in the photoreceptor outer segments and inner segments (arrows) and in the choroid. The non-immune controls (I-L) (rabbit IgG and mouse IgG) used at the same concentration as the primary antibodies showed little or no labeling. ONL = outer nuclear layer, IS = photoreceptor inner segments, OS = photoreceptor outer segments, RPE = retinal pigment epithelium, CH = choroid. Scale bar in L = 10μm.

Fig. 2 <u>Endothelin-1 (ET-1) expression in albino rat retinas by light microscopy.</u> Eyes from adult male Wistar rats were enucleated, fixed, paraffin embedded and sectioned as described in the Methods section. 5μm thick sections were labeled as described in Fig.1 and Methods. As seen in the retinas of pigmented rats, immunoreactive ET-1 was predominant in the RPE layer, that colocalized with the RPE specific protein, RPE65 (arrowheads in D). Retinas from two different albino rats were examined in this study, all

of which were immunoreactive for ET-1 predominantly in the RPE. Non immune controls showed no labeling (not shown). Scale bar in D = 10μm.

Fig. 3 <u>Endothelin-1 (ET-1) expression in human RPE by immunogold transmission electron microscopy (TEM)</u>. Ultrathin sections (50nm) of the human retina (n=2, 74 and 86 year old) were placed on nickel grids and immunostained using rabbit anti-ET-1 (100 μg/ml) and donkey anti-rabbit IgG conjugated to 12nm diameter colloidal gold. Grids were air dried and viewed on a Zeiss 910 electron microscope at 100kV accelerating voltage. Immunoreactive ET-1 was predominant throughout the RPE layer. Within each RPE, clusters of immunogold particles were seen in between large lipid droplets near the apical and basal sides (arrows in B and C). Diffuse immunoreactive ET-1 labeling was observed in rest of the retina albeit at much lower numbers compared to the RPE (not shown). The non-immune rabbit IgG (D and E) showed very few randomly labeled immunogold particles (arrow in E). Scale bar = 2 μm (A, D), 0.5 μm (B,E), 0.2 μm (C).

Fig. 4 <u>Paracellular permeability of C^{14}-mannitol in ARPE-19 cells</u>. Diffusion of D-[1-C^{14}] mannitol (3 μCi/ml) from the apical to the basal side was measured in 4 week-old ARPE-19 cells grown on collagen filters (0.4 μm pore size), n=6. Collagen filters without cells were employed as blanks (n=3). Radiolabeled medium was added to the apical side was maintained at specified time points, 5 μl aliqouts were taken from the basal chamber and counted in a liquid scintillation counter. Flux was calculated as nmoles/min/cm^2.

Fig. 5 <u>Immunoreactive ET-1 in ARPE-19 cells grown on filter supports</u>. ARPE-19 cells were grown on 0.4 μm pore sized collagen coated filters (Transwell-COL). Cells were allowed to grow on filter supports for 3-4 weeks following which they were fixed, permeated and labeled using rabbit anti-ET-1 (5 μg/ml, green), mouse anti-ZO-1 (10 μg/ml, red) and DAPI (blue). Filters were excised from their supports and mounted cell-side facing up on glass slides and coverslips using Fluoro-Save. Cells were visualized on a laser scanning confocal inverted microscope at appropriate wavelengths. Both xy and xz sections were imaged for each slide (n=2). Punctate immunoreactive ET-1 labeling was predominant around the apical belt (arrowheads) around the tight junction peripheral protein, ZO-1 (arrows). The non-immune rabbit IgG showed little labeling.
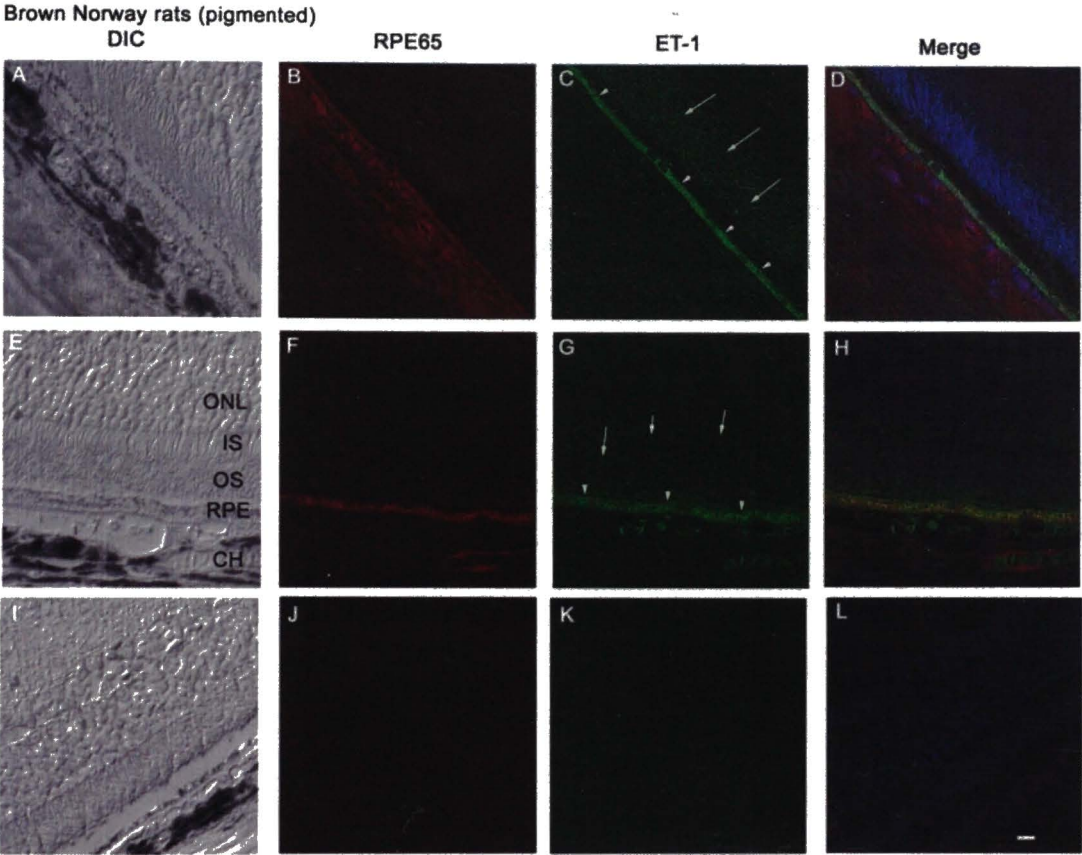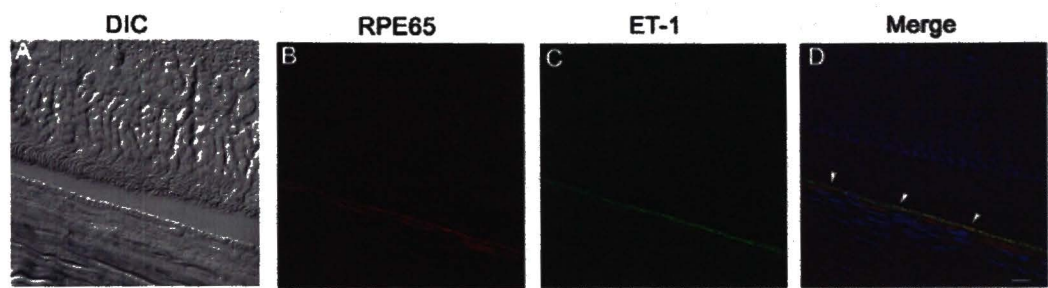
FIGURES

Fig. 1

Brown Norway rats (pigmented)

DIC | RPE65 | ET-1 | Merge

Fig. 2

Wistar rats (male, albino)

| DIC | RPE65 | ET-1 | Merge |

Fig. 3

Outer blood retinal barrier in the human retina (74 yr old), n=2.

Photoreceptor OS
RPE
Bruch's membrane
Rabbit anti-ET-1

Rabbit IgG
(non immune IgG)
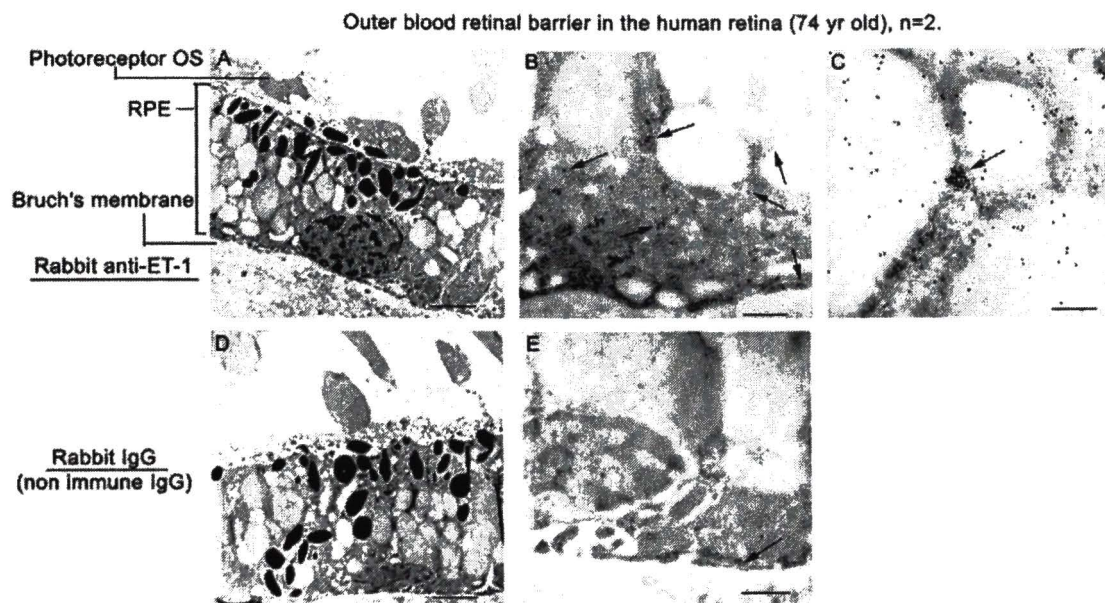
Fig. 4
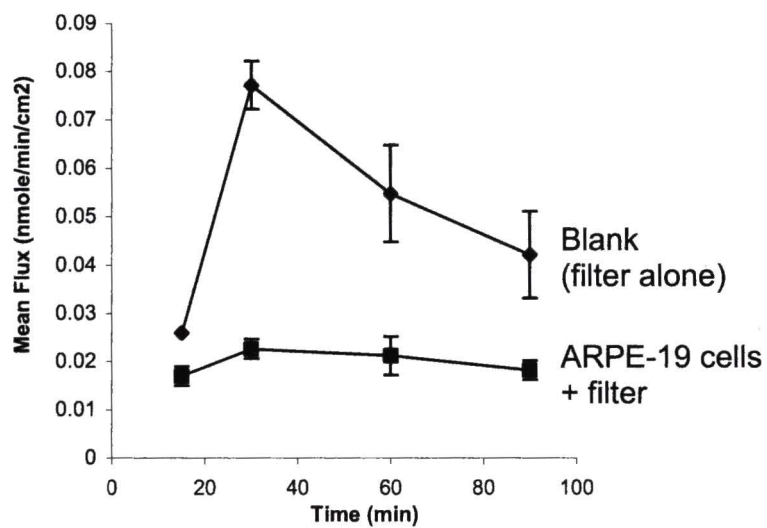
Fig. 5

Anti ET-1 + Anti ZO-1   Non-immune IgG + DAPI
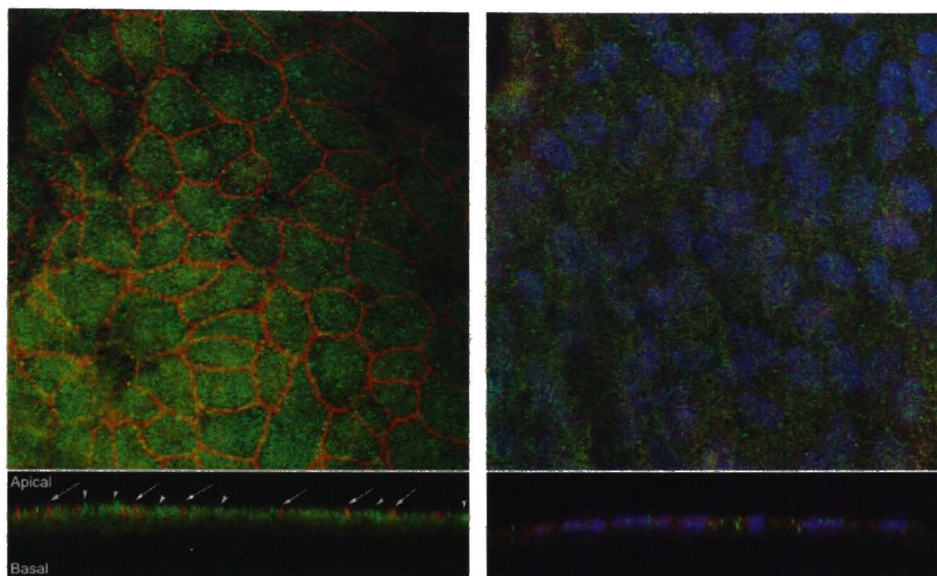
Table I

CONDITION	Secreted ir-ET-1 (pg/mg total protein)	
	Apical side	Basolateral side
Control	13 + 1	13 + 1
Thrombin, 10nM (apical)	17 + 3	19 + 6
Thrombin, 10nM (basolateral)	17 + 4	12 + 2

CHAPTER 5

Thrombin Induced Endothelin-1 Synthesis and Secretion in Retinal Pigment Epithelial

Cells is Rho Kinase (ROCK) Dependent.

Santosh Narayan, Ganesh Prasanna, and Thomas Yorio*.

Department of Pharmacology and Neuroscience, University of North Texas Health Science Center, Fort Worth, Texas 76107, U.S.A.

* Corresponding author:

Thomas Yorio, Ph.D.
Professor and Dean
Department of Pharmacology and Neuroscience
University of North Texas Health Science Center (UNTHSC)
3500 Camp Bowie Blvd,
Fort Worth, Texas 76107.

SUMMARY

The retinal pigment epithelium (RPE) forms the outer blood retinal barrier that is important in providing a controlled environment to the neural retina. We have identified the RPE as a source for endothelin-1 (ET-1) at this region. ET-1 is a potent vasoactive peptide, its function at the site of the RPE remains obscure. Factors that regulate ET-1 synthesis and secretion may provide insight towards delineating its function at this site. Thrombin is one such factor that may act on the RPE following breakdown of the blood-retinal barrier. Thrombin by itself can increase paracellular permeability by altering the cytoskeletal architecture and is also a known inducer of ET-1 synthesis. In the present study we identified the signaling aspects of thrombin mediated ET-1 synthesis and secretion in RPE cells. We report that thrombin mainly acts via the protease-activated receptor-1 (PAR-1) subtype resulting in a rho/ROCK1/2 dependent activation of preproET-1 transcription and mature ET-1 secretion. Additionally, we found that a rise in PAR-1 receptor mediated intracellular calcium may be partially involved in ET-1 production but is independent of a protein kinase C (PKC) mediated mechanism.

INTRODUCTION

The retinal pigment epithelium forms the outer blood retinal barrier that acts as a sentinel preventing macromolecules and blood-borne substances infiltrating the neural retina from the vascular choroidal side (1). Additionally, the RPE offers metabolic and neurotrophic support to the apically located photoreceptors and the basally located choroid. Numerous factors are secreted by the RPE (2) that may play important roles in regulating its immediate environment either in an autocrine and/or paracrine manner. Endothelin-1 (ET-1) is one such factor that was recently shown to be released by RPE cells *in vitro* (3) and is expressed *in situ* in the RPE and photoreceptors as well as in the inner retina (4-7) Endothelins (ET-1, -2 and –3) are 21 amino acid peptides that are potent and versatile regulators of blood flow and pressure (8). ET-1 is one of the most potent vasoconstrictors implicated in several cardiovascular and developmental defects (8,9). ET-1 is widely expressed and secreted especially by endothelial and epithelial cells (10), both of which are critical in maintaining blood-organ barriers . Elevated levels of ET-1 have been reported in conditions that breach the blood-organ barrier, most notably in cerebral ischemia and stroke after subarachnoid hemorrhage (SAH) (11) that involves the breakdown of the blood-brain barrier, and in pre-eclampsia and eclampsia (12,13) that involves placental ischemia after breakdown of the blood-placental barrier, and in certain carcinomas (14).This raises the immediate possibility for secreted ET-1 to mediate actions that promote tissue repair, especially in such situations where rapid control of inflammation is desirable. Little is known about how choroidal and/ or retinal vascular insults influence ET-1 secretion within these regions.

Thrombin, a blood-derived serine protease is implicated in platelet aggregation and clot formation (15). Additionally, thrombin is a potent activator of ET-1 synthesis and secretion (16). Thrombin acts via protease activated receptors including the PAR-1, -3 and –4 subtypes, that cleaves and unmasks active sites on the N-terminal resulting in receptor activation (15,17). PARs like most G-protein coupled receptors are pleiotropic in their ability to activate multiple classes of G-proteins (18,19). These include interaction with $G_{q/11}$, G_i and $G_{12/13}$ G-proteins resulting in transient IP_3 mediated $[Ca^{2+}]_i$ elevation, decrease in intracellular cAMP or activation of rho respectively (20-22). Guanine nucleotide exchange factors for rho (rhoGEFs) including p115 rhoGEF are direct effectors of $G_{\alpha 12/13}$ (23-25) that in turn catalyze GTP loading and activation of rho (26). Rho activation usually results in rearrangement of the cytoskeleton (27,28), changes in paracellular permeability (29), cell division and migration (30) .

Thrombin mediated activation of PAR-1 is associated with both an increase in $[Ca^{2+}]_i$ and rho activation with rho mediated cytoskeletal changes (31). Our previous study with TNF-α and cholinergic actions on ET-1 secretion in RPE indicated that carbachol unlike TNF-α, mediated increase in $[Ca^{2+}]_i$ was not involved in tight junction disassembly or any other morphologically distinct alterations of the cytoskeleton (3) and that TNF-α mediated changes in cytoskeleton resulted in potent activation of ET-1 synthesis and secretion. This is in accordance with other studies that implicate rho activation and not $[Ca^{2+}]_i$ mobilization or pertussis toxin-sensitive G_i protein in inducing cytoskeletal changes (32-34).

We hypothesized that extravasated thrombin following outer blood-retinal barrier breakdown could exert its effects on ET-1 synthesis and secretion in the RPE by inducing cytoskeletal alterations and tight junction disassembly in a rho-dependent manner. The aim of this study was to elucidate the signaling features of thrombin-mediated ET-1 secretion in the retinal pigment epithelial cell.

METHODS

Materials

Thrombin, thrombin receptor activating peptide (TRAP6/ PAR-1 agonist/SFLLR), hirudin (thrombin inhibitor), Ro 31-8425 ((2-[8-(aminomethyl)-6,7,8,9-tetrahydropyrido[1,2-a]indol-3-yl]-3-(1-methyl-1H-indol-3-yl)maleimide, HCl; pan-PKC inhibitor), and Y-27632 ((R)-(+)-trans-N-(4-Pyridyl)-4-(1-aminoethyl)-cyclohexanecarboxamide, 2HCl; ROCK inhibitor) were purchased from Calbiochem/ EMD Biosciences Inc., San Diego, CA. U73122 (1-(6-((17β-3-methoxyestra-1,3,5(10)-trien-17-yl)amino)hexyl)- 1H-pyrrole-2,5-dione, PLC inhibitor) was purchased from Biomol Research Laboratories Inc., Plymouth Meeting, PA. The PAR-4 receptor peptide agonist (pPAR-4/ AYPGKF) was custom synthesized with C-terminal amidation at over > 95% purity by Bioworld, Dublin, OH.

In studies including inhibitors, cells were pretreated with the inhibitor for 20-30 minutes before the agonist treatment except in case of hirudin where the hirudin: thrombin mixture (3:1) was incubated at room temperature for 1 hour before adding it to cells. Mouse anti-ZO-1 was purchased from Zymed Laboratories, San Francisco, CA. Rabbit anti-endothelin-1 (anti-ET-1) was purchased from Bachem/ Peninsula laboratories,

Belmont, CA. The same antibody was used in radioimmunoassay measurements (secreted ET-1) and immunofluorescence experiments (intracellular ET-1). Rabbit IgG and mouse IgG were purchased from Vector laboratories, Burlingame, CA. Secondary antibodies including donkey anti-rabbit IgG and donkey anti-mouse IgG conjugated to HRP were purchased from Amersham Biosciences, Piscataway, NJ. Fluorescent probes including goat anti-rabbit Alexa 488 and goat anti-mouse Alexa 594 were purchased from Molecular Probes, Eugene, OR.

Cell culture

Human retinal pigment epithelial cells (ARPE-19), a spontaneously transformed cell line, was purchased from American Type Culture Collection (ATCC, Manassas, VA). ARPE-19 cells (passage #s: 20-23) were maintained at 37 °C and 5% CO_2 in a 1:1 mixture of Dulbecco's modified Eagle's medium (DMEM) and Ham's F-12 medium (Invitrogen, Carlsbad, CA) supplemented with 10% fetal bovine serum (Hyclone, Logan, UT), 2mM L-glutamine, 23mM $NaHCO_3$ and penicillin and streptomycin (Invitrogen, Carlsbad, CA). ARPE-19 cells were seeded at 1.4×10^5 cells/ well (6 well plate) and maintained in culture for 4-5 weeks (mature RPE or mRPE) developing well-defined tight junctions. according to Dunn et al.(35)

ET-1 extraction and measurement by radioimmunoassay

ARPE-19 cells were grown to mature or differentiated state (4 weeks in culture, mRPE) in 6-well culture plates (35mm diameter/ well, ~ 1.4×10^5 cells/ well) in 1:1 DMEM + Ham's F12 culture medium containing 10% FBS. On the day of treatments, cells were rinsed three times with serum-free 1:1 DMEM + Ham's F12 culture media (SF-DMEM/

F12) and treated with 1 ml SF-DMEM/ F12 containing either thrombin (5, 10, 20nM), SFLLR (pPAR-1, 10, 25, 50 μM) or AYPGKF (pPAR-4, 50 μM). Treatment incubations were for 24 hours in most of the experiments or during a time course (30 minutes, 1hr, 4, 8, 16, 24hr). The extraction protocol for ET-1 was performed as previously described (36). Efficiency of ET-1 recovery was 75 ± 3 % (n = 3). Measurement of immunoreactive ET-1 (ir-ET-1) was according to manufacturer's instructions in a commercially available RIA kit for ET-1 (Peninsula Laboratories, Belmont, CA).

Intracellular Ca^{2+} ($[Ca^{2+}]_i$) measurement

Intracellular Ca^{2+} in mRPE cells was measured at 37 °C by the ratiometric technique using fura-2AM (excitation at 340 nm and 380 nm, emission at 500 nm) according to Prasanna et al.(37).

Immunofluorescence microscopy

ARPE-19 cells were grown on 25mm glass coverslips for 4-5 weeks and treated as indicated. Cells were fixed in 4% paraformaldehyde in PBS (15mM KCl, 468mM NaCl, 580mM $Na_2HPO_4.7H_2O$ and 27mM KH_2PO_4) for 30 minutes at room temperature followed by permeabilization with 0.2 % Triton-X 100 for 15 minutes. Cells were rinsed in PBS and incubated twice in 50 mM glycine, 15 minutes/ incubation. Each coverslip was carefully inverted (cell-side facing solution) onto 200ul of blocking solution containing 3% BSA + 3% normal goat serum in PBS for 30 minutes. The coverslips were then incubated in rabbit anti-ET-1 (10 μg/ml) for 4 hours at 4 °C followed by incubation in a mixture containing rabbit anti-ET-1 (10 μg/ml) and mouse anti-ZO-1 (10 μg/ml), overnight at 4 °C. Coverslips were rinsed and allowed to incubate in a mixture of

secondary antibodies containing donkey anti-mouse Alexa 594 conjugated (5 µg/ml) and donkey anti-rabbit Alexa 488 conjugated (5 µg/ml) for 1 hour in the dark at room temperature. Nuclei were stained with DAPI (300 nM) (Molecular Probes, Eugene, OR) for 10 minutes. Coverslips were mounted on glass slides using FluorSave (Calbiochem, San Diego, CA) and allowed to dry for 20 minutes in the dark. Cells were viewed with a Nikon Microphot FXA digital fluorescent microscope and images at the red, green and blue wavelengths were acquired using a CCD-camera, digitally processed using the IPLab (Scanalytics, Fairfax, VA) image analysis software. All images were deconvolved using the IPLab software and transferred to Adobe Photoshop 7.0 (Adobe Systems, San Jose, CA) for further analysis.

Rho pull- down assay

The rho pull-down assay was performed using the EZ-Detect Rho activation kit from Pierce Biotechnology, Rockford, IL according to manufacturer's protocol. Mature ARPE-19 cells (3-4 weeks in culture) were treated with 10nM thrombin in serum free ARPE-19 medium (1:1 DMEM + F12) at indicated periods. Control cells were incubated in serum free medium alone for the same period. The zero minute time point was when cells in culture was used as is (1:1 DMEM + F12, 10% FBS). Cells were rinsed once with ice-cold phosphate buffered saline (PBS) and lysed using lysis buffer (25mM Tris.HCl, pH 7.5, 150mM NaCl, 5mM $MgCl_2$, 1% NP-40, 1mM DTT, 5% glycerol containing protease inhibitors including aprotinin (10µg/ml), leupeptin (10µg/ml), soy-trypsin inhibitor (10µg/ml), complete mini-EDTA free protease inhibitor cocktail (1 tablet/10ml lysis buffer; Roche, Indianapolis, IN), 1mM PMSF, 25mM NaF and 1mM NaO_4V. 300 µg of

each lysate was used for the pull down. Our initial experiments suggested extremely rapid turnover of activated rho that was barely detectable in our samples even when 1mg of total lysate was used for the pull down. In order to detect activated rho, lysates (300 μg) were mixed with 10mM 0.5M EDTA, pH 8.0 and 0.1mM GTPγS or 1mM GDP for 30 minutes at 30 °C with constant agitation. Reaction was terminated by placing samples on ice with the addition of 60mM MgCl$_2$. Samples were then loaded onto glutathione discs containing the GST-Rhotekin-rho binding domain (GST-rhotekin-RBD fusion protein, 200μg per disc) in a spin column and mixed for 1 hour with gentle rocking at 4 °C. Spin columns were centrifuged and the resin on the column was washed three times with the lysis buffer before adding 50 μl of SDS-sample buffer to it. Samples were boiled for 5 minutes and the column contents were centrifuged into fresh tubes. Samples were separated on 12% SDS-PAGE gels. Unfractionated lysates were used to detect total rho in samples. Gel contents were transferred overnight on to a PVDF membrane (0.45 μm, pore size). Immunoblot analysis was performed as described by the manufacturer using the mouse monoclonal anti-rho antibody (0.5 μg/ml) included in the kit. All blots were developed using the enhanced chemiluminescence kit (Amersham Pharmacia Biotech, Piscataway, NJ), exposed for the same time and developed. Densitometric values were obtained using Scion Image 4.0.

Real time Reverse Transcriptase Polymerase Chain Reaction

Total RNA extraction and cDNA synthesis were performed according to Krishnamoorthy et al.(38). The primer sequences for ppET-1 and β-actin were as follows: ppET-1-

forward/sense 5'-TATCAGCAGTTAGTGAGAGG-3' and reverse/antisense 5'-CGAAGGTCTGTCACCAATGTGC-3' with an expected amplicon/product size of 180 bp; β-actin- forward/sense 5'-TGTGATGGTGGGAATGGGTCAG-3' and reverse/antisense 5'-TTTGATGTCACGCACGATTTCC-3' with an expected amplicon/product size of 514 bp. Quantitative real time PCR (QPCR) was performed using the SYBR-green detection system (Applied Biosystems, Foster City, CA) as described by Zhang et al.(39). Product authenticity was confirmed by DNA sequencing followed by a BLAST homology search of the resulting sequences (data not shown). Quantitation of relative ppET-1 transcript levels in ARPE-19 was achieved using the comparative C_T method (as described in the PE Biosystems User Bulletin #2: http://docs.appliedbiosystems.com/pebiodocs/04303859.pdf

Data Analysis

Quantitative data is represented as mean $\pm$ SEM. Statistical comparisons between control and multiple treatments were made by ANOVA and SNK test. In certain experiments a comparison in the mean value between the untreated control vs. treated sample was made by t-test. In $[Ca^{2+}]_i$ measurements, comparisons between baseline, peak and one minute post peak (not shown) values were made by one way repeated measures ANOVA. Sample size and p values for each experiment are indicated in the figure legends.

RESULTS

Thrombin mediated ET-1 secretion in ARPE-19 cells is PAR-1 dependent

At the posterior segment of the eye, a breakdown of the blood retinal barrier may result in thrombin mediated effects on surrounding cells. In this study we examined whether

thrombin could regulate ET-1 secretion in ARPE-19 cells via the PAR-1 or -4 receptor subtypes. Thrombin significantly increased ET-1 secretion following 24 hours, which was both concentration (fig. 1) and time dependent (fig. 2). To determine if thrombin mediated effects were either PAR-1 or PAR-4 dependent, we tested two synthetic peptides that mimicked the tethered ligand on PAR-1 (pPAR-1/ SFLLR) and PAR-4 (pPAR-4/ AYPGKF). The pPAR-1 but not pPAR-4 ligand significantly increased ET-1 secretion in ARPE-19 cells (fig. 1) suggesting thrombin mediated effects on ET-1 may involve the PAR-1 subtype. Hirudin (anti-thrombin) binds to the catalytic subunit of thrombin (31) and blocks its protease activity. Hirudin alone had no effect on ET-1 secretion but neutralized the thrombin effect when pre-incubated with thrombin before treatment. Time course studies suggested thrombin (10nM) significantly increased ET-1 secretion, first observed at 4 hours with the greatest increase at the end of 16 and 24 hours (fig. 2).

PAR-1 and PAR-4 mediated $[Ca^{2+}]_i$ mobilization in ARPE-19 cells

Protease activated receptors are known to couple $G_{q/11}$ family of heterotrimeric G-proteins that can activate an IP_3-dependent increase in intracellular calcium ($[Ca^{2+}]_i$) (21). To determine if thrombin, pPAR-1 or pPAR-4 mediate elevations in $[Ca^{2+}]_i$ to the similar extent, we examined their immediate effects on $[Ca^{2+}]_i$ following stimulation. Thrombin mediated increase in $[Ca^{2+}]_i$ was concentration dependent with the typical biphasic profile (fig. 1 and table 1). Both pPAR-1 and pPAR-4 ligands significantly increased $[Ca^{2+}]_i$ indicating the presence of both receptor subtypes and that they were both functional. Thrombin was more potent in elevating $[Ca^{2+}]_i$ compared to pPAR-1 or-4 (table 1) and

10-30 nM hirudin and 10 μM U73122 completely attenuated thrombin induced rise in $[Ca^{2+}]_i$ suggesting a PLC-dependent mechanism (table 1).

Thrombin mediated disruption of tight junctions and alterations in cell shape

In all our experiments that involved addition of thrombin or the PAR-1 agonist (pPAR-1) we found significant and rapid alteration of the RPE cytoskeleton that was not seen following addition of the PAR-4 agonist (pPAR-4) (data not shown). Thrombin is known to induce changes in paracellular permeability in endothelial cells (40). In retinal pigment epithelial cells, thrombin mediated changes in cell shape can decrease transepithelial resistance and increase barrier permeability consistent with characteristics of barrier breakdown. We observed similar effects on immunoreactive ZO-1, a peripheral component of tight junctions. Treatment with thrombin resulted in time dependent alterations in cell shape and pronounced disruption of tight junctions (red fluorescence) (fig. 4) that was apparent within the first hour of treatment and progressively damaged the RPE barrier with time.

Activation of rho following thrombin treatment

Rho belongs to the family of monomeric or small GTPases that are thought to exist in one of two states, the ON state where rho has GTP bound and the OFF state where rho has GDP bound (30). This binary mode of existence is crucial for cellular functions that are dependent on G proteins, including cell division, motility, polarity and secretion (30). Since rho is involved in cytoskeletal remodeling and thrombin is a known activator of rho, we examined whether a similar mechanism occurred in RPE. Activated rho was barely detectable in lysates that excluded the non-hydrolysable form of GTP, GTPγS

(data not shown) even at early time points (2 minutes following thrombin addition) suggesting rapid turnover of activated rho. However, when equal amount of lysates were loaded with GTPγS, a detectable signal was observed. Conversely, lysates mixed with GDP failed to detect activated rho (fig. 5A). A comparison of activated rho levels between serum containing media (zero minute), control (untreated/ serum-free alone) and thrombin treatment at 2, 5, 10, 30 and 60 minutes suggested rapid activation within 5 minutes, that peaked at 30 minutes and returned back to basal levels at the end of 60 minutes (fig. 5A and B). This suggested rho, like Ca^{2+}, was a second messenger signal following thrombin stimulation in RPE.

Thrombin induced increase in preproET-1 transcription

Thrombin mediated ET-1 secretion (fig. 1 and 2) was significantly higher than constitutive ET-1 secretion at the end of 4 hours suggesting either earlier events following thrombin receptor activation could be involved in regulating ET-1 synthesis, and/or the radioimmunoassay-based detection for ET-1 was not sensitive enough to detect smaller changes in ET-1 secretion.

To determine if thrombin increased ET-1 synthesis, we employed the real-time PCR technique to quantitatively analyze changes in preproET-1 mRNA at the indicated time points (Fig. 6A). Thrombin partially increased ppET-1 mRNA levels within 30 minutes that was significantly higher than the untreated control after 1 hour. Interestingly, mRNA levels of ppET-1 dropped back to basal levels after the first hour implying that thrombin mediated regulation of ET-1 synthesis was transient. Since rho and $[Ca^{2+}]_i$ elevations were observed within this period, we sought to determine if elevation in ppET-1 mRNA

was dependent on either one cascade or both. Rho associated kinase (ROCK1/2) is a direct rho effector, and like rho, is implicated in alterations in cell motility (41). Inhibition of thrombin mediated activation of the rho/ROCK1/2 pathway by 10 μM Y27632, a ROCK1/2 inhibitor, resulted in complete inhibition of ppET-1 mRNA synthesis while U73122 at 10μM, a PLC inhibitor, only slightly decreased ET-1 synthesis (compared to thrombin alone). This finding implicated the rho/ROCK1/2 pathway as being critical for thrombin induced ppET-1 synthesis.

ROCK1/2 but not PKC modulates PAR-1 receptor mediated ET-1 production in RPE

To examine if prolonged inhibition of ROCK1/2, PLC or PKC had an effect on thrombin induced ET-1 secretion, we preincubated RPE cells with the indicated inhibitors followed by thrombin in the presence of the inhibitor for 24 hours. ET-1 secreted in the media was quantitatively assessed by radioimmunoassay (RIA). Previous studies have implicated agonist-induced rise in $[Ca^{2+}]_i$ with subsequent PKC activation in ET-1 synthesis and secretion (16). In ARPE-19 cells we found the pan-PKC inhibitor, Ro 31-8425 at 100nM had no effect on thrombin mediated ET-1 secretion (fig. 7). Interestingly, the PLC inhibitor, U73122 at 10μM partially attenuated thrombin-induced ET-1 secretion while the ROCK1/2 inhibitor, Y27632 at 10μM completely blocked secretion, a finding similar to that observed in the mRNA studies (fig. 6B).

DISCUSSION

Endothelin-1 is a potent vasoactive 21 amino-acid peptide and was recently shown by our lab to be secreted constitutively by the retinal pigment epithelium *in vitro* (3) and expressed predominantly in the RPE *in situ* in human and rat retinas (42). Additionally,

cholinergics and proinflammatory cytokines like TNF-α can regulate secretion of ET-1 in RPE (3). ET-1 itself is considered proangiogenic and a proinflammatory cytokine (43) that can be induced by other cytokines, growth factors, mechanical stretch and hypoxia (16). Production of mature 21 amino-acid form of ET-1 involves a series of proteolytic steps including the conversion of preproET to proET, proET to bigET that is furin dependent and finally bigET to ET, the rate limiting step that involves an endothelin-converting enzyme (ECE) (44).

Thrombin, a member of the family of serine proteases, is a procoagulant and a known activator of ET-1 (45), and is thought to act at or near the site at which it is produced (31). In the present study, we report that thrombin mediated ET-1 secretion in ARPE-19 cells is time dependent and that secretion may be enhanced by cytoskeletal remodeling and subsequent breakdown of tight junctions. Additionally, we describe a novel signaling cascade for ET-1 synthesis and secretion that is rho/ROCK1/2 dependent and is partially influenced by PAR-1 receptor induced rise in $[Ca^{2+}]_i$.

We found both the PAR-1 (pPAR-1/SFLLR) and the PAR-4 (pPAR-4/AYPGKF) specific peptide agonists were capable of significantly elevating $[Ca^{2+}]_i$ in RPE cells, albeit they were much less potent than thrombin. This suggests that thrombin could mediate other effects that directly sensitize the Ca^{2+} response. Thrombin and pPAR-1 but not pPAR-4 caused a significant increase in ET-1 secretion in ARPE-19 cells, in a concentration and time-dependent manner, implying that PAR-1 and PAR-4 receptor signaling cascades were distinct and that a rise in $[Ca^{2+}]_i$ alone was not enough to mediate ET-1 secretion. PAR-1 receptors are known activators of the pertussis-toxin insensitive $G_{12/13}$ G-proteins,

and dissociation of the G_α subunit can activate rho GEF, a guanine-nucleotide exchange factor for rho. Rho GEFs include lbc, lfc, lsc and p115 (46,47) of which p115 was shown to bind $G_{\alpha12}$ and $G_{\alpha13}$ and mediate Rho activation (23,24). $G_{\alpha13}$ was recently shown to induce preproET-1 transcription in c-jun N-terminal kinase (JNK) dependent manner (48). Additionally, rho GTPases have been implicated in controlling ET-1 production either by directly increasing preproET-1 mRNA transcription (49) or by increasing ECE-1 mRNA transcription (50).

Thrombin caused a transient activation of rho in ARPE-19 cells with visible changes in the cytoskeleton that was accompanied by disruption of the apically localized tight junctions. Quantitative PCR for ppET-1 mRNA suggested that thrombin was a potent activator of ppET-1 mRNA synthesis in these cells, an effect that was transient and most pronounced at the end of the first hour of stimulation. Activated rho has several downstream effectors including direct activation of rho-associated kinase or ROCK1/2 (41). Inhibition of ROCK1/2 with Y27632 also completely inhibited thrombin induced ppET-1 synthesis and ET-1 secretion implicating the predominant role of the rho/ROCK signaling module in ET-1 production in RPE. Additionally, pPAR-1 dependent increase in ET-1 secretion was also completely blocked by Y27632. ROCK1/2 dependent activation of the transcription factor GATA-4 was shown to mediate ET-1 transcription in cardiomyocytes (51).

The signaling cross-talk between rho and calcium dependent pathways is not well established. Activated rhoA was recently shown to interact with IP_3 receptors as well as TRP channel-1 in endothelial cells suggesting that rho may regulate store operated

calcium entry (52) or receptor activated calcium entry (52,53). However, in the present study, phospholipase C dependent IP_3/Ca^{2+} pathway was only partially involved in ET-1 secretion. Synthesis and secretion of ET-1 is known to be protein kinase C (PKC)-dependent (16). Thrombin mediated activation of PKC-α was shown to associate and phosphorylate the rho-guanine nucleotide dissociation inhibitor (rhoGDI), allowing activation of rho and increased paracellular permeability in endothelial cells (Mehta D., 2001). This suggests that PKC may influence rho activation. In ARPE-19 cells however, we found that the pan-PKC inhibitor Ro 31-8425 failed to alter thrombin-mediated ET-1 secretion. Future experiments are planned to address the role of PKC in modulating rho/ROCK activation and ET-1 production in ARPE-19 cells. Figure 8 summarizes the signaling features that may be involved in thrombin-induced ET-1 synthesis and secretion in ARPE-19 cells.

Constitutively active forms of RhoA and Rac1 have been implicated in tight junction disruption in epithelial and endothelial cells (54,55). More recently, a tight junction-associated Rho GEF, lfc/GEF-H1 has been identified (29) and implicated in tight junction function including paracellular permeability. It is tempting to speculate that PAR-1 may be apically or subapically localized that recruits a $G\alpha_{12/13}$ dependent rhoGEF and subsequent rho activation resulting in alteration of cell shape and tight junction disruption. In addition to the above changes in cell shape mediated by PAR-1 activation, ET-1 secretion was significantly enhanced following thrombin addition. Interestingly, secretion of ET-1 was enhanced after 4 hours of thrombin treatment that coincided with progressive disruption of tight junctions.

Our results suggest that rho/ROCK1/2 mediated activation of ET-1 synthesis and secretion may be one of the primary mechanisms involved in the thrombin-ET-1 interaction pathway with concomitant disruption and remodeling of the RPE cytoskeleton. ET-1 thus secreted may mediate wound repair and cell migration, previously identified actions of ET-1 (56,57) or may mediate further damage by increasing nitric oxide production via the ET_B receptor (58). ET-1 released by the RPE may be important in pathologic conditions that involve the blood-retinal barrier breakdown and inflammation as reported in conditions including uveitis (59), retinitis pigmentosa (60), proliferative vitreoretinopathy and diabetic retinopathy (61). The role of constitutive ET-1 production in the RPE is of outstanding interest since its physiologic function at the region of the BRB is presently unknown.

By comparison with breakdown of the blood-brain barrier, excessive secretion of ET-1 may mediate prolong vasoconstriction of retinal and choroidal blood vessels resulting in ischemia. Constitutively secreted ET-1 may play a role in localized RPE migration and wound repair.

ACKNOWLEDGEMENTS

the Yorio lab for their comments and technical expertise. This work is part of S.N's doctoral dissertation.

REFERENCES

1. Marmor, M. F. (1998) in *The Retinal Pigment Epithelium* (Marmor, M. F., and Wolfensberger, T. J., eds), pp. 3-9, Oxford University Press, New York, NY

2. Campochiaro, P. A. (1998) in *The Retinal Pigment Epithelium* (Marmor, M. F., and Wolfensberger, T. J., eds), pp. 459-477, Oxford University Press, New York, NY

3. Narayan, S., Prasanna, G., Krishnamoorthy, R. R., Zhang, X., and Yorio, T. (2003) *Invest Ophthalmol Vis Sci (in press)*

4. MacCumber, M. W., Jampel, H. D., and Snyder, S. H. (1991) *Arch Ophthalmol* **109**, 705-709

5. Wollensak, G., Schaefer, H. E., and Ihling, C. (1998) *Curr Eye Res* **17**, 541-545

6. Stitt, A. W., Chakravarthy, U., Gardiner, T. A., and Archer, D. B. (1996) *Curr Eye Res* **15**, 111-117

7. Ripodas, A., de Juan, J. A., Roldan-Pallares, M., Bernal, R., Moya, J., Chao, M., Lopez, A., Fernandez-Cruz, A., and Fernandez-Durango, R. (2001) *Brain Res* **912**, 137-143

8. Kedzierski, R. M., and Yanagisawa, M. (2001) *Annu Rev Pharmacol Toxicol* **41**, 851-876

9. Russell, F. D., and Molenaar, P. (2000) *Trends Pharmacol Sci* **21**, 353-359

10. Yanagisawa, M., and Masaki, T. (1989) *Biochem Pharmacol* **38**, 1877-1883

11. Salom, J. B., Torregrosa, G., and Alborch, E. (1995) *Cerebrovasc Brain Metab Rev* **7**, 131-152

12. Taylor, R. N., Varma, M., Teng, N. N., and Roberts, J. M. (1990) *J Clin Endocrinol Metab* **71**, 1675-1677

13. Granger, J. P., Alexander, B. T., Llinas, M. T., Bennett, W. A., and Khalil, R. A. (2001) *Hypertension* **38**, 718-722

14. Nelson, J., Bagnato, A., Battistini, B., and Nisen, P. (2003) *Nat Rev Cancer* **3**, 110-116

15. Coughlin, S. R. (1998) *Arterioscler Thromb Vasc Biol* **18**, 514-518

16. Tasaka, K., and Kitazumi, K. (1994) *Gen Pharmacol* **25**, 1059-1069

17. Coughlin, S. R. (1999) *Proc Natl Acad Sci U S A* **96**, 11023-11027

18. Dery, O., Corvera, C. U., Steinhoff, M., and Bunnett, N. W. (1998) *Am J Physiol Cell Physiol* **274**, C1429-1452

19. Coughlin, S. R. (2001) *Thromb Haemost* **86**, 298-307

20. Barr, A. J., Brass, L. F., and Manning, D. R. (1997) *J Biol Chem* **272**, 2223-2229

21. Hung, D. T., Wong, Y. H., Vu, T. K., and Coughlin, S. R. (1992) *J Biol Chem* **267**, 20831-20834

22. Offermanns, S., Laugwitz, K. L., Spicher, K., and Schultz, G. (1994) *Proc Natl Acad Sci U S A* **91**, 504-508

23. Hart, M. J., Jiang, X., Kozasa, T., Roscoe, W., Singer, W. D., Gilman, A. G., Sternweis, P. C., and Bollag, G. (1998) *Science* **280**, 2112-2114

24. Kozasa, T., Jiang, X., Hart, M. J., Sternweis, P. M., Singer, W. D., Gilman, A. G., Bollag, G., and Sternweis, P. C. (1998) *Science* **280**, 2109-2111

25. Hall, A. (1998) *Science* **280**, 2074-2075

26.   Fukuhara, S., Murga, C., Zohar, M., Igishi, T., and Gutkind, J. S. (1999) *J Biol Chem* **274**, 5868-5879

27.   Klages, B., Brandt, U., Simon, M. I., Schultz, G., and Offermanns, S. (1999) *J Cell Biol* **144**, 745-754

28.   Norman, J. C., Price, L. S., Ridley, A. J., Hall, A., and Koffer, A. (1994) *J Cell Biol* **126**, 1005-1015

29.   Benais-Pont, G., Punn, A., Flores-Maldonado, C., Eckert, J., Raposo, G., Fleming, T. P., Cereijido, M., Balda, M. S., and Matter, K. (2003) *J Cell Biol* **160**, 729-740

30.   Etienne-Manneville, S., and Hall, A. (2002) *Nature* **420**, 629-635

31.   Coughlin, S. R. (2000) *Nature* **407**, 258-264

32.   Tigyi, G., Fischer, D. J., Sebok, A., Marshall, F., Dyer, D. L., and Miledi, R. (1996) *J Neurochem* **66**, 549-558

33.   Majumdar, M., Seasholtz, T. M., Goldstein, D., de Lanerolle, P., and Brown, J. H. (1998) *J Biol Chem* **273**, 10099-10106

34.   Jalink, K., and Moolenaar, W. H. (1992) *J Cell Biol* **118**, 411-419

35.   Dunn, K. C., Aotaki-Keen, A. E., Putkey, F. R., and Hjelmeland, L. M. (1996) *Exp Eye Res* **62**, 155-169

36.   Prasanna, G., Dibas, A., Tao, W., White, K., and Yorio, T. (1998) *Exp Eye Res* **66**, 9-18

37.   Prasanna, G., Dibas, A. I., and Yorio, T. (2000) *Invest Ophthalmol Vis Sci* **41**, 1142-1148

38. Krishnamoorthy, R., Agarwal, N., and Chaitin, M. H. (2000) *Brain Res Mol Brain Res* **77**, 125-130

39. Zhang, X., Krishnamoorthy, R. R., Prasanna, G., Narayan, S., Clark, A., and Yorio, T. (2003) *Exp Eye Res* **76**, 261-272

40. Morel, N. M., Petruzzo, P. P., Hechtman, H. B., and Shepro, D. (1990) *Inflammation* **14**, 571-583

41. Riento, K., and Ridley, A. J. (2003) *Nat Rev Mol Cell Biol* **4**, 446-456

42. Narayan, S., Brun, A., and Yorio, T. (2003) *ARVO Abstract [# 337]*

43. Bek, E. L., and McMillen, M. A. (2000) *J Cardiovasc Pharmacol* **36**, S135-139

44. Kido, T., Sawamura, T., and Masaki, T. (1998) *J Cardiovasc Pharmacol* **31 Suppl 1**, S13-15

45. Kurihara, H., Yoshizumi, M., Sugiyama, T., Yamaoki, K., Nagai, R., Takaku, F., Satoh, H., Inui, J., Yanagisawa, M., Masaki, T., and et al. (1989) *J Cardiovasc Pharmacol* **13 Suppl 5**, S132-137; discussion S142

46. Glaven, J. A., Whitehead, I. P., Nomanbhoy, T., Kay, R., and Cerione, R. A. (1996) *J Biol Chem* **271**, 27374-27381

47. Hart, M. J., Sharma, S., elMasry, N., Qiu, R. G., McCabe, P., Polakis, P., and Bollag, G. (1996) *J Biol Chem* **271**, 25452-25458

48. Yamakaw, K., Kitamura, K., Nonoguchi, H., Takasu, N., Miller, R. T., and Tomita, K. (2002) *Hypertens Res* **25**, 427-432

49. Hernandez-Perera, O., Perez-Sala, D., Soria, E., and Lamas, S. (2000) *Circ Res* **87**, 616-622

50.   Eto, M., Barandier, C., Rathgeb, L., Kozai, T., Joch, H., Yang, Z., and Luscher, T. F. (2001) *Circ Res* **89**, 583-590

51.   Yanazume, T., Hasegawa, K., Wada, H., Morimoto, T., Abe, M., Kawamura, T., and Sasayama, S. (2002) *J Biol Chem* **277**, 8618-8625

52.   Mehta, D., Ahmmed, G. U., Paria, B., Holinstat, M., Voyno-Yasenetskaya, T., Tiruppathi, C., Minshall, R. D., and Malik, A. B. (2003) *J Biol Chem*

53.   Ghisdal, P., Vandenberg, G., and Morel, N. (2003) *J Physiol*

54.   Jou, T. S., Schneeberger, E. E., and Nelson, W. J. (1998) *J Cell Biol* **142**, 101-115

55.   Wojciak-Stothard, B., Potempa, S., Eichholtz, T., and Ridley, A. J. (2001) *J Cell Sci* **114**, 1343-1355

56.   Shao, R., and Rockey, D. C. (2002) *J Cell Physiol* **191**, 342-350

57.   Kernochan, L. E., Tran, B. N., Tangkijvanich, P., Melton, A. C., Tam, S. P., and Yee, H. F., Jr. (2002) *Gut* **50**, 65-70

58.   Tsukahara, H., Ende, H., Magazine, H. I., Bahou, W. F., and Goligorsky, M. S. (1994) *J Biol Chem* **269**, 21778-21785

59.   Luna, J. D., Chan, C. C., Derevjanik, N. L., Mahlow, J., Chiu, C., Peng, B., Tobe, T., Campochiaro, P. A., and Vinores, S. A. (1997) *J Neurosci Res* **49**, 268-280

60.   Vinores, S. A., Kuchle, M., Derevjanik, N. L., Henderer, J. D., Mahlow, J., Green, W. R., and Campochiaro, P. A. (1995) *Histol Histopathol* **10**, 913-923

61.   Hiscott, P., and Sheridan, C. M. (1998) in *The Retinal Pigment Epithelium* (Marmor, M. F., and Wolfensberger, T. J., eds), pp. 478-491, Oxford University Press, New York, NY

Figure legends

Fig. 1 <u>Secreted ET-1 in mature ARPE-19 (mRPE) measured by RIA.</u> Cells were treated with the indicated agonists and/or inhibitors for 24 hours in serum-free DMEM/F-12 medium. Immunoreactive ET-1 (ir-ET-1) released in the media was extracted and measured by RIA (refer Methods). In mRPE cells, thrombin significantly increased ir-ET-1 secretion vs. control, an effect that was concentration dependent. Hirudin (30nM) when preincubated with thrombin (10nM) inhibited ET-1 secretion as opposed to thrombin (10 nM) alone. pPAR-1 but not pPAR-4 (both at 50 μM) significantly increased ET-1 secretion suggesting thrombin mediated effects on ET-1 secretion involves the PAR-1 receptor. Data is represented as mean $\pm$ SEM. Statistical comparisons were performed using ANOVA and SNK test. * denotes significance vs. control ($p<0.05$) (n= atleast 6 per treatment).

Fig. 2 <u>Time dependent increase in ir-ET-1 secretion in mRPE cells following thrombin</u> <u>(10 nM) stimulation.</u> Mature ARPE-19 (mRPE) cells were treated with thrombin (10nM) for 1, 4, 8, 16 and 24 hours. The media was collected and assayed for ir-ET-1 content as previously described. Thrombin stimulated ir-ET-1 secretion in a time- dependent manner. A significant increase in ir-ET-1 was observed at the end of 4, 8, 16 and 24 hours compared to control. Secretion of ir-ET-1 reached a plateau after 16 hours. Data is represented as mean $\pm$ SEM. Statistical comparisons were performed by t-test. Asterisk (*), double asterisk (**), pound (#), and double pound symbols (##) denote significance vs. controls at 4, 8, 16 and 24 hours respectively ($p< 0.001$) (n = 9).

Fig. 3. <u>Intracellular [Ca^{2+}]$_i$ measurements in mRPE cells</u>. Representative [Ca^{2+}]$_i$ trends in response to thrombin (10nM), pPAR-1 (50 μM) and pPAR-4 (50 μM) in mRPE cells. There was a concentration dependent rise in thrombin mediated mean [Ca^{2+}]$_i$ mobilization that was attenuated by hirudin and U73122 (see table 1). Thrombin was more potent in mobilizing [Ca^{2+}]$_i$ in mRPE cells compared to pPAR-1 or pPAR-4 (compare y-axes scales and table 1).

Fig. 4 <u>Immunofluorescence analysis in mRPE cells following thrombin (10nM) treatment at the indicated time points</u>. The top row (A-F) represents differential interference contrast (DIC) images and the bottom row (G-L) represents merged fluorscent images of cells labeled using mouse anti-ZO-1 (red), rabbit anti-ET-1 (green) and DAPI (blue). Thrombin (10nM) caused visible breakdown of cell-cell contact and tight junction disruption that was time-dependent. The first detectable change in cell-cell contact was observed at 4 hours and progressive damage thereafter. (scale bar in L = 10μm). Experiments were performed on at least 3 separate coverslips (n=3) per time point.

Fig. 5 <u>Rho pull down assay in ARPE-19 cell lysates following thrombin treatment.</u> Thrombin mediated activation of rho was detected in ARPE-19 cells at 5, 10 and 30 minutes that was higher than unstimulated cells at the similar time points (A, top panels). Total rho in cell lysates remained unchanged (A, lower panels). GDP loading inactivated rho and thus prevented the pull-down. (B) represents the scanning densitometric data plotted as a ratio of activated rho/ total rho at the indicated time points.

Fig. 6 <u>Quantitative real time RT-PCR.</u> Quantitative RT-PCR was performed using the SYBR-green PCR core reagents. Quantitation of ppET-1 transcripts was done by the

comparative C_T method (refer Methods) with β-actin mRNA as the external control. Thrombin mediated significant increase in ppET-1 mRNA that peaked at 1 hour and returned to basal values at all time points tested there after (A). Thrombin induced rise in ppET-1 mRNA was completely inhibited by Y27632, a ROCK1/2 inhibitor but not the PLC inhibitor- U73122 (B). Data is represented as mean ± SEM. Statistical comparisons were performed by t-test. Asterisk (*) denotes significance vs. control, and pound (#) denotes significance vs. thrombin, 1hour (p< 0.05).

Fig. 7 <u>Secreted ET-1 in mature ARPE-19 (mRPE) measured by RIA.</u> Cells were treated with the indicated agonists (thrombin or pPAR-1) or were pretreated with the indicated inhibitors for 20-30 minutes followed by the agonist for 24 hours in serum-free DMEM/F-12 medium. Immunoreactive ET-1 (ir-ET-1) released in the media was extracted and measured by RIA (refer Methods). Thrombin mediated increase in ET-1 secretion was partially blocked by the PLC inhibitor, U73122 and completely inhibited by ROCK1/2 inhibitor, Y27632. The pan-PKC inhibitor (Ro 31-8425) had no effect on thrombin induced ET-1 release. pPAR-1 (SFLLR) mediated ET-1 secretion was also completely inhibited by Y27632. Data is represented as mean ± SEM. Statistical comparisons were performed using ANOVA and SNK test. Asterisk (*) denotes significance vs. control, double asterisk (**) denotes significance vs. thrombin 10nM and pound (#) denotes significance vs. pPAR-1 50 μM (p<0.05) (n= atleast 6 per treatment).

Fig. 8 <u>Thrombin induced ET-1 secretion in RPE is rho/ROCK1/2 dependent.</u> Thombin mediated PAR-1 receptor activation can simultaneously activate the $G_{q/11}$ and $G_{12/13}$ dependent pathways which in turn activates PLC dependent IP_3 and DAG production and

rho activation respectively. IP$_3$ dependent [Ca^{2+}]$_i$ elevation along with DAG can activate PKC that may influence ET-1 synthesis in some cells. The predominant effect of thrombin on ET-1 production in ARPE-19 cells was via the rho/ROCK1/2 dependent pathway. ROCK1/2 may increase ppET-1 mRNA synthesis by activating the GATA family of transcription factors (i.e. GATA-2/4). The physiological function of ET-1 secreted by the RPE is presently unknown. Considering some of the known actions of ET-1, it may mediate tissue repair by acting on its receptors in an autocrine manner or cause further damage to the neural retina by acting on its receptors in the inner retina.

Fig. 1

Secreted ir-ET-1 (pg/mg total protein)
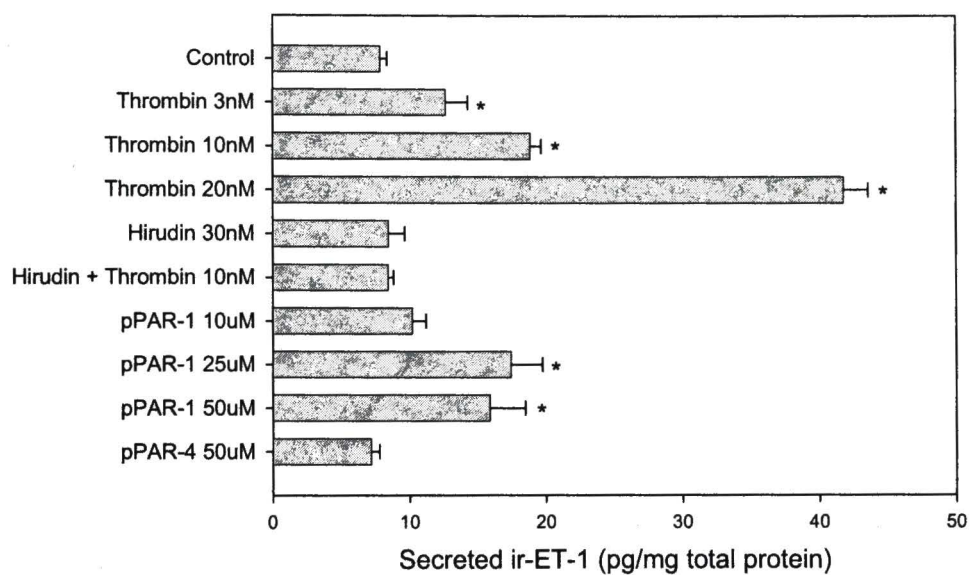
Fig. 2
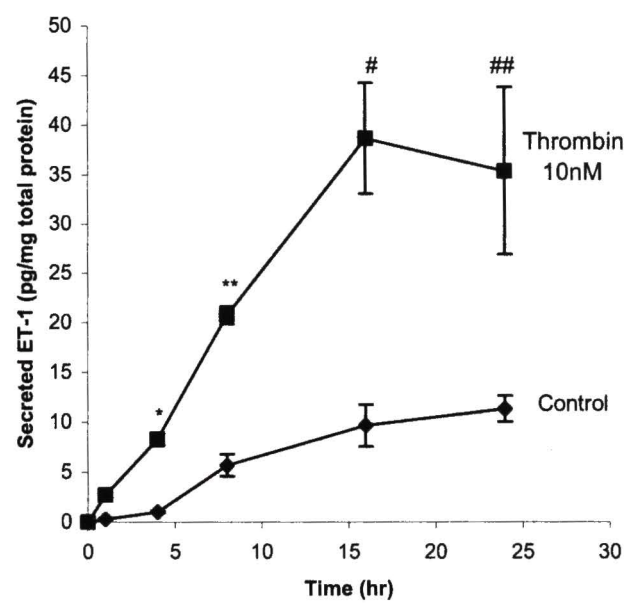
Fig. 3
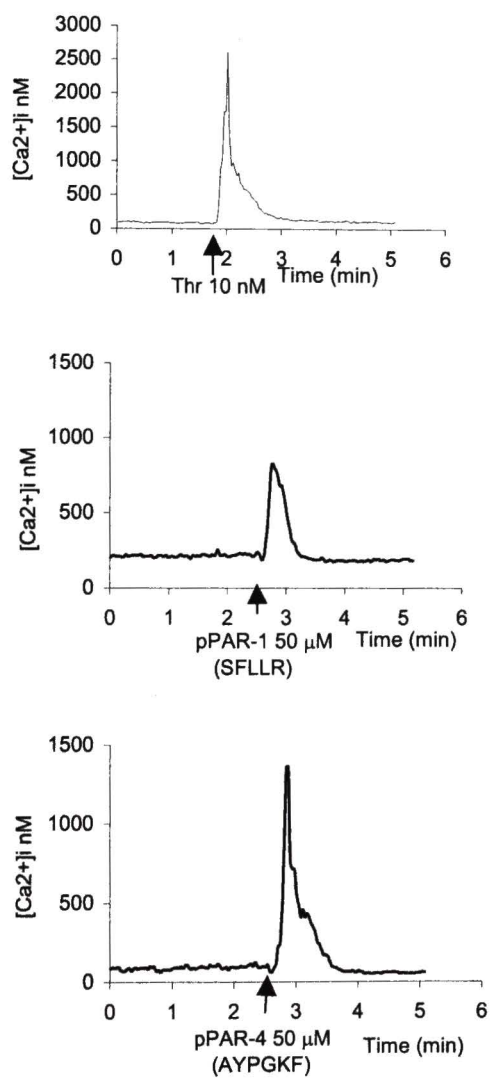
Table 1. (A) Summary of thrombin, pPAR-1 and pPAR-4 mediated $[Ca^{2+}]_i$ mobilization in mRPE cells measured by fura-2AM imaging. (B) Hirudin (anti thrombin) was preincubated with thrombin for 1 hour at room temperature at equimolar or three-fold higher concentration. In U73122 studies, cells were preincubated with 10µM U73122 for 20 minutes before thrombin addition. Asterisk (*) denotes statistical significance between baseline, peak and one minute post peak (not shown) mean values, performed by one way repeated measures ANOVA and SNK method for multiple pair wise comparison ($p<0.001$).

A. Concentration dependent elevation of $[Ca^{2+}]_i$

Treatment	$[Ca^{2+}]_i$ nM, Mean ± SEM	Number of cells (n)
Baseline	70 + 10	11
Thrombin 5 nM	2049 + 184 *	12
Baseline	64 + 5	79
Thrombin 10 nM	2141 + 277 *	79
Baseline	95 + 8	19
Thrombin 20 nM	6164 + 1620 *	19

Baseline	219 + 10	16
pPAR-1 (SFLLR) 50 µM	817 + 52 *	16
Baseline	87 + 9	18
pPAR-4 (AYPGKF) 50 µM	1194 + 177 *	18

B. Inhibition of thrombin mediated elevation in $[Ca^{2+}]_i$

Treatment	$[Ca^{2+}]_i$ nM, Mean ± SEM	Number of cells (n)
Baseline	64 + 5	79
Thrombin 10 nM	2141 + 277 *	79
Baseline	124 + 12	17
Hirudin + Thrombin (10 nM each)	165 + 16	17
Baseline	64 + 5	16

Hirudin + Thrombin (25 nM each)	109 ± 5	16
Baseline/ U73122 $10\mu M$	53 ± 5	16
U73122 + Thrombin 10nM	53 ± 4	16

Fig. 4
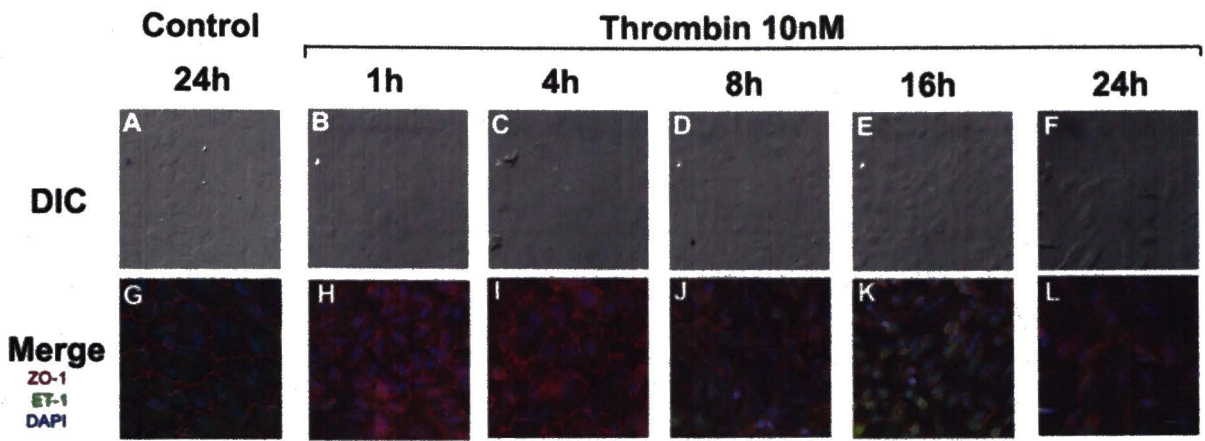
Fig. 5

A.
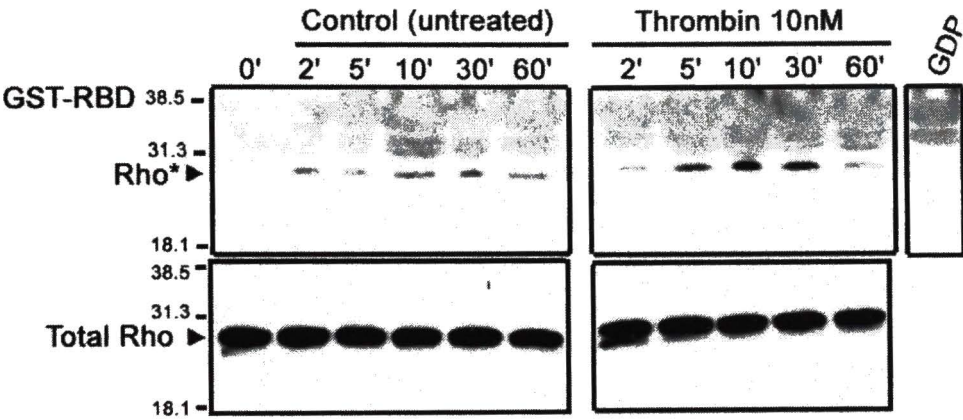
B.
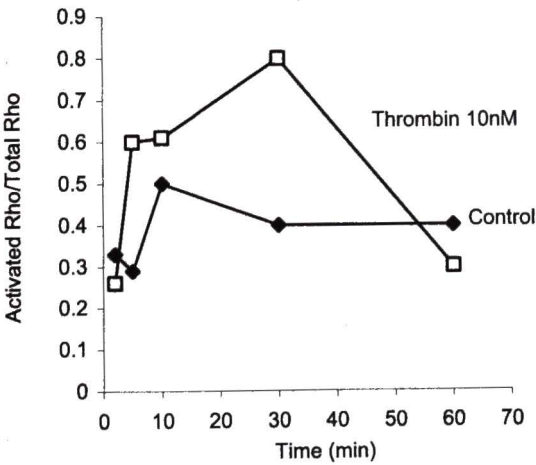
Fig. 6

A.
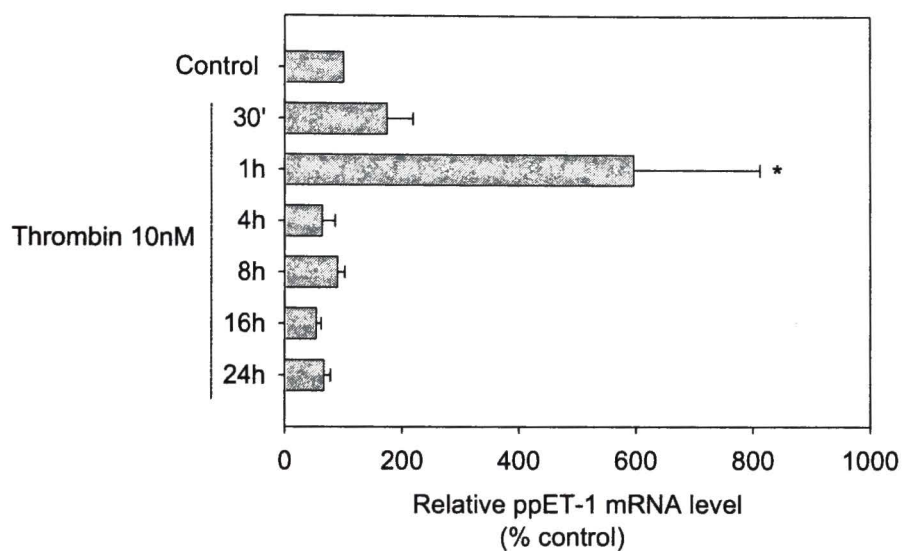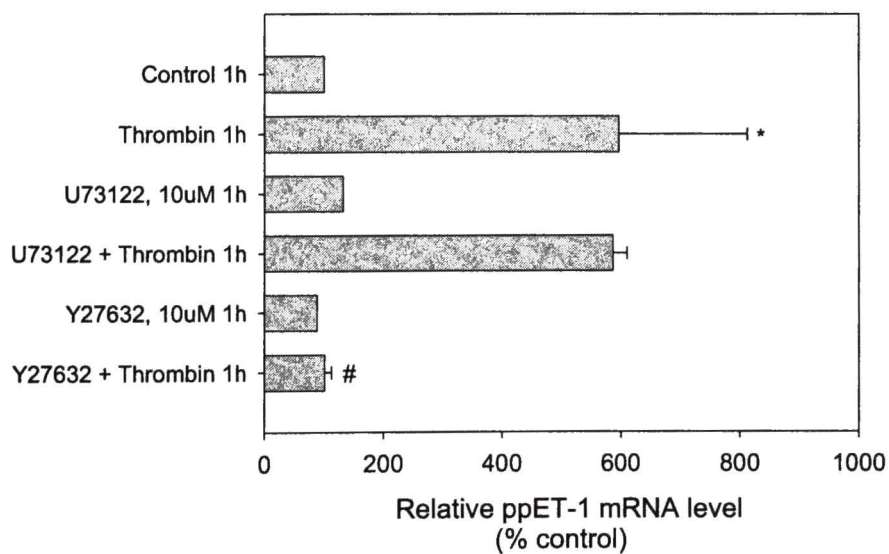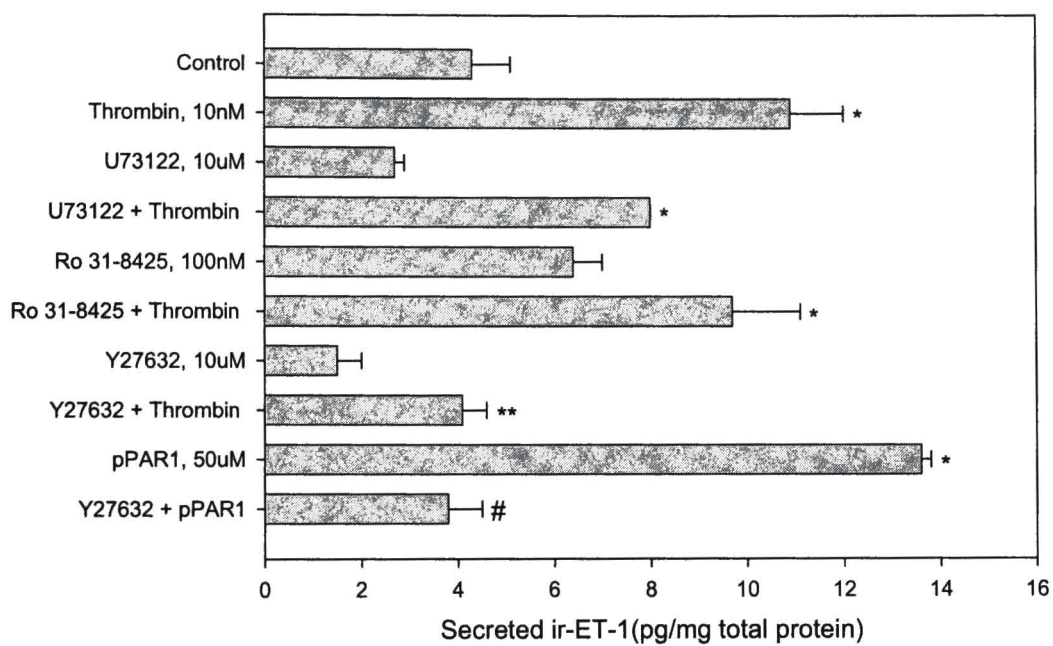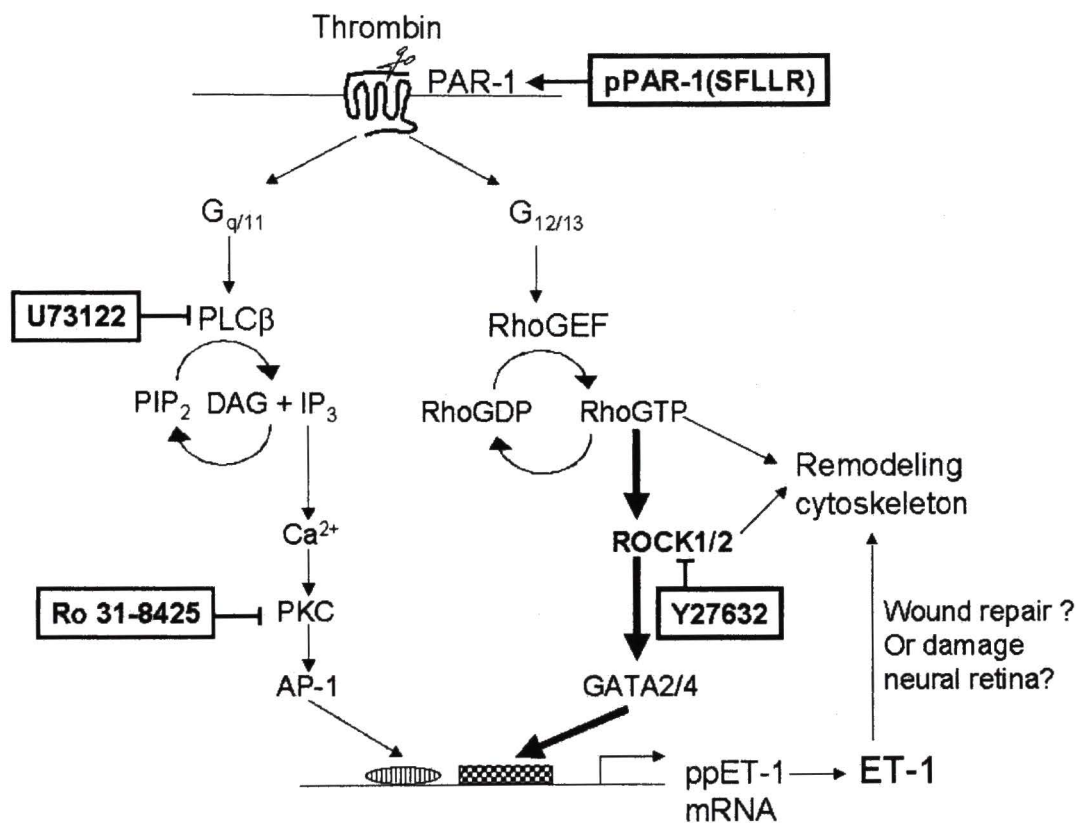

B.

Fig. 7

Fig. 8

CHAPTER 6

CONCLUSIONS AND FUTURE DIRECTIONS

Our study on the outer blood retinal barrier provides comprehensive evidence of ET-1 secretion by the RPE. Using the *in vitro* model of RPE we assessed both constitutive and regulated secretion of ET-1. These results clearly demonstrated that ET-1 is secreted by the RPE and that cholinergics and TNF-α may regulate its secretion. Additionally, TNF-α but not carbachol mediated increase in preproET-1 mRNA and ET-1 secretion in mature RPE cells was time dependent that was concomitant with tight junction disassembly. Expression of ET-1 was predominant in the RPE layer of the retina *in situ* in both rat and human eyes, further strengthening our hypothesis.

Local production of thrombin at the site of blood vessel damage following breakdown may enhance ET-1 secretion in the RPE. We report a novel signaling mechanism by way of thrombin-mediated actions via protease-activated receptor-1 (PAR-1) in RPE cells via the rho-ROCK1/2 signaling pathway.

A figure summarizing our hypothesis is shown below-
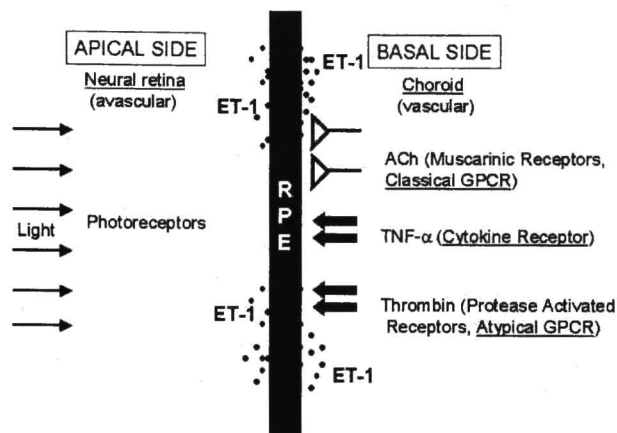
The retinal pigment epithelium may be one of the major sources for ET-1 at the region of the outer blood retinal barrier. Secretion and turover of ET-1 involves furin and endothelin converting enzyme, and endothelin receptors A and B sybtypes. Furin proprotein convertase, and ECE-1 a-d isoforms (slice variants of ECE-1) are expressed by mature RPE cells. Additionally, we found ET_B receptors but not ET_A receptors are expressed by RPE. The ability of cultured RPE cells to secrete ET-1 non-preferentially towards both apical and basolateral directions suggest that ET-1 may act on photoreceptors as well as the choroid.

ET receptors have been detected in photoreceptors and the choroid, but the physiological role of ET-1 at the region of the RPE remains obscure. ET-1 secreted towards the choroid may have a direct influence on choroidal blood flow. Cholinergic nerves innervating the choriocapillaries cause nitric oxide mediated vasodilation. ET-1 secreted by the RPE towards the choroid may act to balance the vascular tone and may

thus regulate blood flow at this region. ET-1 secreted by the RPE at the subretinal space can be measured using a technique developed by Hollyfield et al.

Future experiments with the following design have been planned-

1. C3 transferase is an inhibitor of rho activity. Previous studies have suggested the inability of C3 transferase to completely inhibit rho activity may be due to its poor membrane permeability. Lipofectamine mediated delivery of C3 transferase has achieved greater efficacy. We plan to use this mode of delivery on ARPE-19 cells.

2. Additionally, constitutively active rho (rhoG12V) and dominant negative (rhoT19N) mutants of rho along with kinase dead ROCK1 and –2 will further determine the downstream substrates of this pathway in mediating ppET-1 synthesis.

3. The relative contribution of GATA2/4 and AP-1 transcription factors in activating ppET-1 mRNA synthesis performed by electromobility shift assays (EMSA) and supershift assays are currently in progress.

4. ROCK1/2 has several downstream effectors including GATA. Phosphorylation assays in the presence of the wild type and kinase-dead mutant of ROCK1/2 will determine downstream effectors involved in ET-1 synthesis and secretion.

5. Further examination of the calcium and/or PKC dependent cross-talk with the rho/ROCK pathway will provide useful answers towards understanding how GPCR- dependent activation mechanisms modulate ET-1 production and cytoskeletal changes at the same time.

6. Tight junction disassembly can be induced independent of direct receptor activation either by using peptide inhibitors to the extracellular region of the tight junction resident integral protein- occludin-2 or by transfecting RPE cells with dominant negative ZO-1 followed by ET-1 RIA and PCR analysis. This will determine the role of tight junctions in ET-1 synthesis.

Delineating function

To determine the function of ET-1 at this site, we have currently designed a 'knock-down' approach that is both inducible and tissue specific. Long double stranded RNA (dsRNA) based knockdown is a modification of the siRNA (small interfering RNA) technique that requires a tissue specific promoter. The RPE65 protein is an attractive target because it exclusively present in RPE in vivo. We used the minimal RPE65 promoter upstream of a tetracycline operator (TetO) and dsET-1 (double stranded ET-1 cDNA) that confers an inducible genotype that can be turned on whenever required by feeding transgenic mice with doxycycline.

This approach is especially attractive because of the following anticipated outcome-

ET-1 may be produced in very small amounts in vivo under normal conditions with intact blood retinal barriers. Sodium iodate and optic nerve crush injuries result in breakdown of the blood retinal barrier that may switch ET-1 synthesis to 'hyper-mode'. ET-1 production following an inflammatory challenge may perform the unknown functions. Mice fed with doxycycline prior to inducing inflammation will have lesser amounts of ET-1 available (knocked-down ppET-1 mRNA).

So, how does one measure this phenotype?

We have a few ideas that will address this problem. Labeling retinas with anti-albumin can assess the extent of blood retinal barrier damage. Albumin under normal conditions is impermeable, but studies have shown it to be present in the retina following breakdown of the blood retinal barrier. Comparing wild type, non-induced knockdown and induced knockdown mice during inflammation will provide answers to the role of ET-1 specifically in the retina/choroid. Additionally, fluorescein angiography and electroretinogram (ERG) measurements provide useful methods of assessing the barrier and retinal function in the live animal.

Translational Research

It is possible that ET-1 or components of the ET Axis may be involved in inflammation and angiogenesis in the eye. A genome wide search for mutations in the ET axis in patients susceptible to retinal or choroidal inflammation and in patients with proliferative vitreoretinopathy, choroidal neovascularization, uveitis and diabetic retiopathy may provide an exciting avenue for future research ascertaining the importance of endothelins in the retina and choroid.

On a personal note-

Biologically Inspired Shuttle Wings (BISW): patent pending

The Columbia Space Shuttle disaster and the loss of the entire STS-107 crew including mission experts and payload specialists on February 1, 2003 was a tragic loss that could have been averted. Hindsight is always 20/20 and I think that's what keeps us in the running. In the days after the tragedy, we knew more about the cause of the mishap. The

form material from one of the boosters landed on the left wing during take off that had taken pieces off the insulation. The insulation material it turns out – is made of ceramite, an easily malleable, thermal resistant silicon alloy, the substance commonly used in dental crowns. Shuttle wing insulation is composed of thousands of such ceramite pieces glued together. The impact of the foam resulted in a 'broken barrier'. It was about this time that my research on tight junctions was switching to high gear. Tight junctions communicate from membrane to the nucleus, a breakdown or altered permeability results in activation of known and unknown sensors that communicate to the nucleus to make up for the loss in integrity, either by increasing proliferation or selectively increasing mRNA and protein species that are required to repair the damage. Likewise ceramite pieces could be fitted with tiny sensors (nanomachines) in between them that when disrupted could send signals to a terminal warning the mission crew about structural defects. The day is not far when machine learning for self-repair becomes cliché. The ideal situation would be when defects such as these activate a policing system that allow bio-inspired machines to home in and repair the damage without having humans do such nitty-gritty work requiring fine motor skills.

The Time Is NOW.

Santosh Narayan

August, 2003.

APPENDIX

The following results were part of this dissertation that were not included as part of the chapters, nonetheless, aids in characterizing the RPE as a valid system to access ET-1 synthesis including constitutive and regulated secretion.

TNF-α mediated ET-1 secretion and cytoskeletal remodeling in the RPE is TNF-R1 dependent.

The following studies were designed based on specific aims 2.3b-d that were proposed to examine the expression of TNF-R1 receptor subtype, its relation to TNF-α mediated changes in RPE tight junction architecture and ET-1 secretion.

TNF-α mediated changes in ARPE-19 cells with respect to phetotypic alteration in tight junction assembly (fig.3) as well as ET-1 secretion (fig.2) may be TNF-R1 dependent. It remains to be determined if cytoskeletal alternations and/or tight junction disassembly alone turns on ET-1 synthesis and secretion and whether this could be reversed using selective inhibitors that prevent microtubule disruption and stabilize microtubules as well as inhibitors of tight junction disassembly.

Fig. 1 <u>Western blot analysis of TNF-R1 receptor in ARPE-19 cells.</u> TNF-R1 (55 kD) was detected using mouse monoclonal anti-TNF-R1 (0.8 μg/ml; SantaCruz Biotechnology, Inc., SantaCruz, CA) in ARPE-19 cells.
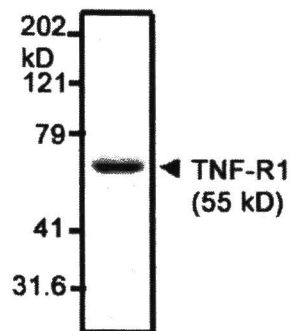
Fig. 2 ET-1 RIA in ARPE-19 cells. Cells were treated with TNF-α (10 nM) for 24 hours in serum-free RPE medium in the presence or absence of a specific TNF-R1 receptor anibody (mouse anti-TNF-R1, 20µg/ml; R & D Systems Inc., Minneapolis, MN). At the end of 24 hours, the culture media (n=3/ condition) were collected, ET-1 was extracted and quantified by RIA. Secreted ET-1 was normalized to total cellular protein.
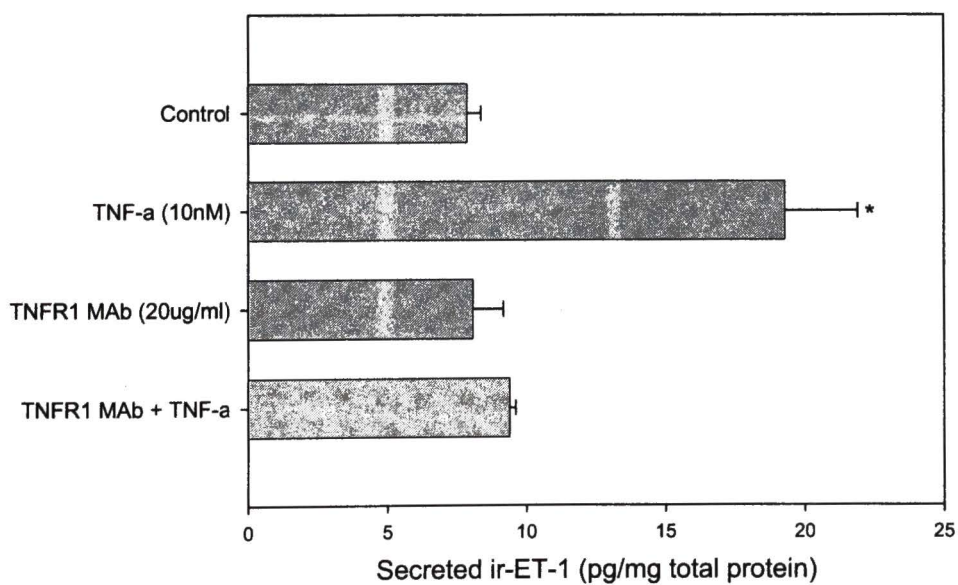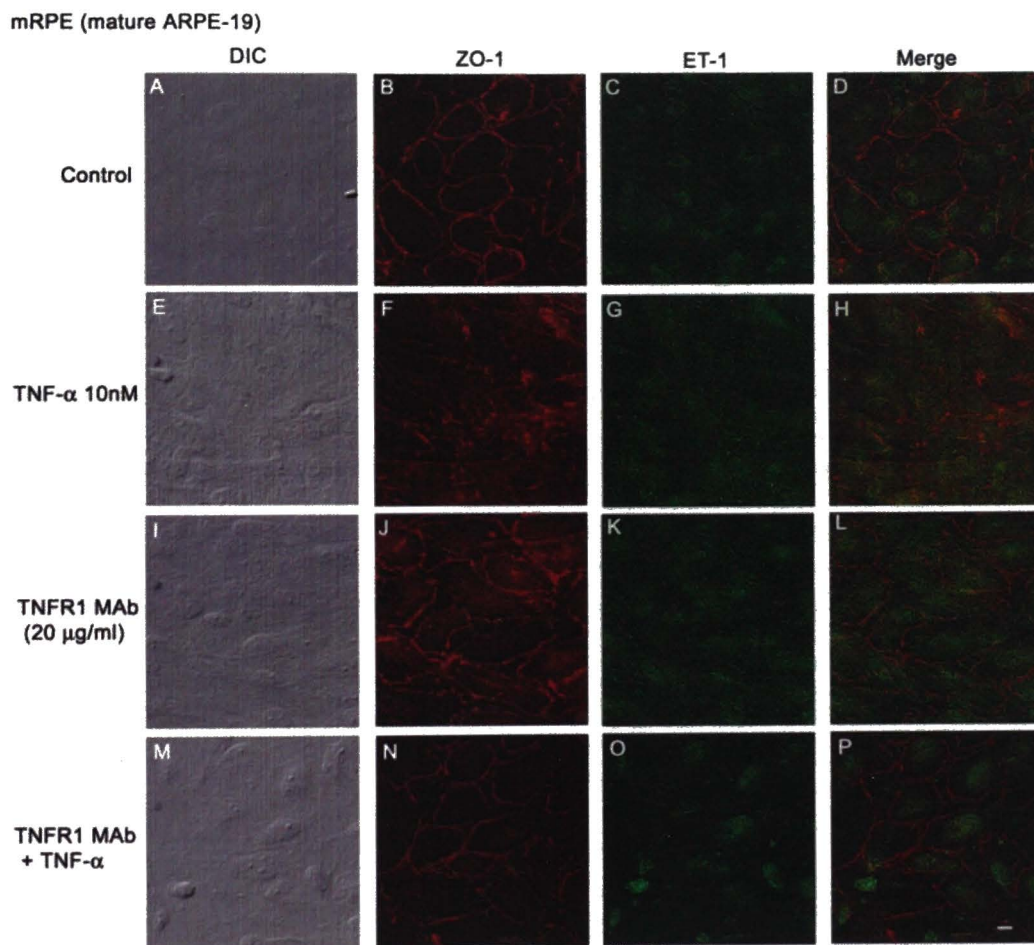
Fig. 3 <u>Indirect immunofluorescence</u>. ARPE-19 cells were treated as in fig. 1, fixed and labeled with the mouse anti-ZO-1 (tight junction associated protein), rabbit anti-ET-1 and the nuclear stain-DAPI. Following secondary antibiody labeling, cells were visualized on a Nikon Microphot fluorescence microscope. Scale in = 10 μm.

The Endothelin-1 Axis in the Retinal Pigment Epithelium

The following study was designed to address part of specific aim 2.4 to determine the expression of furin, a proprotein convertase, endothelin converting enzyme-1 (ECE-1) and its isoforms as well as ET_A and ET_B receptors in ARPE-19 cells. Furin and ECE-1 are involved in the proteolytic processing of preproET-1 to its mature form (ET-1). ET receptors (ET_A and ET_B) are known to regulate extracellular levels of ET-1 by ligand dependent receptor endocytosis.

Furin and the mRNA for ECE-1 isoforms, of which the -1c and -1d isoforms seemed to be more abundant. ET_A and ET_B receptors can regulate the turnover of extracellular ET-1. The ET_B receptor is the 'clearance receptor', activation of which results in internalization and degradion of the receptor-ligand complex in the lysosome. ET_A receptor was undetectable in ARPE-19 cells while bands corresponding to ET_B (34 kD) were present that underwent significant downregulation following ET-1 treatment (30 minutes) that was concentration dependent.

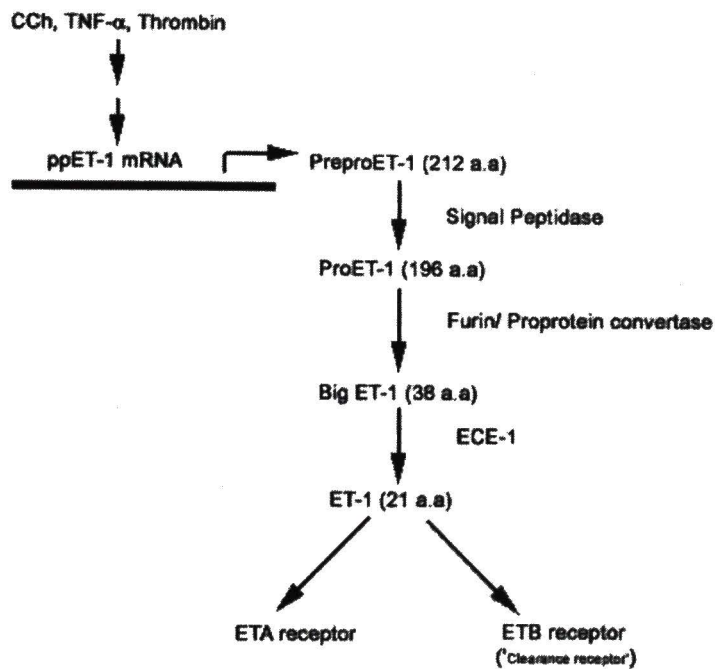Biogenesis of ET-1 and components of the ET Axis

CCh, TNF-α, Thrombin

ppET-1 mRNA → PreproET-1 (212 a.a)

Signal Peptidase

ProET-1 (196 a.a)

Furin/ Proprotein convertase

Big ET-1 (38 a.a)

ECE-1

ET-1 (21 a.a)

ETA receptor   ETB receptor
                    ('Clearance receptor')

Fig. 1 Expression of the proprotein convertase furin in ARPE-19 cells. Furin expressionwas analyzed by western blotting using rabbit anti-furin convertase (1:700; Affinity Bioreagents, Golden, CO). Two bands were detected, one at 100 kD (expected size) and the second band at around 55 kD (size of the putative catalytic domain of furin).
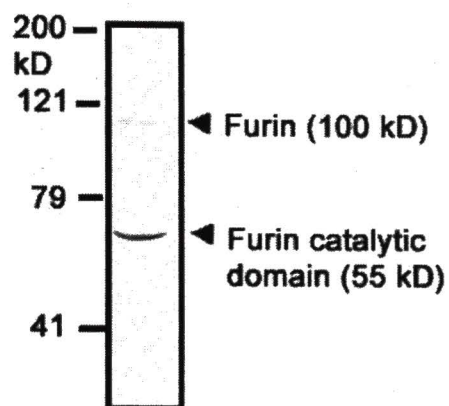
Fig. 2 ECE-1 isoforms in ARPE-19 cells. The mRNA expression of ECE-1 isoforms (1a, b, c, and d) were determined by RT-PCR analysis.
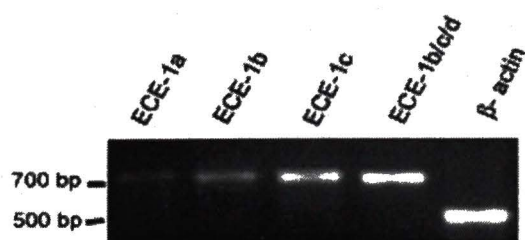
Fig. 3 ET$_B$ receptor subtype in ARPE-19 cells. ARPE-19 cells were treated with ET-1 (1, 10, 100, and 500 nM) for 30 minutes followed by whole cell lysis. Western blot analysis using the rabbit anti-ET$_B$ receptor antibody (1.5 µg/ml; Alomone Labs, Jerusalem, Israel) detected several bands, one of them showed marked downregulation following ET-1 treatement. The antibody : control antigen (1.5: 3) pre-incubation indicated the non-specific bands. ET$_B$ as previously reported by our lab and others migrates around 34 kD.
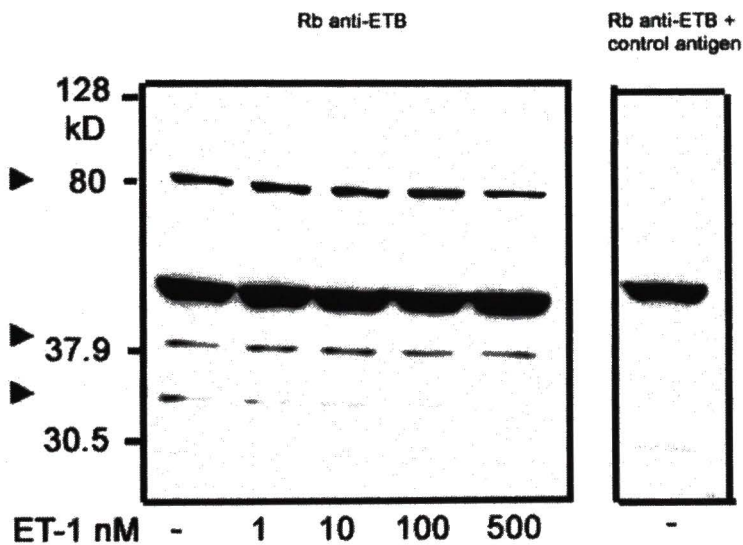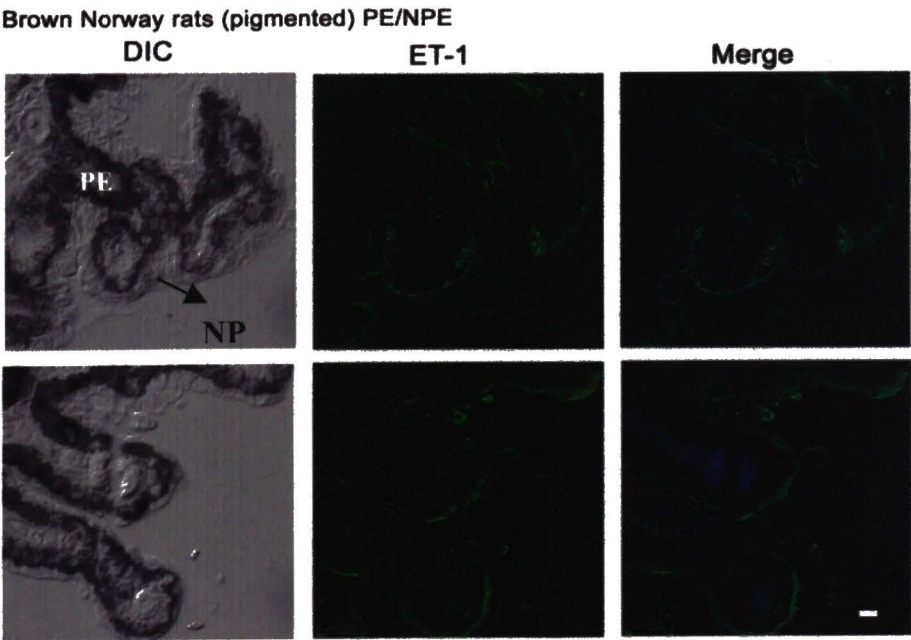
ET-1 in the ciliary epithelium (blood aqueous barrier)

In the anterior chamber, ET-1 is expressed in the non-pigmented epithelium (NPE) that is thought to regulate both aqueous humor production as well outflow facility for the same. The anterior chamber, particularly the NPE clearly indicated the presence of ET-1 by indirect immunofluorescence. Additionally, the result provides confirmation regarding the specificity of the rabbit anti-ET-1 antibody, the same was used in all the posterior segment labeling studies and electron microscopy studies.

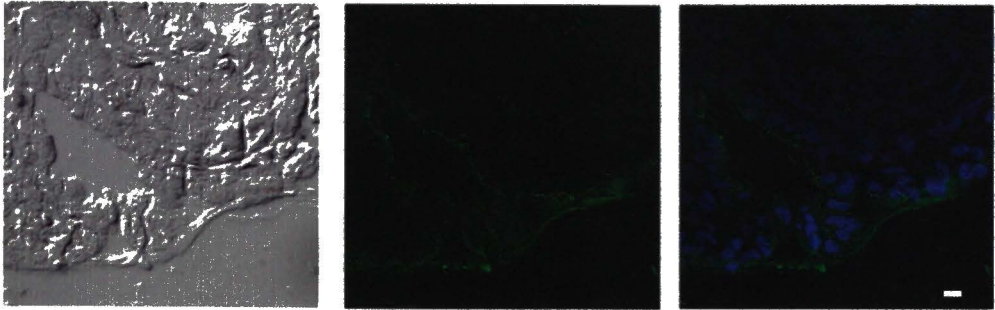**Fig. 1** The blood-aqueous barrier in the anterior chamber and ET-1 immunoreactivity

Brown Norway rat (pigmented) and Wistar (albino) eyes were sectioned and labeled with rabbit anti-ET-1 (10 µg/ml, green) and DAPI (blue). The differential interference contrast (DIC) images on the left indicate the presence and absence of pigments (pigmented epithelium) in A and B respectively. Scale bar = 10µm.

A.

Brown Norway rats (pigmented) PE/NPE

B.

Wistar rats (male, albino) PE/NPE